

International Journal of Applied Sciences and Smart Technologies

Volume 04, Issue 02, December 2022

Sugarcane Production Modeling Using Machine Learning in Western Maharashtra
Chhaya Narvekar, Madhuri Rao

A White Noise Approach to Occupation Times of Brownian Motion
Herry Pribawanto Suryawan

Dijkstra Algorithm Implementation in Determining the Shortest Route of Industrial Gas Distribution in PT Tira Austenite Tbk Cikarang with Python Programming Language
Bernadetha Nathalia Fitra Soverenty, Cyrenia Novella Krisnamurti

An Enhanced Multi-Level Authentication Electronic Voting System
Ayodeji O.J Ibitoye, Halleluyah O. Aworinde, Esther T. Adekunle

**Appropriate Technology-Based Project-Based Learning:
3D Printing Utilization for Learning Media Class**
Monica Cahyaning Ratri

Employee Presence Using Body Temperature Detection and Face Recognition
Arif Ainur Rafiq, Erna Alimudin, Della Puspa Rani

**The Experiment of Wind Electric Water Pumping for Salt Farmers
in Remote Area of Demak-Indonesia**
S. Dio Zevalukito, Y.B. Lukiyanto, F. Risky Prayogo

Response Surface Modelling of the Mechanical Properties of Oil Palm Empty Fruit Bunch Fibre Reinforced Polyester Composites
Chinwe Evangeline Kamma

Comparative Study of Master Oil (MO) and Lophira Lanceolata (Ochnaceae) Oil (LLO) Lubricants in Sewing Machines
J. B. Yerima, G. O. Mokoro, D. William, S. D. Najoji

Design of Someone's Character Identification Based on Handwriting Patterns Using Support Vector Machine
Rosalia Arum Kumalasanti

Optimization of Vacuum Forming Parameter Settings to Minimize Burning Defect on Strawberry Packaging Products Using the Taguchi Method
Th. Adi Nugroho, Adhi Setya Hutama, Perwita Kurniawan

The Effect of the Number of Cooling Pads on the Output Air Condition and Effectiveness of Air Cooler
Wibowo Kusbandono

Pre-service Science Teachers' Competence and Confidence in Scientific Inquiry
Rohandi

p-ISSN 2655-8564 & e-ISSN 2685-9432

CONTENTS

CONTENTS	i
EDITORIAL BOARD	Iii
PREFACE	iv
Sugarcane Production Modeling Using Machine Learning in Western Maharashtra <i>Chhaya Narvekar and Dr.Madhuri Rao</i>	123–130
A White Noise Approach to Occupation Times of Brownian Motion <i>Herry Pribawanto Suryawan</i>	131–140
Dijkstra Algorithm Implementation in Determining the Shortest Route of Industrial Gas Distribution in PT Tira Austenite Tbk Cikarang with Python Programming Language <i>Bernadetha Nathalia Fitra Soverenty, Cyrenia Novella Krisnamurti</i>	141–148
An Enhanced Multi-Level Authentication Electronic Voting System <i>Ayodeji O.J Ibitoye, Halleluyah O. Aworinde, Esther T. Adekunle</i>	149–158
Appropriate Technology-Based Project-Based Learning: 3D Printing Utilization for Learning Media Class <i>Monica Cahyaning Ratri</i>	159–172
Employee Presence Using Body Temperature Detection and Face Recognition <i>Arif Ainur Rafiq, Erna Alimudin, and Della Puspa Rani</i>	173–184
The Experiment of Wind Electric Water Pumping for Salt Farmers in Remote Area of Demak-Indonesia <i>S. Dio Zevalukito, YB. Lukiyanto and F. Risky Prayogo</i>	185–194
Response Surface Modelling of the Mechanical Properties of Oil Palm Empty Fruit Bunch Fibre Reinforced Polyester Composites <i>Chinwe Evangeline Kamma</i>	195–220
Comparative Study of Master Oil (MO) and Lophira Lanceolata (Ochnaceae) Oil (LLO) Lubricants in Sewing Machines <i>J. B Yerima, G. O Mokoro, D. William, and S. D Najoji</i>	221-232
Design of Someone's Character Identification Based on Handwriting Patterns Using Support Vector Machine <i>R. A. Kumalasanti</i>	233-240
Optimization of Vacuum Forming Parameter Settings to Minimize Burning Defect on Strawberry Packaging Products Using the Taguchi Method <i>Th. Adi Nugroho, Adhi Setya Hutama and Perwita Kurniawan</i>	241-254

The Effect of the Number of Cooling Pads on the Output Air Condition and Effectiveness of Air Cooler <i>Wibowo Kusbandono</i>	255-266
Pre-service Science Teachers' Competence and Confidence in Scientific Inquiry <i>Rohandi</i>	267-280
AUTHOR GUIDELINES	281-282

EDITORIAL BOARD

Editor in Chief

Dr. I Made Wicaksana Ekaputra (*Sanata Dharma University, Yogyakarta, Indonesia*)
Email: made@usd.ac.id

Associate Editor

Dr. Pham Nhu Viet Ha (*Vietnam Atomic Energy Institute, Hanoi, Vietnam*)
Dr. Hendra Gunawan Harno (*Gyeongsang National University, Jinju, The Republic of Korea*)
Dr. Iswanjono (*Sanata Dharma University, Yogyakarta, Indonesia*)
Dr. Mukesh Jewariya (*National Physical Laboratory, New Delhi, India*)
Dr. Mongkolsery Lin (*Institute of Technology of Cambodia, Phnom Penh, Cambodia*)
Dr. Yohanes Baptista Lukiyanto (*Sanata Dharma University, Yogyakarta, Indonesia*)
Dr. Apichate Maneewong (*Thailand Institute of Nuclear Technology, Bangkok, Thailand*)
Prof. Dr. Sudi Mungkasi (*Sanata Dharma University, Yogyakarta, Indonesia*)
Dr. Pranowo (*Universitas Atma Jaya Yogyakarta, Yogyakarta, Indonesia*)
Dr. Monica Cahyaning Ratri (*Sanata Dharma University, Yogyakarta, Indonesia*)
Dr. Mahardhika Pratama (*Nanyang Technological University, Singapore*)
Dr. Augustinus Bayu Primawan (*Sanata Dharma University, Yogyakarta, Indonesia*)
Prof. Dr. Leo Hari Wiryanto (*Bandung Institute of Technology, Bandung, Indonesia*)

Editorial Proofreader

Ir. Ignatius Aris Dwiatmoko, M.Sc. (*Sanata Dharma University, Yogyakarta, Indonesia*)
P. H. Prima Rosa, S.Si., M.Sc. (*Sanata Dharma University, Yogyakarta, Indonesia*)

Editorial Assistant

Eduardus Hardika Sandy Atmaja, M.Cs. (*Sanata Dharma University, Yogyakarta, Indonesia*)
Rosalia Arum Kumalasanti, M.T. (*Sanata Dharma University, Yogyakarta, Indonesia*)
Vittalis Ayu, M.Cs. (*Sanata Dharma University, Yogyakarta, Indonesia*)

Administration

Catharina Maria Sri Wijayanti, S.Pd. (*Sanata Dharma University, Yogyakarta, Indonesia*)

Contact us

International Journal of Applied Sciences and Smart Technologies
Faculty of Science and Technology
Sanata Dharma University
Kampus III Paingan, Maguwoharjo, Depok, Sleman
Yogyakarta, 55282
Phone : +62 274883037 ext. 523110, 52320
Fax : +62 272886529
Email : editorial.ijasst@usd.ac.id
Website : <http://e-journal.usd.ac.id/index.php/IJASST>

International Journal of Applied Sciences and Smart Technologies

Volume 4, Issue 2, page iii

p-ISSN 2655-8564, e-ISSN 2685-9432

IJASST is an open-access peer-reviewed journal that mediates the dissemination of research and studies conducted by academicians, researchers, and practitioners in science, engineering, and technology.

PREFACE

Dear readers, we are delighted to serve you Volume 4, Issue 2 of *International Journal of Applied Sciences and Smart Technologies* (IJASST), which is managed and published by the Faculty of Science and Technology, Sanata Dharma University. IJASST is an open-access peer-reviewed journal that mediates the dissemination of research and studies conducted by academicians, researchers, and practitioners in science, engineering, and technology. Its scope also includes basic sciences which relate to technology, such as applied mathematics, physics, and chemistry.

In this edition, we have thirteen papers authored by researchers from Indonesia, India, Turkey, Nigeria, and Palestine. Submitted papers are reviewed fairly using the open journal system (OJS) of IJASST. After the review process, accepted papers of the journal are publicly available for free at the website of IJASST.

For future issues, we are looking forward to your contributions to IJASST.

Dr. I Made Wicaksana Ekaputra
Editor in Chief
IJASST

Sugarcane Production Modeling Using Machine Learning in Western Maharashtra

Chhaya Narvekar^{1, *}, Madhuri Rao²

¹*Department of Information Technology, Xavier Institute Of Engineering ,
Mumbai , India*

²*Thadomal Shahani Engineering College , Mumbai, India*

**Corresponding Author: chhaya.n@xavier.ac.in*

(Received 01-05-2022; Revised 20-07-2022; Accepted 23-07-2022)

Abstract

Agriculture is the most important sector in the Indian economy. India is the world's second-largest producer of sugarcane. Study is undertaken at Shirol tehsil. Kolhapur district, Maharashtra state, India with the aim of modeling sugarcane production forecasting using supervised machine learning algorithms. Sugarcane is mostly cultivated crop in this area. We applied supervised machine learning for forecasting the productivity of sugarcane village wise based on the ten year's data about sugarcane production from the year 2010 to 2020. Sugarcane yield prediction accuracy is around 65%, which is only based on data provided by sugar factory.

Keywords: sugarcane, productivity, machine learning, forecasting.

1 Introduction

The Indian economy relies heavily on sugarcane cultivation. Sugar, as well as enterprises manufacturing alcohol, paper, chemicals, and animal feed, rely on it for raw materials. In India, sugarcane production is processed through a network of sugar mills, as well as various other businesses and backward and forward connections. The demand

for higher sugarcane production in India is increasing due to the multi-purpose usage of sugarcane in India and its byproducts in numerous sectors [1]. Despite rising urbanization around the world, agriculture remains the primary source of income for a huge percentage of the people. Although technological developments have resulted in more accurate weather predictions and increased yields, much work remains to be done to provide farmers with a taking into account local data so they can forecast yields. In the Maharashtra (India) region, the Sugarcane Cultivation Life Cycle (SCLC) spans around 12 months, with plantation starting at three separate seasons. Our method relies on past production data to train a supervised machine learning system and make sugarcane crop predictions.

Climate, production environments and agronomic aspects associated with agricultural management, such as variety selection, cane field age, fertilization, pest and disease control, and weed control, all influence sugarcane yield [2].

Description of study area - Shirol Taluka of Kolhapur district is gifted by the presence of natural irrigation potential on account of five major rivers i.e. Krishna, Panchaganga, Warana, Dudhganga and Vedganga [3]. Soil type here is alluvial. Normal rainfall is during June-October 1019.5mm. Top three crops cultivated are sugarcane 113.9('000 ha), Paddy Rainfed 113.8 ('000 ha) and Groundnut 57.4('000 ha) [4]. India is the world's second-largest producer of sugarcane after Brazil. Sugarcane is grown in all of India's states and at various times of the year. In this study, we propose supervised machine learning based crop yield forecasting model for sugarcane as a principal crop in study area. Crop analysis and agricultural production forecasting always relied on statistical models. Models are applied on ten years production data of the sugarcane. Three algorithms applied for sugarcane productivity prediction and five algorithms are applied for sugarcane yield prediction on ten years sugarcane production data from study area provided by Shree Dutta Sugar Factory, Shirol.

2 Research Methodology

Materials and Methods: Sugarcane is India's most important cash crop. It entails less risk, and farmers may be quite certain of a return even in difficult conditions. Sugarcane is first crop of Kolhapur district [4]. The sugarcane yield data, in tons of cane per hectare [5], originally available at the farmers and village gat number level. Ten years data from the sugar mill which includes farmer name, gat number village, date of sowing and season area of sugarcane cultivated and production. Knowing the size of the sugarcane harvest might assist industry members make better decision [2].

Table 1. Ten year sugarcane cultivation trend in study area

Season-Year	Cultivated AREA	Total Sugarcane Production in Ton
2010-2011	14556.33	1344688.952
2011-2012	13032.36	1229240.511
2012-2013	10824.94	1196219.045
2013-2014	11139.9	1191862.504
2014-2015	337.8816667	67610.66034
2015-2016	11425.21	1294479.054
2016-2017	15058.3365	1224696.921
2017-2018	10524.99	1187021.203
2018-2019	12118.64	1212491.125
2019-2020	11637.48	1047024.887
2020-2021	11272.86	1192268.53

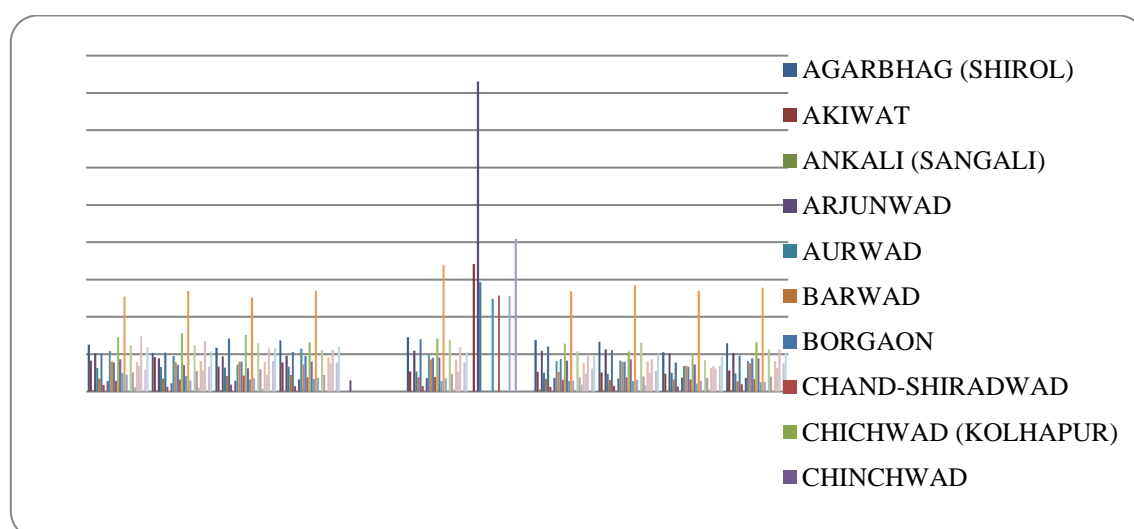


Figure 1. Village wise sugarcane production

From this we added column for productivity and village wise data created and applied machine learning algorithm for predicting the productivity of a particular village. Table 1, shows season wise sugarcane cultivated area and sugarcane production from study area. The model's predictor variables productivity of village is calculated on a yearly basis.

Regression analysis is a basic, technique for modeling the relationship between one or more independent or predictor variables and a dependent or response variable that we want to forecast, and it is one of the tools available in statistical analysis literature [5]. Sugarcane production in study area is summarized in Table 1.

Dataset description

Following Figure 2. shows the sample dataset which is recorded by sugar factory. Year wise production also visualised in Figure 3. For applying machine learning algorithm for yield some of the columns are removed which are less correlated. The features shown in figure 4 are used for training ML regression models after doing the pre-processing such as converting categorical variable in to numerical we get 57495 rows x 11 columns . Dataset is further divided into 80% training and 20 % testing . Performance of model discussed in results section.

	SEASON	VILLAGE_NAME	AREA	WATER_SUPPLY_TYPE	CAME_VARIETY	compute_0012	MATURITY_TYPE	ACTUAL_TON
0	2014-2015	ARJUNWAD	0.40	RIVER	CO-0265	ADASALI	LATE	58.424
1	2014-2015	ARJUNWAD	0.10	RIVER	CO-86032	ADASALI	MIDDLE	15.751
2	2014-2015	ARJUNWAD	0.15	RIVER	CO-0265	ADASALI	LATE	25.740
3	2014-2015	ARJUNWAD	0.40	RIVER	CO-0265	ADASALI	LATE	76.116
4	2014-2015	ARJUNWAD	0.80	RIVER	CO-0265	ADASALI	LATE	129.497

Figure 2. Sample Recorded Data

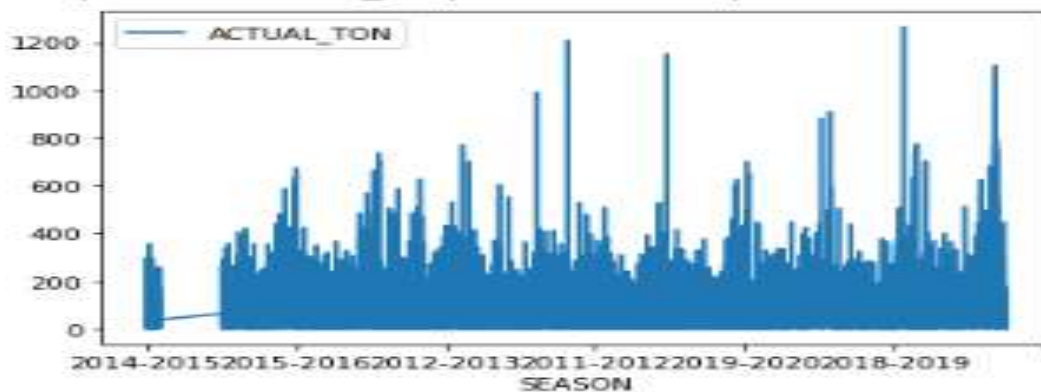


Figure 3. Yearly Production

	AREA	WATER_SUPPLY_TYPE	compute_0012	MATURITY_TYPE	ACTUAL_TON
0	0.40	RIVER	ADASALI	LATE	58.424
1	0.10	RIVER	ADASALI	MIDDLE	15.751
2	0.15	RIVER	ADASALI	LATE	25.740
3	0.40	RIVER	ADASALI	LATE	76.116
4	0.80	RIVER	ADASALI	LATE	129.497

Figure 4. Features Used for Modeling

From the data provided another dataset created which is village wise yearly cultivated area and village wise sugarcane production and productivity of each village calculated per unit area production and machine learning models are trained and tested on this created dataset as well for forecasting productivity of particular village. Productivity compared with national level productivity and state level productivity to get further insights. In both cases climatic, nutrient supply, soil fertility status such parameters are not taken into consideration, which can taken and accuracy would be improved.

3 Results and Discussion

Crop forecasting is the science of estimating crop yields and production ahead of time, usually a couple of months ahead of time. A crucial part of crop production

forecasting is defining the time horizon in terms of time series forecasting approaches. This study included three algorithm for productivity prediction random forest (RF), boosting (GBM), and XGboost which are the most commonly used for agricultural modeling[6]. We tried five different algorithms for modeling yield [4] performance is as shown in Table 2. Performance is not great because there are extrinsic parameters as well which impact on production of crop such as climate, rainfall, soil fertility , management skill and so on which are not considered in the current study.

Table 2. Sugarcane Yield Prediction Model Performance

Machine Learning Algorithm	Accuracy
Linear Regression	62%
Random Forest	65%
XGboost	66%
Gradient Boost	63%
Decision Tree	63%

For sugarcane productivity prediction only village wise area cultivated and production of sugarcane for that particular season is used and target variable is productivity. In this modeling climate data , rainfall , soil quality not considered , parameters used are how much area cultivated, which type of breed, when it is planted, what type of water supply and when crop is taken. Average sugarcane productivity of India is 70-80, average sugarcane productivity of Maharashtra 80.72, [R20], whereas average productivity of the study area is 95. Random forest repressor gives 65% accuracy and other two XGBoost and gradient boosting gave 66% accuracy. When opposed to using a single data model to predict a response, using many model can improve the robustness and accuracy of predictions.

4 Conclusion

The goal of this study was to see if a machine learning approach could provide fresh insights about sugarcane productivity in western Maharashtra. Predicting crop

production may help sugar mills to boost industry revenues by implementing more effective and focused forward selling tactics and logistics planning. The methodology described in this research can readily be applied to other sugarcane-growing regions and agricultural businesses around the world to improve agricultural methods. Sugarcane productivity prediction results demonstrated that the prediction accuracy of the machine learning algorithm is quite promising.

Acknowledgements

The authors are highly grateful to Shree Dutta Sugar Factory, for providing necessary data to carry out this research and thankful to Thadomal Shahani Engineering College, Bandra as well as Xavier Institute of Engineering, Mumbai, India.

References

- [1] P. Mishra, M. A. G. A. Khatib, I. Sardar, J. Mohammed, K. Karakaya, A. Dash, M. Ray, L. Narsimhaiah, A. Dubey, “Modeling and Forecasting of Sugarcane Production in India”, *Sugar tech*, **23**(6), 1317-1324, 2021.
- [2] L. A. Monteiro and P. C. Sentelhas, “Sugarcane yield gap: can it be determined at national level with a simple agrometeorological model?”, *Crop and Pasture Science*, **68**(3), 272-284, 2017.
- [3] I. MAHARASHTRA CELL, “Agriculture Contingency Plan for District: KOLHAPUR”, ICAR_CRIDA_NICRA, 2019.
- [4] Y. Everingham, J. Sexton, D. Skocaj, G. Inman-Bamber, “Accurate prediction of sugarcane yield using a random forest algorithm”. *Agron. Sustain. Dev.* **36**. 27. Springer Verlag/EDP Sciences/INRA. 2016.
- [5] R. G. Hammer, P. C. Sentelhas, J. C. Mariano, “Sugarcane yield prediction through data mining and crop simulation models”. *Sugar Tech*, **22**(2), 216-225. 2020
- [6] R. S. Kodeeshwari and K. T. Ilakkiya, “Different types of data mining techniques used in agriculture-a survey”. *International Journal of Advanced Engineering Research and Science*, **4**(6), 237191. 2017.

A White Noise Approach to Occupation Times of Brownian Motion

Herry Pribawanto Suryawan

Department of Mathematics, Faculty of Science and Technology

Sanata Dharma University, Yogyakarta, Indonesia

Corresponding Author: herrypribs@usd.ac.id

(Received 02-11-2022; Revised 17-11-2022; Accepted 18-11-2022)

Abstract

Occupation times of a stochastic process models the amount of time the process spends inside a spatial interval during a certain finite time horizon. It appears in the fiber lay-down process in nonwoven production industry. The occupation time can be interpreted as the mass of fiber material deposited inside some region. From application point of view, it is important to know the average mass per unit area of the final fleece. In this paper we use white noise theory to prove the existence of the occupation times of one-dimensional Brownian motion and provide an expression for the expected value of the occupation times.

Keywords: occupation times, Brownian motion, white noise analysis

1 Introduction

Technical textiles have attracted great attention to diverse branches of industry over the last decades due to their comparatively cheap manufacturing. By overlapping thousands of individual slender fibers, random fiber webs emerge yielding nonwoven materials that find applications e.g. in textile, building and hygiene industry as integral components of baby diapers, closing textiles, filters and medical devices, to name but a few. They are

produced in melt-spinning operations: hundreds of individual endless fibers are obtained by the continuous extrusion of a molten polymer through narrow nozzles that are densely and equidistantly placed in a row at a spinning beam. The viscous or viscoelastic fibers are stretched and spun until they solidify due to cooling air streams. Before the elastic fibers lay down on a moving conveyor belt to form a web, they become entangled and form loops due to the highly turbulent air flows. The homogeneity and load capacity of the fiber web are the most important textile properties for quality assesment of industrial nonwoven fabrics. The optimization and control of the fleece quality require modeling and simulation of fiber dynamics and lay-down. Available data to judge the quality, at least on the industrial scale, are usually the mass per unit area of the fleece.

Since the mathematical treatment of the whole process at a stroke is not possible due to its complexity, a hierarchy of models that adequately describe partial aspects of the process chain has been developed in research during the last years. A stochastic model for the fiber deposition in the nonwoven production was proposed and analyzed in [4, 5, 7, 10]. The model is based on stochastic differential equations describing the resulting position of the fiber on the belt under the influence of turbulent air flows. In [1] parameter estimation of the Ornstein-Uhlenbeck process from available mass per unit area data, the occupation time in mathematical terms, was done.

Definition 1.1. Let $X = (X_t)_{t \in [0, T]}$, $T > 0$, be a stochastic process and consider an interval $[a, b] \subset \mathbb{R}$. The occupation time $M_{T, [a, b]}(X)$ is defined as

$$M_{T, [a, b]}(X) := \int_0^T \mathbf{1}_{[a, b]}(X_t) dt = \int_0^T \int_a^b \delta_0(X_t - x) dx dt.$$

Here, $\mathbf{1}_{[a, b]}$ denoted the indicator function of the interval $[a, b]$ and δ_0 is the Dirac-delta distribution.

Formally, occupation times models the time the stochastic process spends inside the spatial interval $[a, b]$ during the time interval $[0, T]$. In terms of our physical model for the nonwoven production, the occupation time can be interpreted as the mass of fiber material deposited inside the interval $[a, b]$, i.e. the mass per unit area of the final fleece.

Motivated by the above mentioned problem, in this paper we study the occupation time of one-dimensional Brownian motion. In particular, we show that occupation times of one-dimensional Brownian motion is a white noise distribution in the sense of Hida.

Although it is possible to study the problem by classical probabilistic method, we use a white noise approach to generalize the concept also to higher dimensions in later research. Moreover, in future work an extension to more general process (e.g. with fractional Gaussian noise) is planned. In the next section we provide necessary background on the white noise theory. The main result together with its proof are given afterward.

2 White Noise Analysis

In this section we give background on the white noise theory used throughout this paper. For a more comprehensive discussions including various applications of white noise theory we refer to [8, 9, 12, 13] and references therein. We start with the Gelfand triple

$$\mathcal{S}(\mathbb{R}) \hookrightarrow L^2(\mathbb{R}) \hookrightarrow \mathcal{S}'(\mathbb{R}),$$

where $\mathcal{S}(\mathbb{R})$ is the space of real-valued Schwartz test function, $\mathcal{S}'(\mathbb{R})$ is the space of real-valued tempered distributions, and $L^2(\mathbb{R})$ is the real Hilbert space of all real-valued Lebesgue square-integrable functions. Next, we construct a probability space $(\mathcal{S}'(\mathbb{R}), \mathcal{C}, \mu)$ where \mathcal{C} is the Borel σ -algebra generated by cylinder sets on $\mathcal{S}'(\mathbb{R})$ and the unique probability measure μ is established through the Bochner-Minlos theorem by fixing the characteristic function

$$C(f) := \int_{\mathcal{S}'(\mathbb{R})} \exp(i\langle \omega, f \rangle) d\mu(\omega) = \exp\left(-\frac{1}{2}\|f\|_0^2\right)$$

for all $f \in \mathcal{S}(\mathbb{R})$. Here $\|\cdot\|_0$ denotes the usual norm in the $L^2(\mathbb{R})$, and $\langle \cdot, \cdot \rangle$ denotes the dual pairing between $\mathcal{S}'(\mathbb{R})$ and $\mathcal{S}(\mathbb{R})$. The dual pairing is considered as the bilinear extension of the inner product on $L^2(\mathbb{R})$, i.e.

$$\langle g, f \rangle = \int_{\mathbb{R}} g(x)f(x) dx,$$

for all $g \in L^2(\mathbb{R})$ and $f \in \mathcal{S}(\mathbb{R})$. This probability space is known as the real-valued white noise space since it contains the sample paths of the one-dimensional Gaussian white noise. In this setting a one-dimensional Brownian motion can be represented by a continuous modification of the stochastic process $B = (B_t)_{t \geq 0}$ with

$$B(t) := \langle \cdot, \mathbf{1}_{[0,t]} \rangle,$$

where $\mathbf{1}_A$ denotes the indicator function of a set $A \subset \mathbb{R}$.

In the sequel we will use the Gel'fand triple

$$(\mathcal{S}) \hookrightarrow L^2(\mu) := L^2(\mathcal{S}'(\mathbb{R}), \mathcal{C}, \mu) \hookrightarrow (\mathcal{S})^*$$

where (\mathcal{S}) is the space of white noise test functions obtained by taking the intersection of a family of Hilbert subspaces of $L^2(\mu)$. The space of white noise distributions $(\mathcal{S})^*$ is defined as the topological dual space of (\mathcal{S}) . Elements of (\mathcal{S}) and $(\mathcal{S})^*$ are known as *Hida test functions* and *Hida distributions*, respectively. Within this framework white noise can be considered as the time derivative of Brownian motion with respect to the topology of $(\mathcal{S})^*$. An important tool in white noise analysis is the S-transform which can be considered as the Laplace transform with respect to the infinite dimensional Gaussian measure. The S-transform of $\Phi \in (\mathcal{S})^*$ is defined as

$$(S\Phi)(\varphi) := \langle \langle \Phi, : \exp(\langle \cdot, \varphi \rangle) : \rangle \rangle, \quad \varphi \in \mathcal{S}(\mathbb{R}),$$

where

$$: \exp(\langle \cdot, \varphi \rangle) := C(\varphi) \exp(\langle \cdot, \varphi \rangle),$$

is the so-called Wick exponential and $\langle \langle \cdot, \cdot \rangle \rangle$ denotes the dual pairing between $(\mathcal{S})^*$ and (\mathcal{S}) . We define this dual pairing as the bilinear extension of the sesquilinear inner product on $L^2(\mu)$. The S-transform provides a convenient way to identify a Hida distribution $\Phi \in (\mathcal{S})^*$, in particular, when it is hard to find the explicit form for the Wiener-Itô chaos decomposition of Φ .

Theorem 2.1. [12]

1. The S-transform is injective, i.e. if $S\Phi(\varphi) = S\Psi(\varphi)$ for all $\varphi \in \mathcal{S}(\mathbb{R})$, then $\Phi = \Psi$.
2. If a stochastic distribution process $X : I \rightarrow (\mathcal{S})^*$ is differentiable, then $S \frac{d}{dt} X(t)(\varphi) = \frac{d}{dt} SX(t)(\varphi)$ for all $\varphi \in \mathcal{S}(\mathbb{R})$.

In the following we state a sufficient condition on the Bochner integrability of a family of Hida distributions which depend on an additional parameter.

Theorem 2.2. [11] Let $(\Omega, \mathcal{A}, \nu)$ be a measure space and $\lambda \mapsto \Phi_\lambda$ be a mapping from Ω to $(\mathcal{S})^*$. If

- (1) the mapping $\lambda \mapsto S(\Phi_\lambda)(\varphi)$ is measurable for all $\varphi \in \mathcal{S}(\mathbb{R})$, and
- (2) there exist $C_1(\lambda) \in L^1(\Omega, \mathcal{A}, \nu)$, $C_2(\lambda) \in L^\infty(\Omega, \mathcal{A}, \nu)$ and a continuous seminorm $\|\cdot\|$ on $\mathcal{S}(\mathbb{R})$ such that for all $z \in \mathbb{C}$, $\varphi \in \mathcal{S}(\mathbb{R})$

$$|S(\Phi_\lambda)(z\varphi)| \leq C_1(\lambda) \exp(C_2(\lambda)|z|^2 \|\varphi\|^2),$$

then Φ_λ is Bochner integrable with respect to some Hilbertian norm which topologizing $(\mathcal{S})^*$. Hence $\int_\Omega \Phi_\lambda d\nu(\lambda) \in (\mathcal{S})^*$, and furthermore

$$S\left(\int_\Omega \Phi_\lambda d\nu(\lambda)\right) = \int_\Omega S(\Phi_\lambda) d\nu(\lambda).$$

Let $0 < T < \infty$ and $B = (B_t)_{t \in [0, T]}$ be a one-dimensional standard Brownian motion. The corresponding Donsker's delta distribution is given by

$$\delta_0(B_t - x) = \delta_0(\langle \cdot, \mathbf{1}_{[0, t]} \rangle - x) = \frac{1}{2\pi} \int_{\mathbb{R}} \exp(i\lambda(\langle \cdot, \mathbf{1}_{[0, t]} \rangle - x)) d\lambda.$$

It has been proved that $\delta_0(B_t - x) \in (\mathcal{S})^*$. Furthermore, its S-transform is given by

$$S\delta_0(B_t - x)(\varphi) = \frac{1}{\sqrt{2\pi t}} \exp\left(-\frac{1}{2t}(\langle \varphi, \mathbf{1}_{[0, t]} \rangle - x)^2\right),$$

for any $\varphi \in \mathcal{S}(\mathbb{R})$. For details and proofs see e.g. [8, 12]. The Donsker delta distribution is an important research object in the Gaussian analysis. For example, it can be used to study local times, self-intersection local times, stochastic current and Feynman integrals, see e.g. [2, 3, 6, 14, 15, 18]. The derivatives of Donsker's delta distribution has been also studied in [16]. In [17] Donsker's delta distribution is analyzed in the context of stochastic processes with memory.

3 Main Result

Now we are ready to prove the main finding of the paper.

Theorem 3.1. *Let $B = (B_t)_{t \in [0, T]}$ be a one-dimensional standard Brownian motion and consider an interval $[a, b] \subset \mathbb{R}$. The occupation time*

$$M_{T, [a, b]}(B) := \int_0^T \int_a^b \delta_0(B_t - x) dx dt$$

is a Hida distribution.

Proof: It is apparent, at least formally, that occupation times can be obtained by integrating Donsker’s delta distribution with respect to the product measure on $[a, b] \times [0, T]$. In this regard we will use Kondratiev-Streit integration theorem (Theorem 2.2) to prove the statement. Observe that for any $\varphi \in \mathcal{S}(\mathbb{R})$

$$S\delta_0(B_t - x)(\varphi) = \frac{1}{\sqrt{2\pi t}} \exp\left(-\frac{1}{2t} \left(\int_0^t \varphi(s) ds - x\right)^2\right)$$

is a measurable function with respect to the product measure on $[0, T] \times [a, b]$. Now for any $z \in \mathbb{C}$ and $\varphi \in \mathcal{S}(\mathbb{R})$ we have

$$\begin{aligned} & |S\delta_0(B_t - x)(z\varphi)| \\ &= \left| \frac{1}{\sqrt{2\pi t}} \exp\left(-\frac{1}{2t} \left(\int_0^t z\varphi(s) ds - x\right)^2\right) \right| \\ &= \frac{1}{\sqrt{2\pi t}} \left| \exp\left(-\frac{1}{2t} (\langle z\varphi, \mathbf{1}_{[0,t]} \rangle - x)^2\right) \right| \\ &= \frac{1}{\sqrt{2\pi t}} \left| \exp\left(-\frac{1}{2t} (\langle z\varphi, \mathbf{1}_{[0,t]} \rangle^2 - 2x \langle z\varphi, \mathbf{1}_{[0,t]} \rangle + x^2)\right) \right| \\ &= \frac{1}{\sqrt{2\pi t}} \exp\left(-\frac{x^2}{2t}\right) \left| \exp\left(-\frac{1}{2t} \langle z\varphi, \mathbf{1}_{[0,t]} \rangle^2\right) \exp\left(\frac{x}{t} \langle z\varphi, \mathbf{1}_{[0,t]} \rangle\right) \right| \\ &\leq \frac{1}{\sqrt{2\pi t}} \exp\left(-\frac{x^2}{2t}\right) \exp\left(\frac{1}{2t} |\langle z\varphi, \mathbf{1}_{[0,t]} \rangle|^2\right) \exp\left(\left|\frac{x}{t} \langle z\varphi, \mathbf{1}_{[0,t]} \rangle\right|\right) \\ &= \frac{1}{\sqrt{2\pi t}} \exp\left(-\frac{x^2}{2t}\right) \exp\left(\frac{1}{2t} |z|^2 |\langle \varphi, \mathbf{1}_{[0,t]} \rangle|^2\right) \exp\left(\frac{|x|}{\sqrt{t}} \frac{|z|}{\sqrt{t}} |\langle \varphi, \mathbf{1}_{[0,t]} \rangle|\right) \\ &\leq \frac{1}{\sqrt{2\pi t}} \exp\left(-\frac{x^2}{2t}\right) \exp\left(\frac{1}{2t} |z|^2 |\varphi|^2 |\mathbf{1}_{[0,t]}|^2\right) \exp\left(\frac{x^2}{2t}\right) \exp\left(\frac{1}{2t} |z|^2 |\varphi|^2 |\mathbf{1}_{[0,t]}|^2\right) \\ &= \frac{1}{\sqrt{2\pi t}} \exp(|z|^2 |\varphi|^2). \end{aligned}$$

The first factor

$$C_1(t, x) = \frac{1}{\sqrt{2\pi t}}$$

is an integrable function on $[0, T] \times [a, b]$ while the second factor

$$C_2(t, x) = \exp(|z|^2 |\varphi|^2)$$

is a bounded function of t and x . Theorem 2.2 gives the desired result. ■

Corollary 3.2. *The S-transform of the occupation times of Brownian motion is given by*

$$SM_{T,[a,b]}(B)(\varphi) = \int_0^T \frac{1}{\sqrt{2\pi t}} \int_a^b \exp\left(-\frac{1}{2t} \left(\int_0^t \varphi(s) ds - x\right)^2\right) dx dt,$$

for any $\varphi \in \mathcal{S}(\mathbb{R})$.

Proof: Since $M_{T,[a,b]}(B) \in (\mathcal{S})^*$ then according to Theorem 2.2 for every $\varphi \in \mathcal{S}(\mathbb{R})$ it holds

$$\begin{aligned} SM_{T,[a,b]}(B)(\varphi) &= S \int_0^T \int_a^b \delta_0(B_t - x) dx dt(\varphi) \\ &= \int_0^T \int_a^b S \delta_0(B_t - x)(\varphi) dx dt \\ &= \int_0^T \int_a^b \frac{1}{\sqrt{2\pi t}} \exp\left(-\frac{1}{2t} \left(\int_0^t \varphi(s) ds - x\right)^2\right) dx dt \\ &= \int_0^T \frac{1}{\sqrt{2\pi t}} \int_a^b \exp\left(-\frac{1}{2t} \left(\int_0^t \varphi(s) ds - x\right)^2\right) dx dt. \blacksquare \end{aligned}$$

Corollary 3.3. *The expected value of the occupation times of Brownian motion is given by*

$$\mathbb{E}_\mu(M_{T,[a,b]}(B)) = \int_0^T \frac{1}{\sqrt{2\pi t}} \int_a^b \exp\left(-\frac{x^2}{2t}\right) dx dt.$$

Proof: The expected value with respect to the white noise measure of the occupation times of Brownian motion is obtained by taking the S-transform and evaluating the value at 0:

$$\begin{aligned} \mathbb{E}_\mu(M_{T,[a,b]}(B)) &= SM_{T,[a,b]}(B)(0) \\ &= \int_0^T \frac{1}{\sqrt{2\pi t}} \int_a^b \exp\left(-\frac{1}{2t} \left(\int_0^t 0 ds - x\right)^2\right) dx dt \\ &= \int_0^T \frac{1}{\sqrt{2\pi t}} \int_a^b \exp\left(-\frac{x^2}{2t}\right) dx dt. \blacksquare \end{aligned}$$

4 Conclusions

We give a mathematically rigorous meaning to the occupation times of a standard Brownian motion as a Hida distribution. An expression for the expected value for the occupation times is also obtained. For the application point of view it is desirable to have a more explicit form for the expected value. This will be done in the future work. We would like also to mention that our present result is limited to one-dimensional setting. For further research we plan to generalize the result to higher spatial dimensions.

Acknowledgements

The author would like to thank anonymous reviewers for their valuable comments and suggestions. Financial support from the Institute for Research and Community Service (LPPM) Universitas Sanata Dharma through research grant No. 017/Penel./LPPM-USD/IV/2022 is gratefully acknowledged.

References

- [1] W. Bock et al, "Parameter estimation from occupation times—a white noise approach," *Communications on Stochastic Analysis*, **26**(3), 29-40, 2014.
- [2] W. Bock, J. L. da Silva, and H. P. Suryawan, "Local times for multifractional Brownian motion in higher dimensions: A white noise approach," *Infinite Dimensional Analysis, Quantum Probability and Related Topics*, **19**(4), id. 1650026, 16 pp, 2016.
- [3] W. Bock, J. L. da Silva, and H. P. Suryawan, "Self-intersection local times for multifractional Brownian motion in higher dimensions: A white noise approach," *Infinite Dimensional Analysis, Quantum Probability and Related Topics*, **23**(1), id. 2050007, 18 pp, 2020.
- [4] T. Götz et al, "A stochastic model and associated Fokker-Planck equation for the fiber lay-down process in nonwoven production processes," *SIAM Journal of Applied Mathematics*, **67**(6), 1704-1717, 2007.
- [5] M. Grothaus et al, "Application of a three-dimensional fiber lay-down model to nonwoven production processes," *Journal of Mathematics in Industry*, **4**(4), 1-19, 2014.
- [6] M. Grothaus, F. Riemann, and H. P. Suryawan, "A White Noise approach to the Feynman integrand for electrons in random media," *Journal of Mathematical Physics*, **55**(1), id. 013507, 16 pp, 2014.
- [7] M. Herty et al, "A smooth model for fiber lay-down processes and its diffusion approximations," *Kinetic and Related Models*, **2**(3), 489-502, 2009.
- [8] T. Hida et al, "White Noise. An Infinite Dimensional Calculus," *Kluwer Academic Publisher, Dordrecht*, 1993.

- [9] Z.Y. Huang and J. Yan, "Introduction to Infinite Dimensional Stochastic Analysis," *Kluwer Academic Publisher, Dordrecht*, 2000.
- [10] A. Klar, J. Maringer, and R. Wegener, "A 3D model for fiber lay-down nonwoven production processes," *Mathematical Models and Methods in Applied Sciences*, **22**(9), 1-18, 2012.
- [11] Y. Kondratiev et al, "Generalized functionals in Gaussian spaces: The characterization theorem revisited," *Journal of Functional Analysis*, **141** article number 0130, 301-318, 1996.
- [12] H.H. Kuo, "White Noise Distribution Theory," *CRC Press, Boca Raton*, 1996.
- [13] N. Obata, "White Noise Calculus and Fock Space," *Springer Verlag, Berlin*, 1994.
- [14] H.P. Suryawan, "A white noise approach to the self intersection local times of a Gaussian process," *Journal of Indonesian Mathematical Society*, **20**(2), 111-124, 2014.
- [15] H.P. Suryawan, "Weighted local times of a sub-fractional Brownian motion as Hida distributions," *Jurnal Matematika Integratif*, **15**(2), 81-87, 2019.
- [16] H.P. Suryawan, "Derivative of the Donsker delta functionals," *Mathematica Bohemica*, **144**(2), 161-176, 2019.
- [17] H.P. Suryawan, "Donsker's delta functional of stochastic processes with memory," *Journal of Mathematical and Fundamental Sciences*, **51**(3), 265-277, 2019.
- [18] H.P. Suryawan, "Pendekatan analisis derau putih untuk arus stokastik dari gerak Brown subfraksional," *Limits: Journal of Mathematics and Its Applications*, **19**(1), 15-25, 2022.

This page intentionally left blank

Dijkstra Algorithm Implementation in Determining the Shortest Route of Industrial Gas Distribution in PT Tira Austenite Tbk Cikarang with Python Programming Language

Bernadetha Nathalia Fitra Soverenty¹, Cyrenia Novella Krisnamurti^{1,*}

¹*Department of Mathematics Education, Sanata Dharma University,
Yogyakarta, Indonesia*

**Corresponding Author: cyrenianovella@usd.ac.id*

(Received 23-06-2022; Revised 27-09-2022; Accepted 28-09-2022)

Abstract

Mathematics is used in various fields of human life, one of them is in the industrial field. In the field of industrial mathematics can be used in finding the shortest route in distributing industrial gas. Finding the shortest route was done using Dijkstra's algorithm and developing the Python programming language. The purpose of this study is to determine the shortest route on industrial gas distribution at PT Tira Austenite Tbk Cikarang using the Python programming language. This type of research is applied research. The results obtained from this study are the Python programming language that can be used to find the shortest route of industrial gas distribution and users only enter the starting point and endpoint data on the program.

Keywords: shortest route, industrial gas distribution, Dijkstra algorithm, Python

1 Introduction

Mathematics can be used in various areas of human life. The use of mathematics starts from simple things, such as home numbering, to complicated things, such as the application of mathematics to other sciences. One of the areas that use mathematics is the industrial field. Based on Law No. 5 of 1994 on industry, industry is an economic activity that manages raw materials, semi-finished goods, and finished goods into high-value goods of their use. Over time, the industrial field in Indonesia also began to develop. Industrial gases are one form of industrial development and the main gases available are Oxygen (O_2), Nitrogen (N_2), Carbon Dioxide (CO_2), Argon (Ar), Hydrogen (H_2), Helium (He), and Acetylene (C_2H_2)[1].

Industrial gas is widely used by various fields such as hospitals, universities, or other companies providing goods resulting in an increasing need for industrial gas. Therefore, there are various companies that offer industrial gas and one of them is PT Tira Austenite Tbk Cikarang. PT Tira Austenite Tbk Cikarang sells, produces, and distributes industrial gas. The company certainly expects all activities to run efficiently. Activities that are usually carried out by the company in distributing its products by delivering products to 4 to 5 consumers based on the same direction in one trip. Distribution activities can run more efficiently by searching for the shortest route to 5 consumers. The process of finding the shortest route can indicate that mathematical science is applied in human life. Finding the shortest route on PT Tira Austenite Tbk Cikarang which includes open companies can help in auditing the company's finances to estimate the fuel costs incurred.

The process of finding the shortest route can be done with a graph that will represent the travel map. The graph consists of 2 infinite sets, namely a blank set of dots ($V(G)$) and a set of lines ($E(G)$) [2]. Based on the type of line, the graph is divided into directional graphs and undirected graphs. Directional graph is a graph whose side has a direction while an undirected graph is a graph whose side has no direction [3]. In the representation of the graph of PT Tira Austenite Tbk Cikarang with consumers will be

used directional graphs. Directional graphs are used because on the map there is a one-way path. It will also use labeled graphs. A labeled graph is a graph whose lines are each line assigned a value or label [4].

When the representation of the travel map graph from PT Tira Austenite Tbk Cikarang with consumers has been formed, finding the shortest route can be done with various algorithms and one of them Dijkstra algorithm. Dijkstra's algorithm is an algorithm that uses the greedy principle that each step in choosing a minimum weight line then inserts it in the solution set [5]. The selection of this algorithm is based on its advantages, which are simple and have a good level of accuracy and produce the shortest route that is quite accurate [6]. During this time, the process of finding the shortest route is usually done manually without utilizing technology. However, over time technology is used to facilitate human life.

Python programming language can be used as one of the alternatives to help the process of finding the shortest route. In Python there are keywords, data types, and operators that can help keep programs running as commanded. Some keywords contained in Python such as `and`, `def`, `break`, `return`, and `global`. Then the data types contained in Python are integers, floating points, complexes, strings, lists, and tuples [7]. There are several operators in Python. The operators that assist in the process of mathematical calculations are arithmetic operators e.g. `+` which are useful for addition and `*` which are useful for multiplication [8]. Assignment operators are useful for placing data into variables, such as `=` to assign values in the right operand to left operands. Then the comparison operator is useful for comparing the left pass with the right pass. Comparison operators include `==`, `!=`, `>`, `<`, `>=`, and `<=`. While logic operators are useful for determining the true value of a value. Logical operators consist of `and`, `or`, and `not` [9]. The Python programming language was chosen because in addition to being free and easy to learn, the calculation results have a high level of accuracy so as to provide valid results on the program [10].

Based on the background that has been presented, the purpose of this study is to determine the shortest route in the distribution of industrial gases from PT Tira

Austenite Tbk Cikarang to 5 consumers with the most purchases of industrial gas in the most types of industrial gas sold in January 2020 to June 2021, namely PT Annisa Mitra Husada, PT Indocement Tunggul Prakarsa, Jiangxi Thermal Power Construction, PT Solusi Bangun Indonesia Tbk, and Universitas Kristen Indonesia with Python programming language.

2 Research Methodology

The type of research used is applied research. Applied research is conducted with the aim of applying, testing, and evaluating the ability of a theory applied to solve practical problems[11]. The study will apply Dijkstra's algorithm to determine the shortest route of industrial gas distribution to 5 consumers. The subject of this study is google maps which is useful in knowing the distance between PT Tira Austenite Tbk Cikarang and 5 consumers. Meanwhile, the object of this study is the route that connects every consumer in the distribution of industrial gas. This research method is a literature study to gather accurate information related to Dijkstra's algorithm and its application in determining the shortest route. The libraries used are reference books and scientific journals.

3 Results and Discussion

The process of distributing industrial gases from PT Tira Austenite Tbk Cikarang to PT Annisa Mitra Husada, PT Indocement Tunggul Prakarsa, Jiangxi Thermal Power Construction, PT Solusi Bangun Indonesia Tbk, and Universitas Kristen Indonesia there is a possibility not to be done every day. Therefore, 1 day is chosen which is the frequency of days most often distributed products to each consumer. Based on sales data from January 2020 to June 2021, the companies that most often distributed products on Mondays are PT Annisa Mitra Husada, PT Solusi Bangun Indonesia Tbk, and Universitas Kristen Indonesia. Meanwhile, for Wednesday is PT Indocement Tunggul Prakarsa and Jiangxi Thermal Power Construction and Friday is Jiangxi Thermal Power Construction.

Use of Python programming language in finding the shortest route of industrial gas distribution at PT Tira Austenite Tbk Cikarang using a GUI (Graphical User Interface) window. The use of a GUI can make it easier for users in the process to find the shortest route. The syntaxes used in creating the GUI window use the data types, keywords, and operators available in Python. The developed Python program will display a GUI window then it needs a tkinter module in its syntax.

The view that will be seen first by the user after the program in the run is a GUI window that has been created. In the GUI window contains several components that can help users in finding the shortest route. The components that will appear are like buttons. There are 3 buttons that users will see in the initial display, namely the ‘Hari Senin’, ‘Hari Rabu’, and ‘Hari Jumat’ buttons. The button corresponds to the day in the distribution of industrial gases. In addition, there is also a box for users to enter the starting point and endpoint and information for the user regarding the starting point and endpoint that can be entered in the box. Here's the initial view that the user will see.

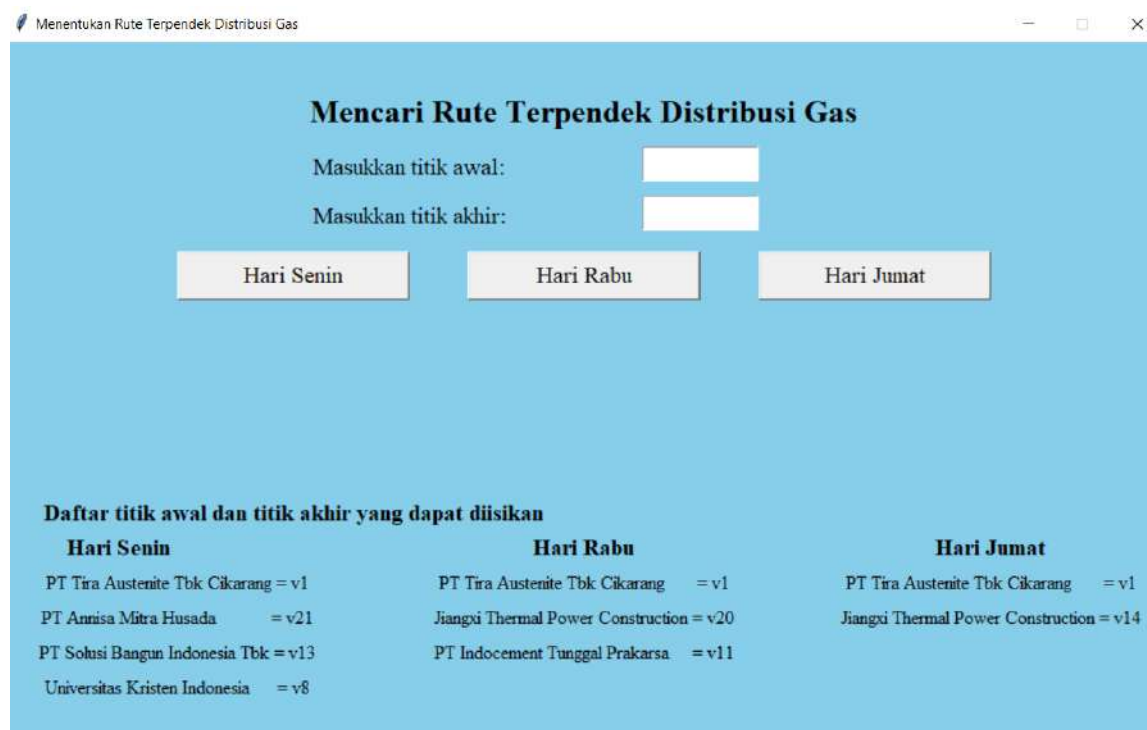


Figure 1. Program Start View

The user can enter the starting point and endpoint according to the information that has been provided. On the available information the starting point and the end point of

Monday, Wednesday, and Friday are different. This is due to the difference in the company that the distribution process does on each day. After the user fills in the starting point and endpoint, the user can press the ‘Hari Senin’, ‘Hari Rabu’, and ‘Hari Jumat’ buttons based on the shortest route to search. When one of the day buttons is pressed, the user will see results in the form of the length of the track and the route to be traversed. Here is one example when a user confuses v11 as the starting point and v20 as the endpoint and presses the ‘Hari Rabu’ button on the program.

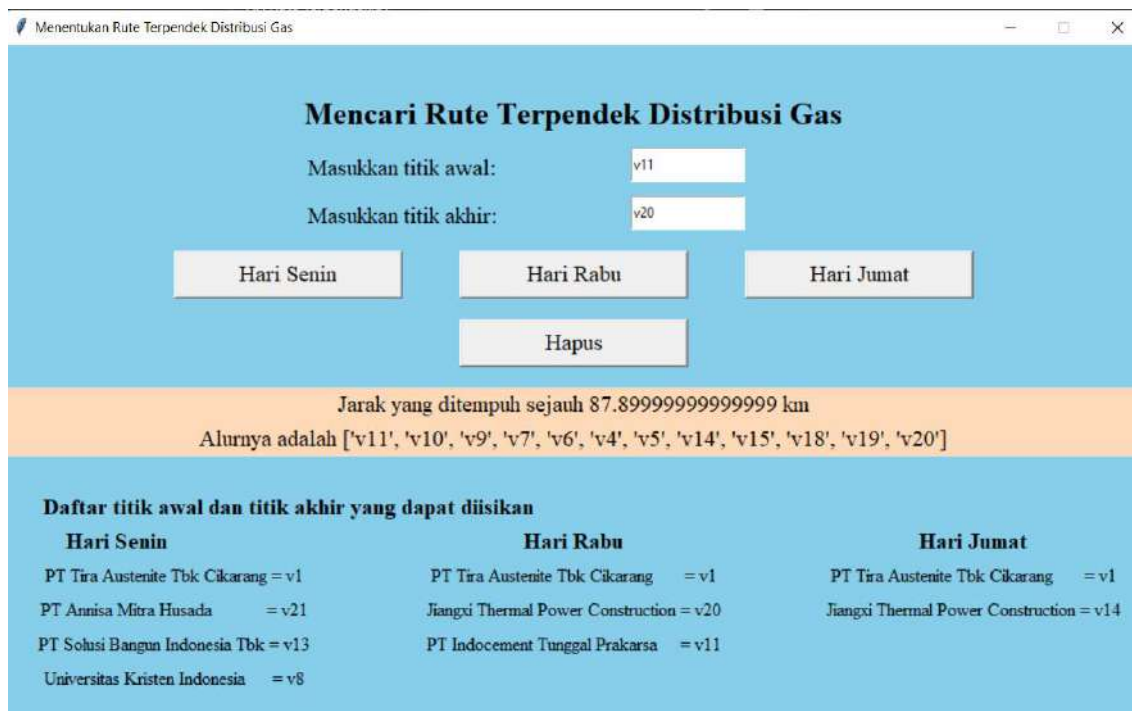


Figure 2. Program Running

This program was created to help and make it easier for users to find the shortest route. Therefore, users will be able to search for the other shortest routes with this program. Users can press the delete button when they want to delete the previous data and perform another shortest route search process. Here is the view that the user will see when pressing the ‘Hapus’ button.

The Python GUI program that has been created is proven to help users in finding the shortest route, especially in distributing industrial gases at PT Tira Austenite Tbk Cikarang. The results displayed are also in accordance with the results of manual calculations.

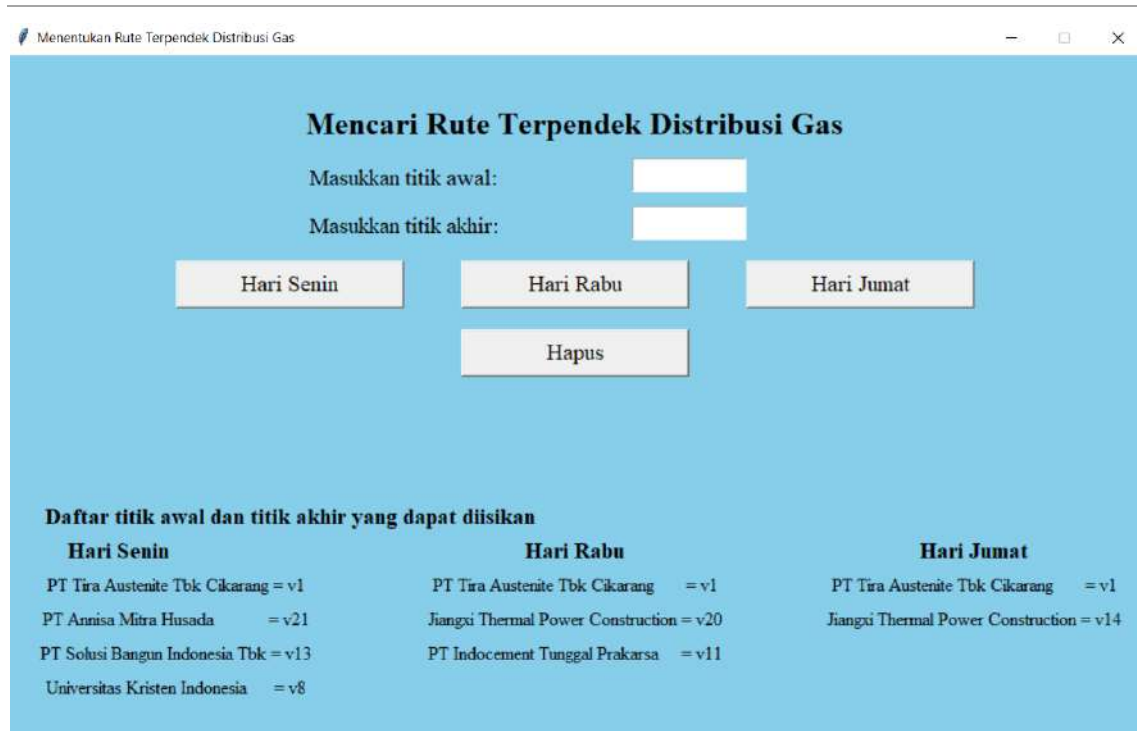


Figure 3. After Pressing the Delete Button

4 Conclusion

The Python programming language is utilized in the process of finding the shortest route of industrial gas distribution at PT Tira Austenite Tbk Cikarang with Dijkstra algorithm by developing GUI windows. GUI window development can make it easier for users to use programs and make the look more attractive. When the user will search for the shortest route can enter the starting point and endpoint on the program. Results will appear when the user presses the Day button which corresponds to the frequency of the day most often distributed to each consumer. Users can also search for other shortest routes without closing the GUI window by pressing the Delete button then all data will be deleted.

References

- [1] Irma Nuriska, "Penetapan Harga Gas Industri di Tinjau dari Undang-Undang Nomor 5 Tahun 1999 Tentang Larangan Praktek Monopoli dan Persaingan Usaha Tidak Sehat (Studi Kasus: Putusan Nomor 09/KPPU-L/2016)", *Doctoral dissertation*, Jakarta: Universitas Yarsi, 2018.

- [2] Jong Jek Siang, “Riset Operasi dalam Pendekatan Algoritmis”, Yogyakarta: CV Andi Offset, 2011.
- [3] D. Anggraeni, “Graf Berarah Fuzzy (fuzzy Digraf)”, *Mathunesa: Jurnal Ilmiah Matematika*, **2**(3), 2013.
- [4] K. S. Dewi, W. Wamiliana, M. Ansori, “Penentuan Banyaknya Graf Tak Terhubung Berlabel Titik Berorde Tujuh Tanpa Loop Loop”, *Jurnal Siger Matematika*, **2**(2), 77-89, 2021.
- [5] S. Andayani and E. W. Perwitasari, “Penentuan Rute Terpendek Pengambilan Sampah di Kota Merauke Menggunakan Algoritma Dijkstra”, *Semantik*, **4**(1), 2014.
- [6] R. R. Al Hakim, *et al.*, “Aplikasi Algoritma Dijkstra dalam Penyelesaian Berbagai Masalah”, *EXPERT: Jurnal Manajemen Sistem Informasi dan Teknologi*, **11**(1), 42-47, 2021.
- [7] H. Bhasin, “Python Basics A Self-Teaching Introduction”, *Virginia: Mercury Learning and Information*, 2019.
- [8] D. Amos, D. Bader, J. Jablonski, F. Heisler, “Python Basics: A Practical Introduction to Python 3”, Real Python, 2020.
- [9] J. P. Mueller, “Beginning Programming with Python for Dummies”, Kanada, John Wiley & Sons, Inc., 2018.
- [10] A. Hidayah, “Program Perencanaan Plat Beton Bertulang Berdasarkan SNI 2847-2013”, *Doctoral dissertation*, Universitas Muhammadiyah Surakarta, 2017.
- [11] Sugiyono, “Metode Penelitian Kuantitatif, Kualitatif, dan R&D”, Bandung, Penerbit Alfabeta, 2013.

An Enhanced Multi-Level Authentication Electronic Voting System

Ayodeji O.J Ibitoye^{1*}, Halleluyah O. Aworinde¹, Esther T. Adekunle¹

¹ *Computer Science Dept., Bowen University, Iwo, Osun State, Nigeria*
Corresponding Author: ayodeji.ibitoye@bowen.edu.ng

(Received 06-10-2022; Revised 01-11-2022; Accepted 14-11-2022)

Abstract

Originally, manual voting systems are surrounded with issues like results manipulation, errors and long result computation time, ineligible voters, void votes among others. Electronic voting system helped in overcoming the challenges with manual voting system, to engendered other problems of phishing, men in the middle attack alongside voter's impersonation. By these challenges, the integrity of an election results in a distributed system has become another top concern for e-voting system based on reliability. To achieve an improved voters' authentication and result validation with excellent user experience, here, a Facial Recognition Electronic Voting System that is power-driven by Blockchain Technology was developed. The entire election engineering activities are decentralised with improved security features to enhance transparency, verifiability, and accountability for each vote count. The self-service voting system was built by smart contract and implemented on the Ethereum network. The obtained reports and evaluations reflected a non-editable and self-sufficiently certifiable system for voting. It also has a competitive edge over fingerprint enabled e-voting system. Aside its excellent usability and general acceptance, the developed method discarded to a larger extent, intended fraudulent actions from election activities by eliminating the involvement of a middleman while facilitating privacy, convenience, eligibility and satisfactory voters' right.

Keywords: blockchain technology, facial recognition, electronic voting system, smart contracts, Ethereum network.

1 Introduction

The advent of democracy as a system of government, and the freedom of expression by the citizen through voting has become a norm in the process of selecting a leader all over the world. While, the right and power of citizen through voting without malpractice cannot be underestimated, voting remains a way of resolving conflicting and inconsistent viewpoints in major decision of policies and/or who leads over a period. Although the processes may be controversial, depending on the adopted voting system, yet the unruffled decision becomes communal after each electorate has express his/her opinion [1]. For Instance, candidates belonging to a political party are elected to the Local Government, State, Or Federal either for executive or legislative positions in Nigeria over a period. With fairness and existing democratic rule as factors for consideration, the voting processes and context remains an evolving domain from manual system to electronic with the goal of building a credible, verifiable, transparent and integrity driven e-voting system. While the electronic system of voting is also filled with potential possibilities of denial-of-service attack (DOS), server hacking, hardware malfunction, administrative manipulation among others, e-voting is being investigated widely, and countless operational models have been deployed and in used as stable solution for voters' freedom and right across multifaceted faces of the society.

By this development, e-voting remains the most optimal system of voting with capacity for innovative improvement on its shortfalls when compared with the manual systems of voting. Hence, the process of improving openness, vote privacy, invulnerability and verifiability, especially in a decentralised voting ecosystem is more important today as technology keeps improving in proportionate direction with cybercrimes [2]. In more recent times, blockchain technology has been adopted for secured and transparent processes. For instance, the number of groups actions irrespective of volume and currencies can be tracked clearly and in real time despite the dispersed wallets in Bitcoin. By this, a central authority is not required on a Point to Point based system and through the use of cryptographic approach, the system is kept secured and unbroken [3].

Therefore, in e-voting, a decentralised blockchain system with end-to-end encryption can be used to address vote tampering, while promoting vote tallying in real time. However, it is important to embed such e-voting systems with biometric or computer vision infrastructure in order to curb human generated challenges of ineligibility, verifiability and impersonation in an e-voting cycle of registration, validation, collection and tallying. Several biometric features such as fingerprint with blockchain technology has been used to build an e-voting system, the essence of this work is to fuse a facial recognition software with blockchain technology in e-voting system development. Thus, in section two (2), an overview of related works on e-voting system is presented. Section 3 discussed the multi-level e-voting system using facial recognition and Blockchain technology. Sample experimental evolutions and findings is presented in section four (4) before conclusion and recommendation in section five (5).

2 Sample Related Works

In a democratic system, voting remains an important tool for people to express their opinion regarding policies, choice of leadership and more. Over the years, different methods have been integrated to define a sustainable election process. Some of this include the use of paper wherein voters use pencil or thumb print on the preferred candidate. Then, an optical scanner [4] or hand counting is used in tallying, and results are computed on Microsoft Excel sheet or calculated using modern calculator in some instances. As the world evolve with technology, some countries still trust the paper ballot voting system either for its disadvantage in order to satisfy self-interest or genuinely due to problems of digital infrastructure, change process or its advantages. As the technologically growth spans, an electronic system for recording, storing and processing voters' data into digital form was developed. E-voting, as an instance uses digital ballot instead of the paper ballot; then, the entire voting cycle from registration to result computation is also performed electronically. For instance, a Direct Internet and Electronic (DRE) machines as a portable computer has been built for the exhibition of ballot choices from electronic recording votes. By pressing the touch screen, voters' decision is authenticated [5] and vote audit of recount has the case may be is possible through the Voter-Verified (or Verifiable) Paper Audit Trail (VVPAT). [6] also encoded fingerprints on smart card through secret splitting algorithm to develop an Electronic Biotechnology Voting System (EBTVS), for voter's verification.

Consequently, with the advent of blockchain technology, several e-voting systems have been developed overtime. [7] deployed an e-voting system, which uses a biometric device for validation during registration on a smart contract through an Ethereum network. The application explores the latent use of decentralised networks to audit and understand electoral procedures. Similarly, the application of blockchain technology for the deployment of a distributed e-voting system was appraised by [8]. It also recognised the legal and technological restrictions of using blockchain technology as a service for e-voting systems.

In the bid to advance the need for blockchain technology in e-voting, [9] encouraged electoral involvement through a decentralised blockchain technology; the solution addresses vote tampering, upheld transparency in vote cast while protecting the voters. Indeed, as the call for a decentralised voting system heightens, [10] projected a decentralised e-voting system with blockchain. The developed two-level architectural system provided a safe voting process that is exclusive of redundancy. The application also ensured that necessary voting criteria are satisfied for an anonymous but transparent vote count. Subsequently, a permission driven multichain platform for voting was developed by [11]. The software allows a distinct administrator to arrange the Blockchain based desired specification while voter's distinctiveness was confirmed through a fingerprint recognition system to secure vote cast. Aside, a crypto-voting system by [12] through two linked blockchains, [13] provided requisite information to voters on the difficulties and risk associated with blockchain e-voting system through an Architecture Trade-off Analysis Method (ATAM). Computational cryptographic trust has proven to be more reliable than human trust in voting. By this and more, smart contract was also deployed by [14] with to goal to address challenges with voting accuracy, security and privacy. Futhermore, hashing was deployed by [15] to ascertain that each vote count while preserving the anonymity of the voter. This is related to the electronic voting protocols by [16], whose system ensures the security of the identity of every voter while recorded vote results are tamper-proof. No doubt, Blockchain technology has continued to provide positive support for e-voting system with fingerprint technology. It is secured from human corruption, however, due to the fallouts of fingerprint technology and the fast adoption of facial recognition systems, a blockchain distributed facially recognised e-voting system is presented in section three (3) for consideration.

3 Multi-level Authentication E-voting System

The object detection model used here is YOLO V3. The raspberry pi, due to its limited computing power, cannot be used to implement the original YOLO model. Hence, we use YOLO Tiny, a tiny and yet efficient version of YOLO. For the datasets we used Google’s open images dataset V6. To train the model, we have to set the number of batches for the datasets so as to determine the iteration of training the model. The ideal number of iterations should be 2000 batches per number of objects. In our case we are dealing with 7 objects so the batches should be 14,000. While the model is training the prime objective of the algorithm is to decrease the average loss. We started with average loss of 4.5 and reached to an average loss of 1.08. Figure 1 shows the graph depicting the decrease in average loss as the number of iteration increases.

The electronic facial recognition e-voting system uses Ganache blockchain technology to manage voters and administrative activities in a voting cycle. The voting procedures are deployed using Smart contract on an Ethereum network (Blockchain). The architecture of this system as presented in Figure one (1) showed how several modules of the system synergises to attain the goal of authentic, verifiable, invulnerable, convenience and transparent voting system.

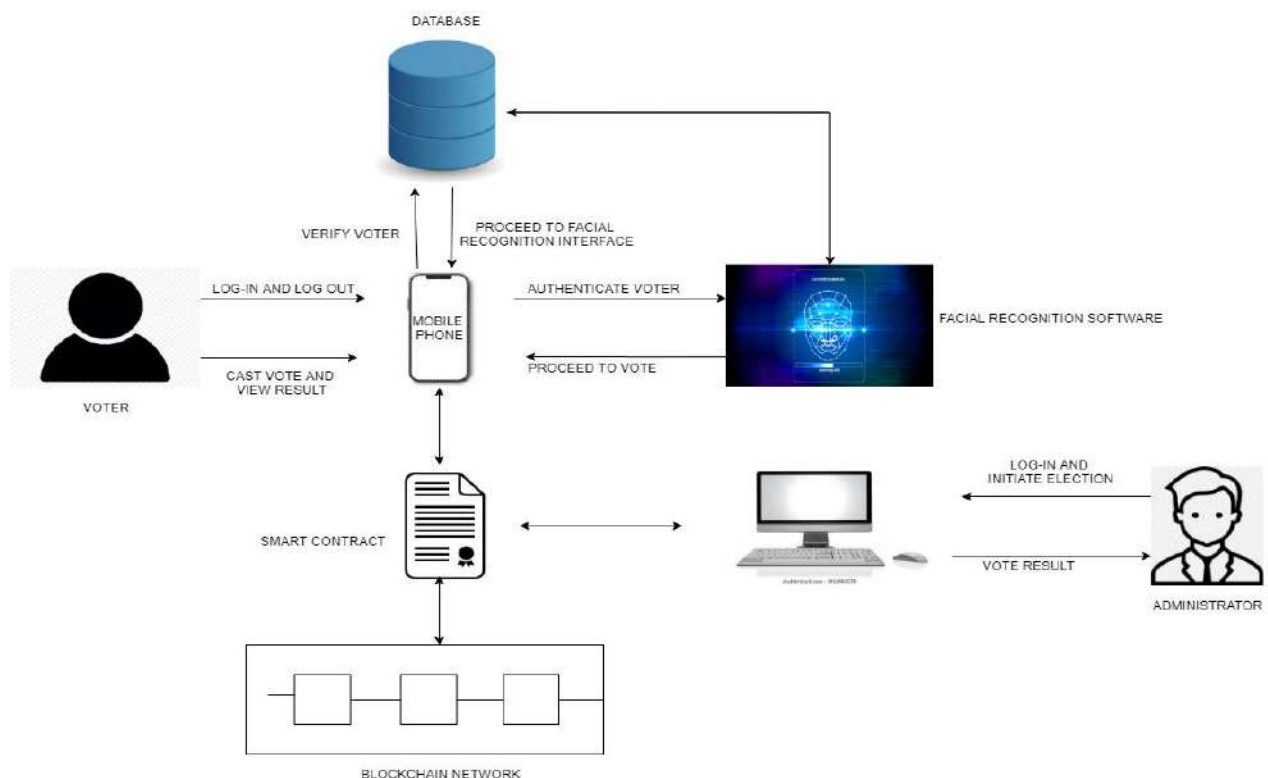


Figure 1. Facial Recognition E-voting System Using Blockchain

Initially, from the available dataset, voters who do not satisfactorily meet the voting criteria were eliminated to avoid data repetition and inconsistency. Then, 215 voters with the right voting criteria validated their preregistered information to obtain an Ethereum private key as a vote accreditation certificate. At this instance, multiple user images were captured from different angles for a more detailed training set. By this, the voters' data, which also included their faceprint are matched and stored in the database. From Figure one above, the face geometry, which included the users, length of the jawline, the form cheekbones, the depth eye sockets, and more were captured and analysed, using the Local Binary Pattern (LBP) algorithm. In order to vote, the voter's login to the mobile application; first, with the unique username and password before validating the user face with the embedded LBP facial recognition algorithm as a two-factor authentication procedure.

Sequel to the existing training and preprocessing procedures for registered images, the face of the voter is scanned to ascertain a matching degree from the array of images in the database whenever the voting system is being used, as the voters face is presented, the following procedures takes effect:

1. LBPs are extracted before the resulting histograms from each of the cells are weighted and concatenated differently just like the training data.
2. k-NN (with $k=1$) is subsequently performed with the x^2 distance with the goal of finding the closest face in the e-voting training data.
3. The user face print is associated with the smallest x^2 distance in the final classification if found.

These extracted features as further illustrated in Figure two (2) is packaged to activate face remembrance at every authentication and validation protocol call. This is possible through direct conversion of facial analog information to a digital equivalence tagged faceprint. Then, features are extracted from the faces through vector point analysis before the classification is obtained. While each faceprint is unique to an individual just like the thumbprint, face validation activities are executed to match and compare the users face with the stored information during capturing for further decision

support before a voter or administrator access the developed e-voting system. Therefore, if there exists a match, the voter is granted approval to cast a vote by choosing the choice candidate then clicking the button “Vote”. In addition, voters can also ascertain that his/her vote decision is not manipulated in an ongoing electoral process. Once schedule election period is over, vote collection takes place before tallying. Then, the Administrator announces the vote results with satisfactory evidence.

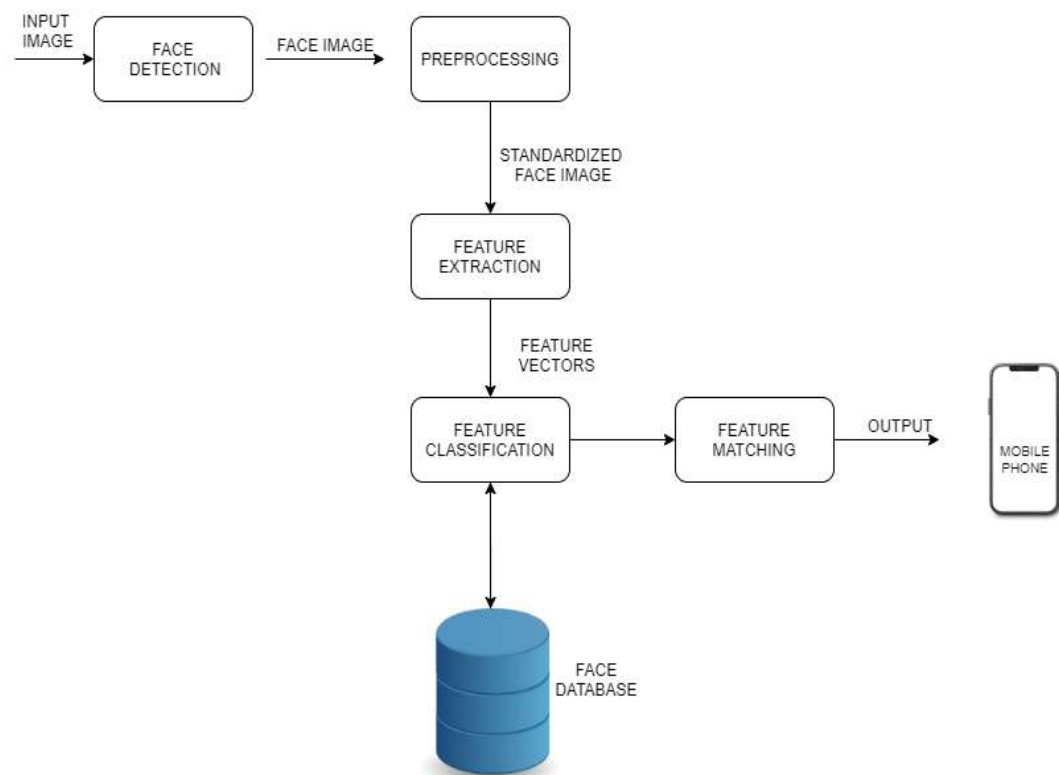


Figure 2. Block Diagram of a Facial Recognition System.

4 Evaluation Report

The developed blockchain e-voting system with face recognition achieved excellence when evaluated based on the principles of:

- a. **Eligibility:** The ability to allow only registered voters to vote just once based on the defined electoral procedures. Thus, with the two-factor authentication, only authorised voters can access the voting system.

- b. **Privacy:** The ability to leverages cryptographic properties of blockchain towards ensuring that each vote is kept secret through vote hashing.
- c. **Verifiability:** The ability of a voter to track vote statues in the tallying system through the unique Ethereum ID
- d. **Convience:** The ability of an eligible voter to vote easily without biases or discrimination
- e. **Usability:** The ability to measure how well a user can use the application based on process and design flow.

The following analysis as presented in Figure 3 is obtained

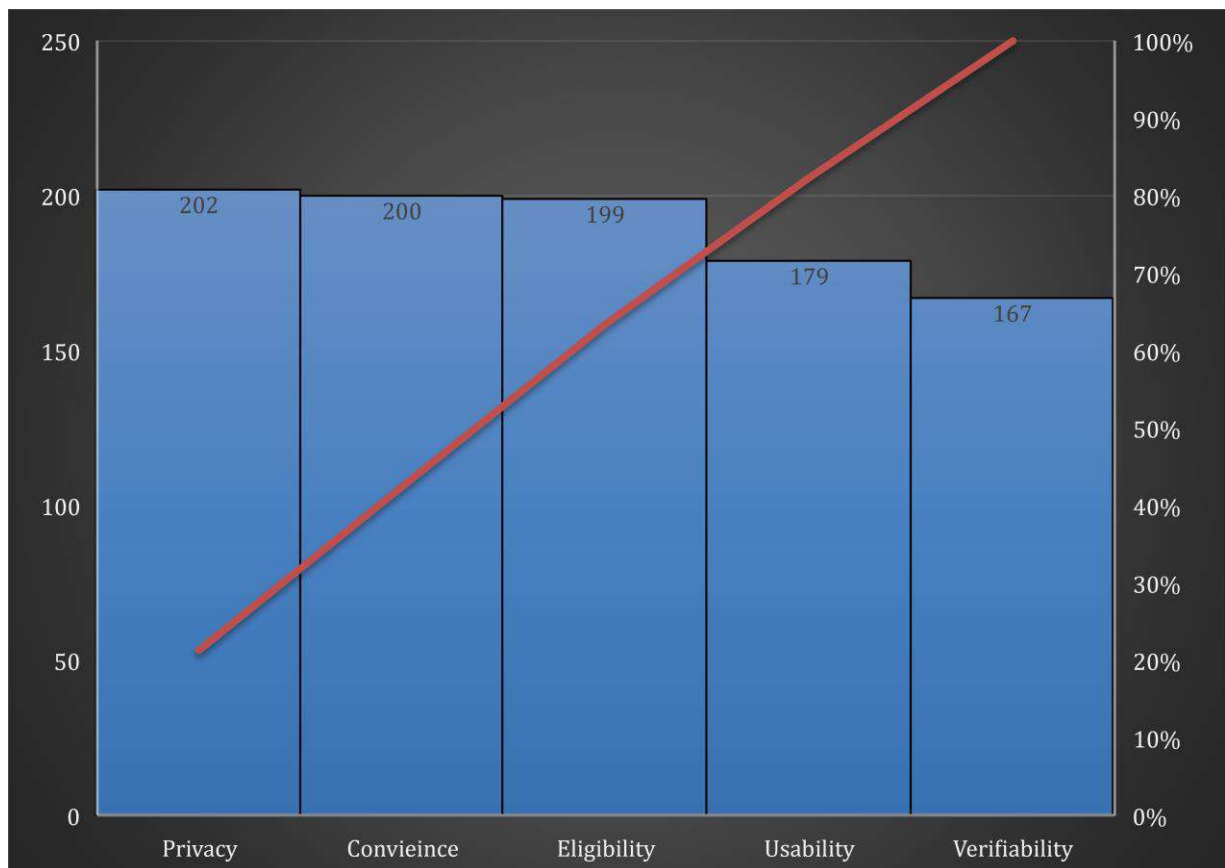


Figure 3. Sample Voters Evaluation Report

Overall, the Facial Recognition voting system also helped in resolving the challenge of varying fingerprint patterns, which cannot be recreated or rendered. In addition, with

the new normal where people are encouraged to touch less, a self-service remote face ID verification can be achieved. However, voters disguising or wearing face shield remains a challenge for future development and not within the scope of this research activities.

5 Conclusion

Overall, the Facial Recognition voting system also helped in resolving the challenge of varying fingerprint patterns, which cannot be recreated or rendered. In addition, with the new normal where people are encouraged to touch less, a self-service remote face ID verification can be achieved. However, voters disguising or wearing face shield remains a challenge for future development and not within the scope of this research activities.

References

- [1] Y. Xie, “Who Over reports Voting?”, *J J.Am.Polit.Sci.Rev.* **80**, 613–624, 2017.
- [2] C. Ayo, O. Daramola, A. Azeta, “Developing A Secure Integrated E-Voting System”, In *Handbook of Research on E-Services in the Public Sector: E-Government Strategies and Advancements*, IGI Global, USA, 278–287, 2011.
- [3] S. Nakamoto, “Bitcoin: A Peer-to-Peer Electronic Cash System” Available: <https://bitcoin.org/bitcoin.pdf>, 2009.
- [4] M. Rockwell, “Bitcongress – Process for block voting and law”, Available: <http://bitcongress.org/> [Accessed: December 2017].
- [5] A. Ndem, “Three risks posed by electronic voting - The Election Network”, Available: <http://theelectionnetwork.com/2018/10/25/three-risks-posed-by-electronic-voting/>, 2018.
- [6] O.O Adeosun. Ayodeji O.J. Ibitoye, J.O Alabi, “Real Time E-Biotechnology Voting System; Using Secret Splitting”, *International Journal of Electronics Communication and Computer Engineering*, **6**(6), 2015.
- [7] A. Benny, “Blockchain based E-voting System”, *SSRN Electronic Journal*, 2020.

- [8] F. P. Hjalmarsson, G. K. Hreioarsson, M. Hamdaqa, G. Hjalmtysson, “Blockchain-Based E-Voting System”. *IEEE International Conference on Cloud Computing, CLOUD, 2018-July*, 983–986., 2018.
- [9] H. V. Patil, K. G. Rathi, M. V. Tribhuwan, Science, C., College, D. Y. P. A. C. S., “A Study on Decentralized E-Voting System Using Blockchain Technology”, *International Research Journal of Engineering and Technology (IRJET)*, **5**(11), 48–53, 2018.
- [10] K. Isirova, A. Kiian, M. Rodinko, A. Kuznetsov, “Decentralized electronic voting system based on blockchain technology developing principals”, *CEUR Workshop Proceedings*, 2608, 211–223, 2020.
- [11] K. K. Sharma, J. Raghatwan, M. Patole, V. M. Lomte, “Voting system using multichain blockchain and fingerprint verification”, *International Journal of Innovative Technology and Exploring Engineering*, **9**(1), 3588–3597, 2019.
- [12] F., Fusco, M. I. Lunesu, F. E. Pani, A. Pinna, “Crypto-voting, a blockchain based e-voting system”, *IC3K 2018 - Proceedings of the 10th International Joint Conference on Knowledge Discovery, Knowledge Engineering and Knowledge Management*, **3**, 223–227, 2018.
- [13] D. Thebus, O. Daramola, “E-voting System for National Elections Using a Blockchain Architecture”, In *Pan African International Conference on Science, Computing and Telecommunications Book of Proceedings*, University of Swaziland, Kwaluseni, Swaziland, 2019.
- [14] K. Sadia, M. Masduzzaman, R. K. Paul, A. Islam, “Blockchain Based Secured E-voting by Using the Assistance of Smart Contract”, 2019.
- [15] R. Suganya, A. Sureshkumar, P. Alaguvathana, S. Priyadharshini, K. Jeevanantham, “Blockchain Based Secure Voting System Using IoT”, *International Journal of Future Generation Communication and Networking*, **13**(3), 2134–2142. 2020.
- [16] C. C. Z. Wei and , C. C. Wen, “Blockchain-based electronic voting protocol”. *International Journal on Informatics Visualization*, **2**(4–2), 336–341, 2018.

Appropriate Technology-Based Project-Based Learning: 3D Printing Utilization for Learning Media Class

Monica Cahyaning Ratri^{1*}

*Chemistry Education Study Program, Faculty of Teacher Training and Education,
Sanata Dharma University, Yogyakarta, Indonesia*

**Corresponding Author: monicacahyaningr@usd.ac.id*

(Received 01-10-2022; Revised 04-11-2022; Accepted 07-11-2022)

Abstract

Indonesia has more than ten thousand islands, making it an archipelago; therefore, the distribution of learning media and facilities over the country is difficult. This condition may affect the learning material delivery and the student's understanding. Thus, the *do-it-yourself* (DIY) learning media helps to overcome this condition. We investigated the usefulness of applying appropriate technology through the 3D printing technique to fabricate learning media inspired by local wisdom to meet the needs of learning media. The students were guided by a project-based learning (PjBL) method to find the problem, design their learning media, fabricate it using a 3D printer, and expected to be applied to deliver the teaching material in the class. This study aimed to observe the implementation of the designing process based on theory to reality. A qualitative method and questionnaire were used to measure student's responses. We found that PjBL learning based on a 3D printing project increases students' motivation through creativity and effectiveness in delivering the teaching materials.

Furthermore, 3D printed-based learning media can easily be fabricated, producing less waste.

Keywords: actuators and sensors, TCP socket, object detection

1 Introduction

Indonesia is a country with more than ten thousand islands, well known as one of the biggest archipelagos. Not only is the island huge, but the population of more than 275 million people also vary with various background and ethnic group, making it so diverse. Regional autonomy was chosen for the government system to maximize regional potential. Several problems arise due to those conditions in the education system and facilities.[1, 2] As the number of islands and the population wider, it will not be easy to even out the education facilities over the country.

Education is one of the crucial aspects of achieving a better society.[3] However, that stage remains challenging with the various ethnic backgrounds in Indonesia. The limited access to education facilities, the shortage of capable teachers, problems in the curriculum, and a high tuition fee to afford for most Indonesian are the challenging problems that need to be solved.[4-6] The solution should be found at the moment to solve that recent problem. Thus, education goals in Indonesia are soon to be achieved.

Chemistry is a mandatory subject that has to be taken during high school in Indonesia. Thus, the understanding of chemistry subject is one of the essential capabilities, even though chemistry has many abstract concepts.[7, 8] The structure of the compound is an example of the abstract phenomena in chemistry which has to be implemented in real life.[9] Therefore, the strategy to give a deep understanding of this matter is crucial. Moreover, chemistry subject also requires the student to recognize and capture the abstract molecule model of the compound. Hence, unlimited visualizing of abstract models is needed.[10] In chemistry, the boundary in the visualizing ability of students on abstract phenomena could be helped with the 3D imaging software using the computer or adjustable do-it-yourself (DIY) media.

The likelihood of media visualizing the abstract concept in chemistry is preferable in delivering teaching material to achieve a deep understanding. Learning media plays a significant role in making abstract matter more real in teaching and learning, particularly. The effectiveness and efficiency of achieving learning objectives are increased with the involvement of learning media.[11] Chemistry is not a subject that is easy to be explained only verbally; however, the visuals also will help in the explanation of the new and novel ideas in chemistry. [12] Visual media help student to make the idea more accessible than the textbook material.[13] Based on those understanding, a recent learning media which can help students to increase the reality of the concept by involving the local wisdom to prevent the problem of the needed material and that easily made is necessary this recent time. Thus, the learning media not only help the student to understand more about the abstract concept, moreover help the teacher to visualize the theoretical ideas.

The problem in transportation to connect one island to another in Indonesia affects the mobility of school facilities such as learning media. Therefore, a new strategy, on-site fabrication learning media by utilizing local wisdom and appropriate technology, is required. Appropriate technology emerges as the new end-use product based on society's need with the integrated system.[14] The need for a product from the area is gathered into one data and based on that, a new design to fulfill the need is made. The fabrication of the designed product follows this, and the product is sent and able to be used by people, in this case, students.[15] 3D printing is the implication of appropriate technology able to meet the needs of learning media based on local wisdom. 3D printing is a process of fabrication of 3D design of the digital model and can be processed by various 3D printer type, layer by layer to make 3D object by joined and solidified with a computer.[16] The 3D printing technique allows the fabrication of complex designs easily with less waste.

In order to figure out the solution to the problem mentioned above, we designed a project-based learning (PjBL) activity in the learning media class. PjBL allows the student to look for the solution to the problem they face and design a plan to solve it.[17] Thus, the students could creatively create a new learning media based on local wisdom and the subject's needs using 3D printing technology. We investigate the

effectiveness of the application of the 3D printing technique in the learning media class on the fabrication of learning media. The students' motivation and response were measured with the questionnaire through the google form. The students' response mentioned that learning media fabrication through PjBL with 3D printing was easy to design, fabricate, and maintain, and they thought that this learning media helps deliver teaching material in chemistry subject.

2 Research Methodology

The sample was one class of students in the learning media class, Chemistry Education study program, Sanata Dharma University, Yogyakarta. We used PjBL-based research with six steps approach.[18] We took 5 weeks to conduct this project. During the first meeting, students were introduced to the 3D printing technique, the basic information about a cartesian 3D printer used for this project, and the basic information about the 3D design software. Then, we applied the PjBL learning method in this class and gave the students project to be solved by utilizing the 3D printer to make DIY learning media. Students were allowed to identify the problem in learning material delivery that could be solved with the learning media.

The students were encouraged to find the problem in delivering the teaching material in high school chemistry subject as the first step. The second step was making a plan to solve the problem they found. The third step was scheduling the project, followed by students' weekly reports. Then, the student presented their results in the student exhibition, and the final step was reflections. The project started with the fabrication of the learning media based on students' findings. The first fabrication step was designing the learning media inspired by local wisdom into 3D digital design using Tinkercad. Then it was followed by a printing process using the 3D printer Ender 3 Pro with polylactic acid (PLA) filament as material. Weekly reports were mandatory to be handed to the teacher by students to control the students' progress, and discussion was opened during this time. After all, were done, the student had to present their result in an exhibition and explain the function and purposes of their learning media. In the end, we did the class reflection to reflect on our findings after we finished the project.

The effectiveness of this project was measured by a questionnaire, including the student motivation, the easiness of the fabrication, and their response to the potential application. The questionnaire was given to the student through Google form after all the processes were completed; thus, the student's response was based on their experience.

3 Results and Discussion

Appropriate technology named with 3D printing technique was chosen for DIY learning media fabrication due to the simple instrument and its fabrication effectivity. Moreover, a 3D printer which is a relatively small instrument, only needs PLA filament as the material and is easy to travel to many places, even rural areas. Indonesia is an archipelago with a transportation problem to reach the rural area; however, it has prodigious local wisdom that inspires DIY learning media fabrication. In reference to those reasons, we conducted the study by applying the PjBL method to measure the effect of the application of appropriate technology on student motivation and the effectiveness of teaching delivery of chemistry subjects.

The research steps are presented in Figure 1, and the step started with a discussion on finding the problem. After students find the problem in delivering chemistry teaching material, then students make a plan to solve those problems. The solution involved the 3D printing in creating the new learning media. The scheduling project is the next step to continue the plans. After starting the fabrication step using 3D printing, students have to report their progress weekly to control the project's progress. The next step is after students complete their project; they present their results in the student exhibition (Supplementary Figure 1), followed by students' reflections. The reflection was then conducted to complete the step in this cycle and to, recall their experience during the project and share their motivation and the effectiveness of the 3D printing-based learning media.

In the last step, which was the reflection, the questionnaire was included on it. There were two parts of the question in the questionnaire about fabrication and the potential application of 3D printed learning media. The first part was about the students'

responses on the fabrication, and the student's responses on the application were in the second part. The questions in every part are listed below:

1. Fabrication of learning media based on 3D printing is easy to design
2. Fabrication of learning media based on 3D printing trigger the creativity
3. Fabrication of learning media based on 3D printing is easy to fabricate
4. Fabrication of learning media based on 3D printing is easy to handle the waste
5. Fabrication of learning media based on 3D printing is easy to maintain
6. Application of learning media is maintainable (easy to maintain)
7. Application of learning media is usability (easy to operate and use)
8. Application of learning media is reusable
9. Application of learning media is effective and efficient
10. Application of learning media is the easy to delivered teaching material

Students' feedback was then collected and analyzed.

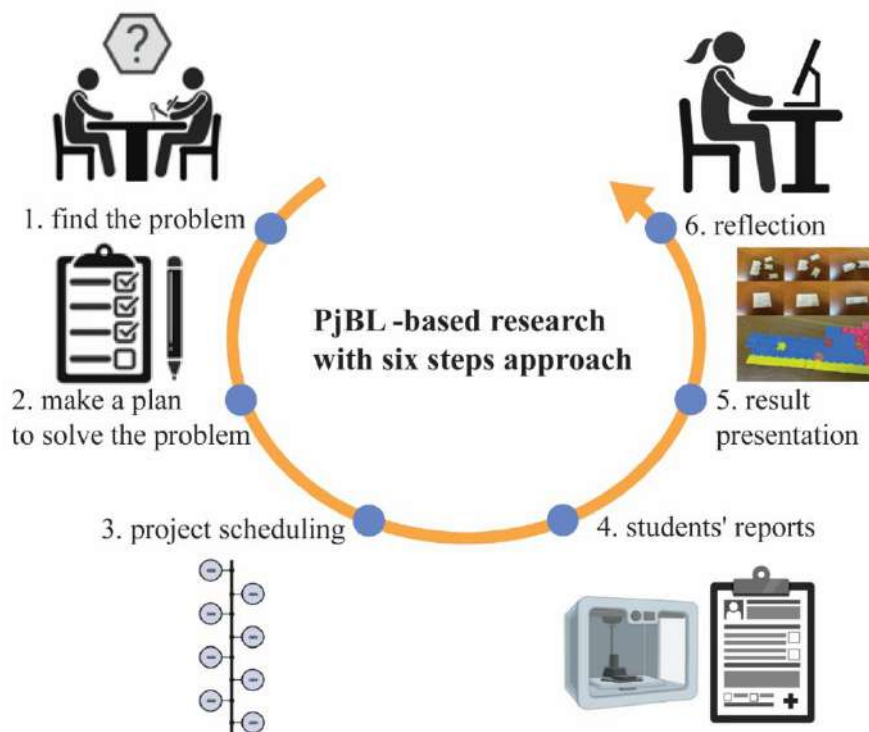


Figure 1. The experimental step on applying PjBL-based research with the six-step approach to measure the effectiveness of applying appropriate technology on the student's motivation and teaching material delivery.

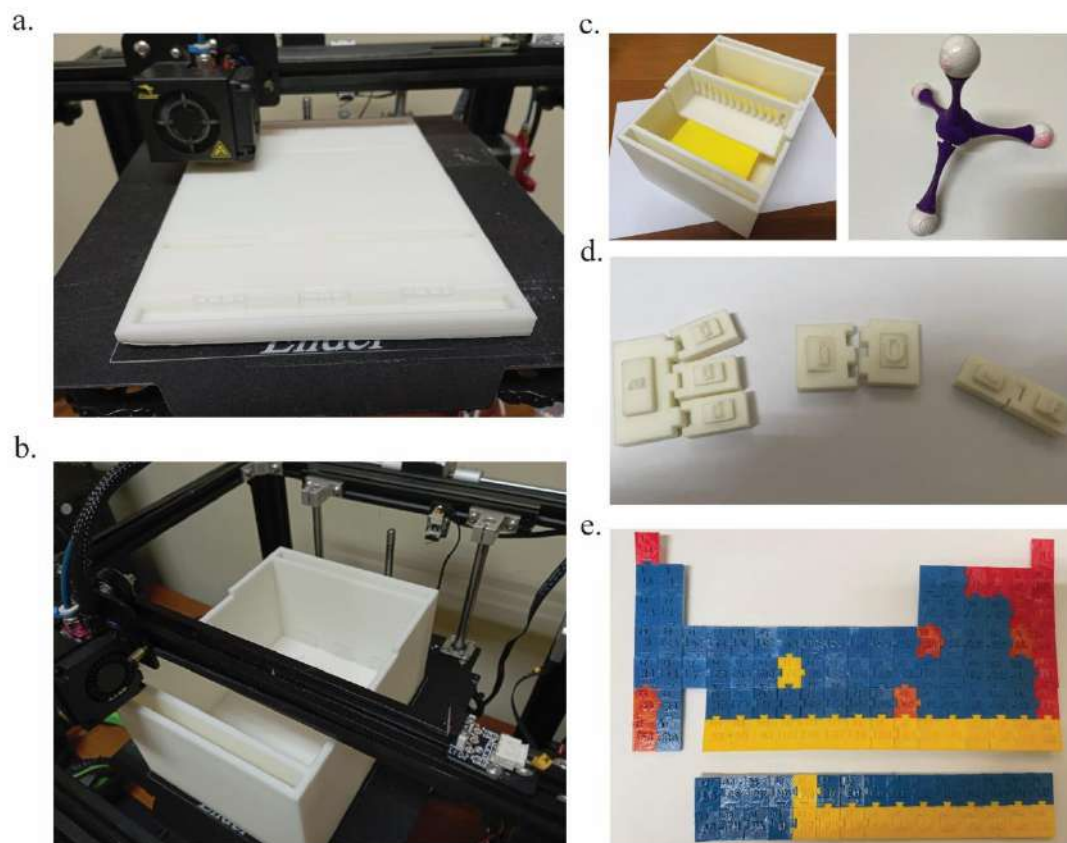


Figure 2. The printing process and 3D printed product for learning media. **a** and **b** are the printing process using the cartesian 3D printer for learning media products. **c.** 3D printed resemble electrophoresis instruments and molymod. **d.** 3D printed puzzle ionic bond and **e.** 3D printed embossed-periodic system of elements with specific colors based on their properties.

The PjBL cycle was conducted for 5 weeks. Students were given a chance to finish their projects and report their progress weekly on the learning management system (LMS) site. The report was needed to control the progress of students, and the teacher was able to discuss and give suggestions if needed. Figure 2 a and b show the fabrication process of learning media using a 3D printing technique that made a 3D learning media resemble electrophoresis instruments layer by layer using a cartesian 3D printer. The finished 3D printed learning media are shown in the Figure 2 c, d and f. In the Figure 2c, a resembling 3D electrophoresis instrument and molymod can be seen. A

resembling 3D electrophoresis instrument is useful for explaining the electrophoresis process to students. Molymod also helps the teacher to explain the abstract concept of the molecular structure of the molecule to students. A 3D shape and visual presentation allow the students to construct an abstract concept to be more realistic; therefore, students' understanding can be enhanced.[19] The 3D-printed puzzle ionic bond is shown in Figure 2d. The puzzle is a traditional game in Indonesia; inspired by this local wisdom, the puzzle is aimed at giving the student another alternative in the learning process. The puzzle gaming method in delivering ionic bond topic potential to help students to heighten their motivation and learning result. [20] The 3D-printed embossed-periodic table of elements is shown the Figure 2e. The 3D embossed-periodic table of elements with specific colors based on their properties aimed to strengthen students' understanding of the difference of elements' properties visually.

The fabrication of learning media was governed by appropriate technology using the 3D printing technique. In the application of appropriate technology, we have to consider several things, such as the effectiveness of the technique in fulfilling the need, the easiness of fabrication, and also waste handling. Thus, the student's opinion of this technology should be known by surveying through the questionnaire. The student's response to this fabrication technique is presented in Figure 3. Based on the survey, students said the 3D printer was easy to maintain. Therefore, the 3D printer is usable in many places, even with minimal facilities, as long as electricity is provided. PLA filament was used as the material due to its affordability; PLA is a degradable biopolymer that is harmless to the environment.[21] Based on the survey, students said that the waste of this fabrication was easy to handle due to its biodegradability. 80% of students said the fabrication step was easy, and the rest said that it was difficult. This finding explains that student has a different level of motivation. Thus, the responses were different. All students agreed that this project motivated them by triggering their creativity. Students were obligated to solve the problems by creating learning media based on 3D printing inspired by local wisdom. Furthermore, a 3D electronic design was required for working with a 3D printer; therefore, students must learn how to make a 3D design based on their needs. Even though 10% of students agree that designing 3D objects was not easy, most students agree that the 3D design was easy to make.

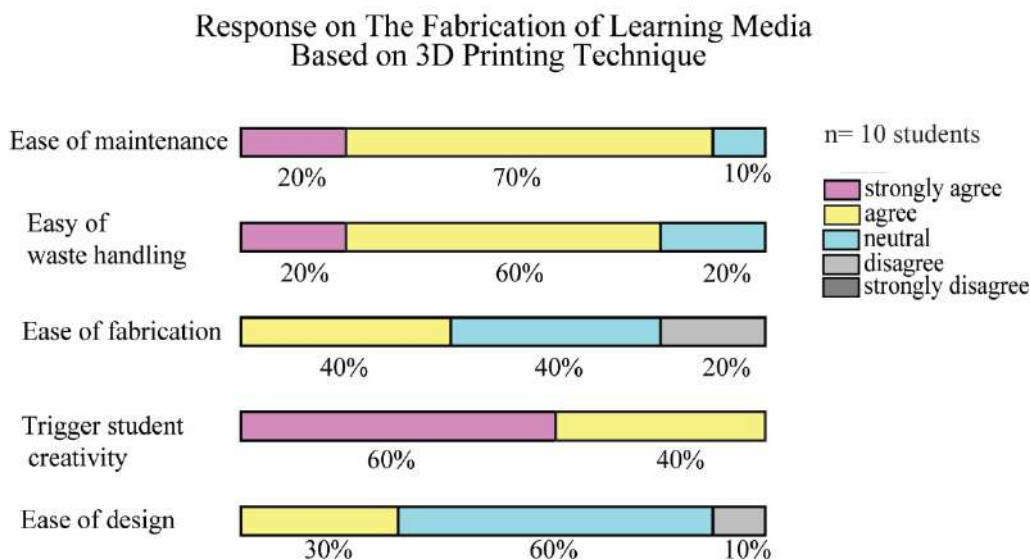


Figure 3. Summary of students' responses on the fabrication of learning media based on 3D printing technique. Students' responses were based on their motivation, which was expressed by their creativity and willingness to learn new techniques and designs.

A survey measured the effectiveness of the application of 3D printed learning media. The sample was students of a learning media class. Five indicators were used as representatives of the success of the learning media application. The indicators were: 1. learning media is maintainable (easy to maintain); 2. learning media usability (easy to operate and use); 3. learning media is reusable; 4. learning media is effective and efficient in delivering the teaching material; 5. learning media is easy to deliver teaching material. Student response on the application of learning media was great. The students were agree that 3D printed based learning media is easy to maintain during the delivering of the teaching material. The application of learning media was usefull for the students. That is importance because of the utilization of learning media able to maintain students interest, increase their analytical skill and enhance student attention.[19] Recently, due to the environmental problem and increased awareness of environmental sustainability, the fabricated learning media should be reusable. The survey shows that this 3D-printed learning media can potentially be used several times. Because chemistry is one of the subjects where most of the topics are abstract, the real

learning media for chemistry subjects is preferred. The learning media ought to be visually accessible and present abstract concepts in reality.[12, 13] The students agreed that the learning media's application fulfilled that necessity. Based on the survey, students said that the learning media is effective and efficient in delivering the abstract concept in reality and easy to explain the abstract concept to be understandable. Therefore, this PjBL project's result shows us the potential of DIY learning media fabrication to fulfill the needs of local wisdom-inspired learning media.

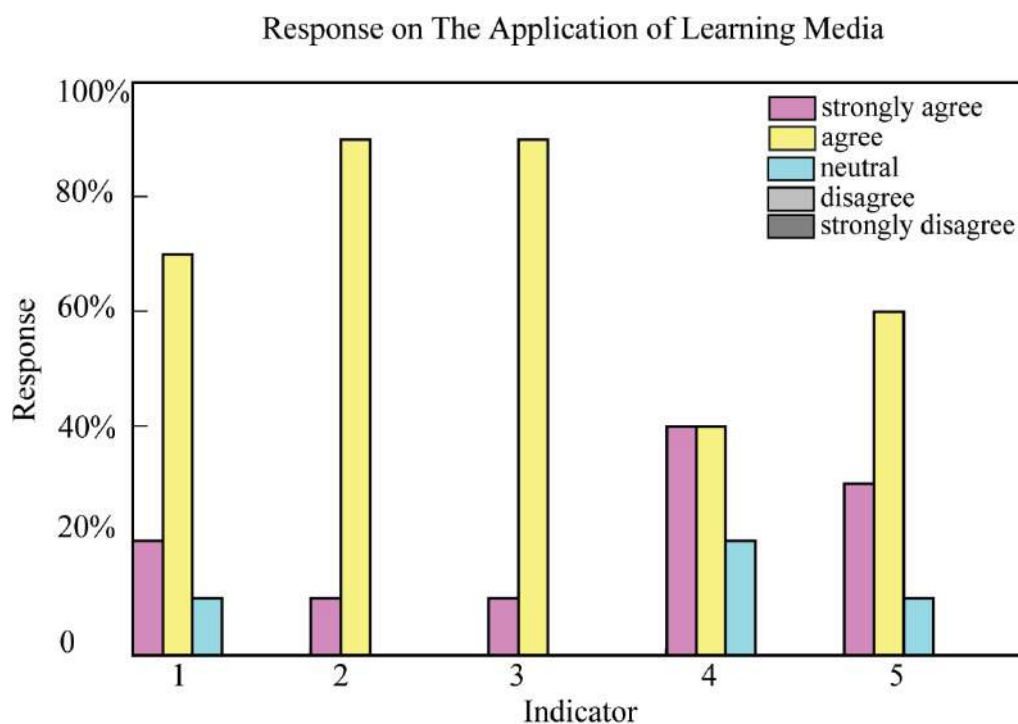


Figure 4. Summary of students' responses on the application of learning media based on 3D printing technique. Students' responses were based on the questionnaire, including the easiness of use, reusability, and the effectiveness of delivery of teaching material

4 Conclusion

The result of this study can be concluded that the PjBL-based 3D printed learning media fabrication enhanced students' motivation, easy to handle, operate and use. 3D printed learning media is also helpful and effective in delivering learning material. The material used for the filament is affordable and biodegradable, thus, harmless to the

environment. The easiness of travel the 3D printer make this 3D printing technique potentially used in many places, even in rural area.

Acknowledgment

The author wants to acknowledge the very generous contributions of Mr. Johnsen Harta and all the students in the learning media class, Chemistry Education Study Program, Sanata Dharma University. National research foundation of Korea for providing the 3D printer instrument for this research.

References

- [1] L. Hakim, “Pemerataan akses pendidikan bagi rakyat sesuai dengan amanat Undang-Undang Nomor 20 Tahun 2003 tentang Sistem Pendidikan Nasional”, *EduTech: Jurnal Ilmu Pendidikan Dan Ilmu Sosial*, **2**(1), 2016.
- [2] R. Niswaty, M. Nasrullah, and H. Nasaruddin, “Pelayanan publik dasar Bidang Pendidikan tentang sarana dan prasana di Kecamatan Pulau Sembilan Kabupaten Sinjai”, in *Seminar Nasional LP2M UNM*, **1**(1), 2019.
- [3] C. Hopkins and R. McKeown, “Education for sustainable development: an international perspective”, *Education and sustainability: Responding to the global challenge*, **13**, 13-24, 2002.
- [4] A. B. Santosa, “Potret pendidikan di tahun pandemi: dampak COVID-19 terhadap disparitas pendidikan di Indonesia”, *CSIS Commentaries*, 1-5, 2020.
- [5] D. Hairi, “Respon Pemuda Perbatasan Dalam Menghadapi Keterbatasan Fasilitas Pendidikan Pada Pulau Combol Desa Selat Mie Kecamatan Moro Kabupaten Karimun”, *Universitas Maritim Raja Ali Haji*.
- [6] I. D. P. Subamia, “Analisis kebutuhan tata kelola tata laksana laboratorium IPA SMP di Kabupaten Buleleng”, *JPI (Jurnal Pendidikan Indonesia)*, **3**(2), 2015.
- [7] A. O'Dwyer and P. E. Childs, “Who says organic chemistry is difficult? Exploring perspectives and perceptions”, *Eurasia Journal of Mathematics, Science and Technology Education*, **13**(7), 3599-3620, 2017.
- [8] G. Sirhan, “Learning difficulties in chemistry: An overview”, 2007.

- [9] H. K. Wu, J. S. Krajcik, and E. Soloway, “Promoting understanding of chemical representations: Students' use of a visualization tool in the classroom”, *Journal of Research in Science Teaching: The Official Journal of the National Association for Research in Science Teaching*, **38**(7), 821-842, 2001.
- [10] T. A. Holme, “Can We Envision a Role for Imagination in Chemistry Learning?”, *Journal of Chemical Education*, **98**(12), 3615-3616, 2021.
- [11] Y. D. Puspitarini and M. Hanif, “Using Learning Media to Increase Learning Motivation in Elementary School”, *Anatolian Journal of Education*, **4**(2), 53-60, 2019.
- [12] G. Salomon, “Media and symbol systems as related to cognition and learning”, *Journal of educational psychology*, **71**(2), 131, 1979.
- [13] P. S. Cowen, “Film and text: Order effects in recall and social inferences”, *ECTJ*, **32**(3), 131-144, 1984.
- [14] C. Brivio, “Off main grid PV systems: appropriate sizing methodologies in developing countries”, 2014.
- [15] M. Jiménez, L. Romero, I. A. Domínguez, M. d. M. Espinosa, and M. Domínguez, “Additive manufacturing technologies: an overview about 3D printing methods and future prospects”, *Complexity*, 2019.
- [16] M. C. Ratri, A. I. Brilian, A. Setiawati, H. T. Nguyen, V. Soum, and K. Shin, “Recent Advances in Regenerative Tissue Fabrication: Tools, Materials, and Microenvironment in Hierarchical Aspects”, *Advanced NanoBiomed Research*, **1**(5), p. 2000088, 2021.
- [17] J. Choi, J.-H. Lee, and B. Kim, “How does learner-centered education affect teacher self-efficacy? The case of project-based learning in Korea”, *Teaching and Teacher Education*, **85**, 45-57, 2019.
- [18] N. H. Fiktoyana, I., S. Arsa, P., Adiarta, A., “Penerapan Model Project Based Learning Untuk Meningkatkan Hasil Belajar Dasar Dan Pengukuran Listrik Siswa Kelas X-TIPTL 3, SMKN 3 Singaraja”, *Jurnal Pendidikan Teknik Elektro Undiksha*, **7**(3), 90-101, 2018.

- [19] I. N. H. Fiktoyana, P. S. Arsa, and A. Adiarta, “Enhancing student interest in English Language via multimedia presentation”, *International Journal of Applied Research*, **2**, 275-281, 2016.
- [20] S. Y. Cheung and K. Y. Ng, “Application of the Educational Game to Enhance Student Learning, (in English)”, *Frontiers in Education*, Original Research **6**, 31 March 2021.
- [21] H. Tsuji and S. Miyauchi, “Enzymatic Hydrolysis of Poly(lactide)s: Effects of Molecular Weight, l-Lactide Content, and Enantiomeric and Diastereoisomeric Polymer Blending”, *Biomacromolecules*, **2**(2), 597-604, 2001.

This page intentionally left blank

Employee Presence Using Body Temperature Detection and Face Recognition

Arif Ainur Rafiq^{1,*}, Erna Alimudin¹, and Della Puspa Rani¹

¹*Department of Electronics Engineering, Polytechnic State of Cilacap
Cilacap, Indonesia*

**Corresponding Author: aar@pnc.ac.id*

(Received 18-08-2022; Revised 16-09-2022; Accepted 21-09-2022)

Abstract

Employee performance can be measured by their presence or attendance, which applies to both civil servants and non-civil servants. Because the attendance system still uses the manual technique, it is considered inefficient due to the potential for data fraud and attendance problems. In addition, the government is adopting precautions against viruses in office buildings to maintain business continuity while the pandemic is being addressed. The goal of this study was to employ a facial recognition system and temperature measurement to lower the danger of COVID 19 transmission while also minimizing paper use by using a facial recognition system as a substitute for presences. It has so far permitted the digitization of formerly manual sights. The OpenCV library allows computers to detect faces using the haar cascade classifier approach and Python as a programming language. A Logitech C930e webcam with a resolution of 1080p at 30fps was used to capture facial data, which was then processed on a Raspberry Pi 4 microprocessor. It uses an MLX90614 sensor to monitor body temperature, which is controlled by an



Arduino Uno microcontroller. It is well integrated into the database based on body temperature testing and facial recognition. The development of a more accurate temperature sensor reading method for distance and employee body temperature is a priority for future research.

Keywords: arduino uno, haar cascade classifier, presence, temperature detection, face recognition

1 Introduction

The presence or attendance of employees, both civil servants and non-civil servants, is one sign of their performance. It examines the relevance of attendance data collecting, its relationship to performance indicators that become quality standards, and material for evaluating and improving the quality of public services, based on Regulation of Government of The Republic of Indonesia No. 30 of 2019 concerning the Work Assessment of Civil Servants. [1] Manually filling attendance from for recording attendance data is certainly inefficient because of the potential for fraud, such as data falsification or human error. Furthermore, administrative recapitulation is done manually which takes a long time because a lot of data must be entered. Many attendance systems have been built with pattern recognition that recognizes unique human physical traits, such as facial recognition and fingerprint recognition, as technology advances. These distinct reduce fraud during the registration procedure. [2]

There are many biometric identification method used for attendance system. The implementation of biometric recognition systems can be based on physical or behavioral characteristics, such as the iris, voice, fingerprint, and face. [3] One of well-discussed field nowadays in biometric identification is fingerprint. Fingerprint is considered a secured way because it has a unique pattern that is different for each person. [4] Unfortunately, systems that use fingerprints require the user to make direct physical contact with the fingerprint reader for a few seconds to perform fingerprint pattern recognition. This can increase the risk of contamination by harmful pathogenic microbes or cross-contamination of food and air by other users. [5] To avoid contamination by

physical contact in Corona Virus Disease (COVID) 19, the presence system can use other biometric identification, one of which is face recognition. Face recognition has often been done for various purposes. Security systems and administrative management through face recognition systems have also started to be used and developed in industry, business, and offices. [6] A face recognition-based attendance system has been carried out and also obtained a high accuracy score of 80%. In this study, the eigenface and haar cascade classifier methods were used for student attendance.[7] The object detection method created by Paul Viola and Michael Jones is the haar cascade algorithm, which is divided into several areas of the face such as the eye area, nose area, mouth area, and others. It depends on the image that has been trained. [8]

Decree of The Health Minister of The Republic of Indonesia Number Hk.01.07/Menkes/382/2020 about Community Health Protocol in Public Places and Facilities for Prevention and Corona Virus Disease Control 2019 (COVID-19) states that there must be a body temperature measurement at the guest entrance and employees. If the temperature is found greater than 37.3 °C, employee or guest will not allowed enter unless stated negative/ non-reactive COVID-19 after laboratory examination in the form of RT-PCR examination is valid for 7 days or rapid test valid for 3 days, before entering the office. [9] Moreover, Guidelines for the Prevention and Control of Corona Virus Disease 2019 (COVID-19) in Offices and Industries in Supporting Business Continuity in a Pandemic Situation from Minister of Health of the Republic of Indonesia's Decree No. HK.01.07/MENKES/328/2020 states that people with fever ($\geq 38^{\circ}\text{C}$) or a history of fever; or symptoms of respiratory system disorders such as runny nose / illness throat/cough and no other cause based on convincing clinical picture and in the last 14 days before the onset of symptoms had a history of travel or living in countries/regions that report local transmission or have history of contact with confirmed cases of COVID-19 classified as Person Under Monitoring. [10].

Based on the decree from Minister of Health of the Republic of Indonesia which has been described, conclude that temperature measurement is one of the important steps to prevent COVID 19 transmission. Therefore, it is necessary to design a device that can

measure the body temperature of each employee before entering the office. This is done to prevent the spread of Covid-19. This device also replaces the manual presence that still uses paper. Thus, manipulation of presence data can be avoided. The proposed device is expected to be used in the office.

2 Research Methodology

Methodology used here The working procedure of the tool is depicted using block diagrams. Later on, this block diagram will be utilized as a guide for completing the final project. The system's block diagram is shown in Figure 1.

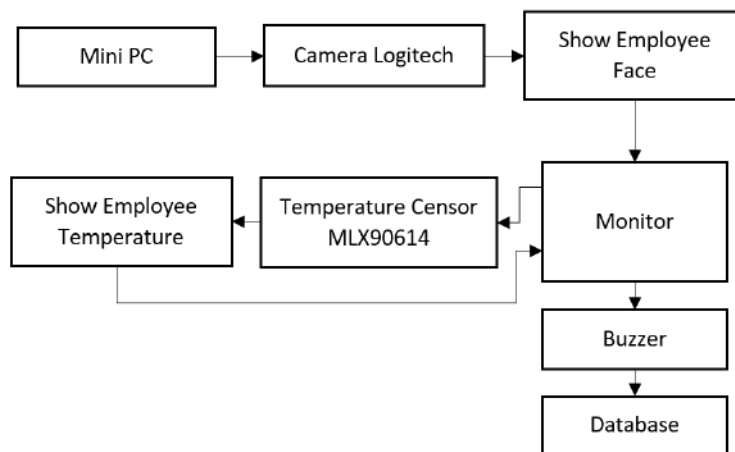


Figure 1 System Block Diagram

The following is an explanation of the block diagram system's function:

1. The Raspberry Pi serves as the system's controller.
2. The temperature sensor is used to determine an employee's body temperature.
3. Monitor functions include keeping track of staff temperature readings.
4. The camera take photographs employees' faces as an indication of their presence.
5. A sound indicator in the form of a buzzer.
6. The database is used to keep track of staff attendance.

The system will operate based on the following principle: The camera will work when personnel is objects or faces. It will then appear on the monitor screen. Furthermore, the temperature sensor will work when the thing is in front of the sensor. The results will be presented on the monitor screen and directly recorded into the database. The flowchart is a standard to describe the process. The system design flowchart that is carried out can be seen in Figure 2.

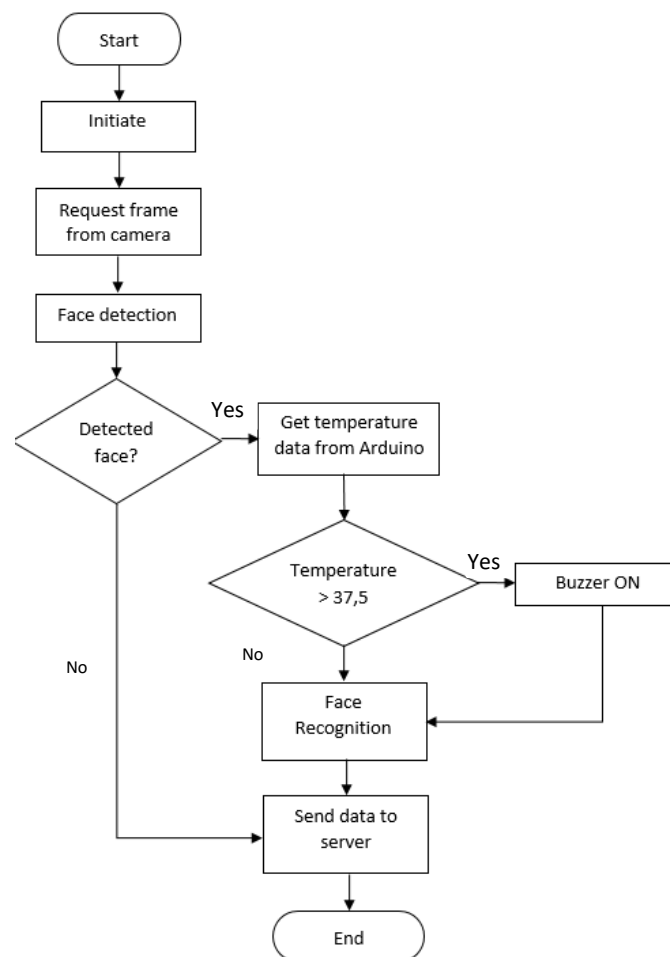


Figure 2 *Flowchart Design System*

When an object is detected, the camera detects the employee's face, and if it fits, the temperature sensor immediately reads the employee's temperature. If the temperature is less than 38°C, the staff have arrived and will enter the room directly. If the employee's

temperature rises above 38 degrees Celsius, he will be followed up on his medical history and subjected to health protocols, such as self-isolation at home. Employee data will also be entered into the database.

The design of the tools to be created is referred to as mechanical design. The skeleton section of the gadget is built of a triplet base material. The camera is made up of aluminum in parts. The frame is made of wood since it is easy to develop and arrange out components like Raspberry, Arduino, and monitors. The mechanical design is shown below. Figure 3 (a) shows the front view, and Figure 3 (b) shows the back view of the mechanical design of the tools created.

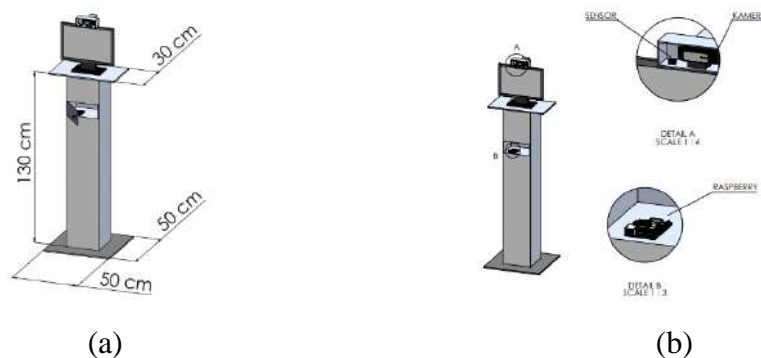


Figure 3 Mechanical design from (a) front view and (b)

3 Results and Discussions

This section shows how the system was tested after it was built. Obtain data to determine whether or not the tool designed was successful.

3.1 MLX Sensor Temperature Measurement Testing

The face was brought closer to the MLX temperature sensor with a predetermined distance of 1 meter, and a Non-Contact Infrared Thermometer was used as a comparison. Table 1 shows the results of temperature sensor testing using a non-contact infrared thermometer.

Table 1. Temperature Sensor Comparison Test with Non-Contact Infrared Thermometer

No	MLX Temperature Sensor	Termometer Infrared Non Contact	Difference Score	User
1	35,6°C	36,5°C	0,9°C	1 Dita
2	34,5°C	36,2°C	1,7°C	2 Jahrona
3	34,8°C	35,9°C	1,1°C	3 Della
4	34,6°C	35,5°C	1,1°C	4 Ira
5	35,1°C	35,9°C	0,8°C	5 Vemmi
6	35,8°C	36,4°C	0,6°C	6 Ferahma

According to the findings of the testing, there was a discrepancy between the MLX sensor readings and the Non-Contact Infrared Thermometer, with the lowest contrast distinction of 0.6°C and the highest distinction of 1.7°C. The temperature was shallow while monitoring body temperature because the temperature detection distance is too far from the sensor, causing the temperature sensor to be less accurate when reading body temperature.

3.2 User Identification Testing

The goal of the test is to collect photos of people's faces as data, which will be stored in a folder that will be used as a database to match the system to face detection. Because object detection accuracy in the haar cascade classifier approach depends on the impacts of the training, images were taken as much as feasible to maximize the detection results. Figure 4 shows the identification test results at a distance of one meter. The results of successful and unsuccessful identification are shown in Table 2.

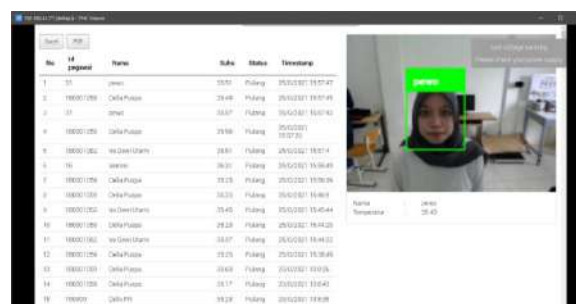


Figure 4 User face identification in 1 meter away

Table 2 User's Face Identification

No	User	1 st Trial	2 nd Trial	3 rd Trial
1	User 1 Dita	Unsuccessful	Successful	Successful
2	User 2 Jahrona	Unsuccessful	Successful	Successful
3	User 3 Della	Successfull	Successful	Successful
4	User 4 Ira	Unsuccessful	Successful	Successful
5	User 5 Vemmi	Unsuccessful	Successful	Successful
6	User 6 Ferahma	Unsuccessful	Successful	Successful
7	User 7 Ali	Successful	Successful	Successful
8	User 8 Azhar	Successful	Successful	Successful

Table 2 shows the result of three times testing. There were several unsuccessful experiments. In the first experiment, several obstacles caused the camera and temperature sensor not to work optimally, such as excessive lighting effects, being too far from the camera position, and the temperature sensor. In the second and third experiments, data obtained that the maximum limit of lighting and distance has been determined. Then, the system were tested in further distance to know how far the system can recognize user. The result shows in Table 3.

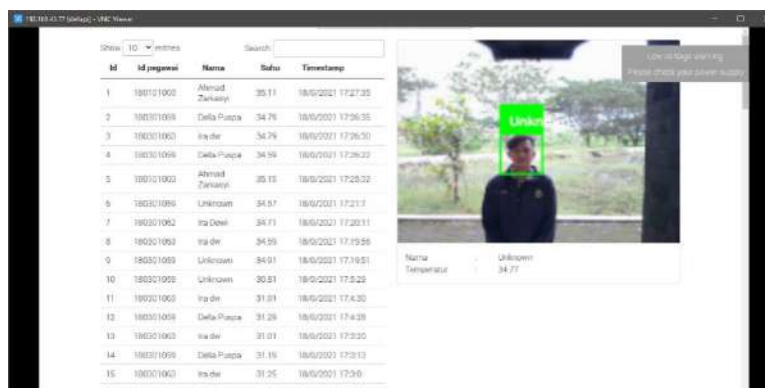


Figure 5 User face identification in 2 meter away

Table 3 shows testing system when the user stand in two meters away from camera. System shows status unknown. Whether the user was already registered the system could not recognize the face user. This testing shows that the camera only able to recognize face up to 1.5 meters away.

3.3 Buzzer Testing,

Speaker testing is used to ensure that the speakers can produce a clear sound. The following Table 3 is the result of buzzer testing.

Table 3 *Buzzer Testing*

No	Temperature	Categorize	Speaker
1	33°C	Normal	Speaker Off
2	34°C	Normal	Speaker Off
3	35°C	Normal	Speaker Off
4	36°C	Normal	Speaker Off
5	>37,5°C	High	Speaker On

Based on the data in Table 3, if the detected temperature is at an average temperature, the speaker is "OFF" or off. Furthermore, if the detected temperature is above the average temperature or >37.5°C, the speaker is active and gives instructions as a warning.

3.4 Database Testing

In database testing, several experiments were carried out to determine how the database system stores data. The results of the database test can be seen in Figure 5.

No	Username	Time IN	Temperature IN	Time OUT	Temperature OUT
1	Ahmad Zarkasyi	27/0/2021 14:25:39	34.23	27/0/2021 14:26:0	33.85
2	Ali	27/0/2021 14:25:8	34.17	27/0/2021 14:25:17	33.85
3	anggi ap	26/0/2021 14:13:22	31.73	-	-
4	Babas	27/0/2021 13:45:29	35.25	-	-
5	catur	27/0/2021 12:7:0	34.85	-	-

Figure 5. Data Testing Result

In this test, faces that have done training can be saved directly to the database. If people who have not been identified or have been identified but are not suitable in facing the room on faces that previously did data training. The database will store the results of face detection and body temperature of employees who enter and will go home when the employee enters the office and when the employee will go home.

4 Conclusions

The results of testing the tool as a whole show that the tool works according to its function. The camera only able to recognize face up to 1.5 meters away. Buzzer as a sign of a user who has a fever will sound at a body temperature above 37.5°C. From the six sensor tests, there are slight differences between the sensor readings and the MLX and Non-Contact Infrared Thermometer. The temperature measured on the MLX sensor is lower than the temperature on the Infrared Contact Thermometer because the temperature detection distance is too far from the sensor causing the temperature sensor to be less accurate when reading body temperature. Meanwhile, in the first facial identification experiment, there were still 2 failures out of 8 trials. This is because the location where the face was shot makes the camera get too much exposure. After the camera was moved to a more suitable location, the results obtained were successful in the second and third experiments for 8 users.

References

- [1] Republic Indonesia, "Republic of Indonesia Government Regulation No. 30 year 2019", 1945.
- [2] M. Hernandez-de-Menendez, R. Morales-Menendez, C. A. Escobar, and J. Arinez, "Biometric applications in education", *Int. J. Interact. Des. Manuf.*, **15**(2–3), 365–380, 2021.
- [3] S. C. Hoo and H. Ibrahim, "Biometric-Based Attendance Tracking System for Education Sectors: A Literature Survey on Hardware Requirements", *J. Sensors*, **2019**, 7410478, 2019.
- [4] V. P. Singh, S. Srivastava, and R. Srivastava, "Automated and effective content-based image retrieval for digital mammography", *J. Xray. Sci. Technol.*, **26**, 29–49, 2018.
- [5] K. Okereafor, I. Ekong, I. Okon Markson, and K. Enwere, "Fingerprint Biometric System Hygiene and the Risk of COVID-19 Transmission", *JMIR Biomed. Eng.*, **5**(1), e19623, 2020.
- [6] F. Susanto, F. Fauziah, and A. Andrianingsih, "Lecturer Attendance System using Face Recognition Application an Android-Based", *J. Comput. Networks, Archit. High Perform. Comput.*, **3**(2), 167–173, 2021.
- [7] T. E. Prabowo, R. Hartanto, and S. Wibirama, "Prototype of Student Attendance Application Based on Face Recognition Using Eigenface Algorithm," *IJITEE (International J. Inf. Technol. Electr. Eng.)*, **3**(1), 23, 2019.
- [8] A. Ghoshal, A. Aspat, and E. Lemos, "OpenCV Image Processing for AI Pet Robot," *International Journal of Applied Science and Smart Technologies (IJASST)*, **3**(1), 65–82, 2021.
- [9] Widiharso, "Teknik Dasar Elektronika Telekomunikasi. Kementerian Pendidikan dan Kebudayaan", 2013.
- [10] Health Minister of The Republic Of Indonesia, "Decree of The Health Minister of The Republic of Indonesia Number HK.01.07/Menkes/382/2020 about

Community Health Protocol in Public Places and Facilities for The Prevention and Control of Corona Virus Disease 2019 (Covid-19)". Indonesia, 2019.

The Experiment of Wind Electric Water Pumping for Salt Farmers in Remote Area of Demak-Indonesia

S. Dio Zevalukito¹, YB. Lukiyanto^{1,*} and F. Risky Prayogo¹

¹*Department of Mechanical Engineering, Sanata Dharma University,
Yogyakarta, Republic of Indonesia*

**Corresponding Author: lukiyanto@usd.ac.id*

(Received 09-11-2022; Revised 14-11-2022; Accepted 29-11-2022)

Abstract

Local villagers in the remote area of Wedung, Demak, northern of Central Java, Indonesia utilized special equipment called wind-pump for sea water lifting and circulating on salt production processes. The salt farmer has skill to produce, manufacture and maintain his own traditional wind-pump. In the windpump structure unit consisted of four blades horizontal axis windmill and reciprocating pump. This experiment study separated both windmill and pump by 50 meters. The pump was low speed centrifugal type pump. The windmill shaft was connected electrically to the pump shaft. The electric transmission components were an AC generator, diodes circuits and an DC motor. The experiment is carried out in a place that has the same characteristics as the original place at southern region of Bantul, Yogyakarta, Indonesia. The variation of experiment was pump head of 55 cm and 85 cm during 6 hours each variation. The average wind speed at the time of data collection at the head of 55 and 85 cm were 3.9 and 3.8 m/s. The volume flow rate and the volume produced by the pump during 6 hours of operation were 0.134 and 0.215 liter/s and 2901.6 and 4640.6 liters.



Keywords: wind-pump, salt production processes, four blades, electric transmission

1 Introduction

Salt production in Indonesia is still using a traditional technique. This technique applies solar heat and solar radiation to evaporate seawater [1]. The salt production process is usually in a dry season. This process is the easiest and cheapest method. Typically, the salt ponds are spread across the coastline. The salt ponds are plentiful on the north coast of Java-Indonesia.

Wind energy for water pumping is spread worldwide, especially in developing countries [3]. The application of renewable energy for water pumping still exists. The traditional methods use windpump and the modern methods, such as photovoltaic and wind turbine technologies for water pumping [4]. Especially in remote areas, salt farmers do not have electricity or fuel to power the pumps [5]. The salt farmers respond to their issues and built the windmills [2,5]. This windmill is used to assist salt farmers in salt production.

The salt farmers from Demak use the windmill for water pumping [2,5]. Commonly, salt farmers use a reciprocating pump as an instrument for transporting water [2]. This traditional technique is usually called windpump. There are two types of purposes for this windpump. The first type was built to transport water from the sea to salt ponds, and the second type was built to transport water from one pond to another pond [2].

The purpose of this study is to discuss salt farmers' windmills of Demak for water pumping with a slow-speed centrifugal pump. There are two variations on the net head on this research, there are 55.00 cm and 85.00 cm. The dissimilarity on the net head could expand other assistances for salt farmers. The results are windspeed to volume flow rate, efficiency and volume produced in a day.

The study purpose is to investigate the performance of four blades salt farmer's windmill from Demak-Indonesia for water pumping coupled with a centrifugal pump, with two variations of the water level (55.00 cm and 85.00 cm). Velasco et al. [6] explained the theory of wind-electric water pumping. Zevalukito and Lukiyanto [7]

investigated the salt farmer's windmill from Demak for water pumping with a low-speed centrifugal pump. The transmissions utilize electric transmissions, with electric generators and electric motors. Iswanjono et al. [8] investigated the performance of transmissions with some type of generator, motor, and cable. Lukiyanto and Wahisbullah [9] examined the double U pipe configuration for a centrifugal pump. The double U pipe arrangements aim to escalate efficiency because double U pipe configurations have lower losses than a sliding orifice.

Site and Data Description. The data collection process has completed at Kuwaru Beach (Bantul, Special Region of Yogyakarta, Indonesia). The windpump system was installed about 50 m from the coastline. The windmill was fitted on a beach and the centrifugal pump was arranged 50 m away from the windmill. There was no vast difference in the wind speed range between Kuwaru Beach and Demak's coastline. The place has uncontrollable wind speed by the reason of the natural conditions of the coastline. The data collection was started in the morning until the afternoon on local time (GMT+07.00). The wind speed was ranging between 2.2 up to 3.9 m/s. The information required was wind speed and the windmill's shaft speed on the windmill, and the volume flow rate of the centrifugal pump. The data informations were recorded every 6 minutes.

2 Research Methodology

Fig. 1. illustrates the wind pumping system. The windmill's shaft attached with the AC generator's shaft subsequently produces AC electricity. DC electricity is produced as a result of AC electricity transform into DC electricity by a diodes circuit (Wheatstone bridge). The DC electricity is linked with the DC electric motor. The DC electric motor shaft is coupled with a low-speed centrifugal pump. When the low-speed centrifugal pump rotates, then the water is supplied with centrifugal force. The centrifugal force pushes the water upward.

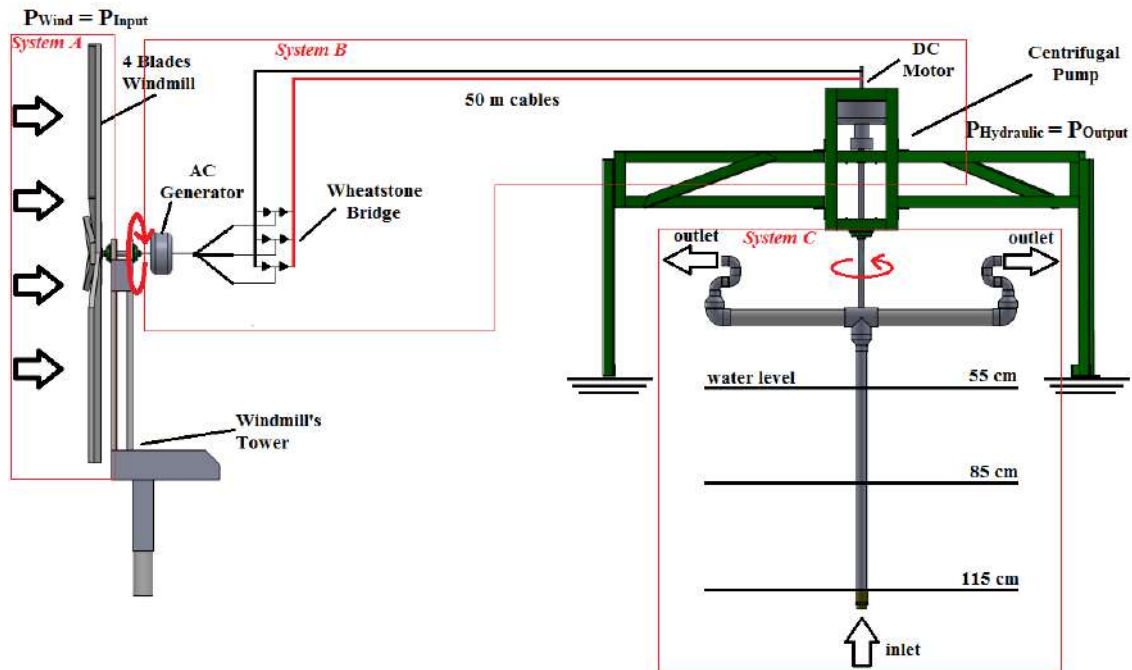


Figure 1. Schematics of Wind Pumping System

This wind pumping system in this study has three principal parts shown in Fig. 1. There are windmills [5], a transmissions system [8], and a centrifugal pump [9]. In this study, the windpump system was used an AC generator and DC electric motor as electric transmissions. Fig. 2. Shows energy losses during energy converting.

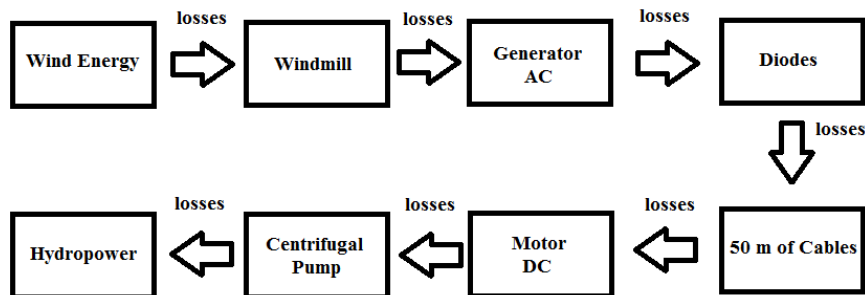


Figure 2. Energy Losses of The System

Windmill (System A). The windmill used in this study purchased directly from one of the salt farmers from Demak-Indonesia. The windmill is arranged with four blades and maybe rearranged with two blades [5]. The windmills have dimensions of 200.00 cm diameter, 22.25 cm wide, and 2.50 cm width. The windmill is attached to a shaft with dimensions of 2.00 cm in diameter and 25.00 cm in length. The shaft is fitted horizontally between the two UCF 204 bearings. The wooden tower was used to install the windmill.

Usually, the wooden tower is instantly installed above the pond's fence. The wooden tower is attached to the rigid structure due to research purposes.

The performance of windmills was examined by Zevalukito et al. [5]. The windmill has a Coefficient of Performance (C_p) of 10.2% and has maximum torque (T) of 1.90 Nm. The maximum wind energy captured by this windmill is 10.2% could be converted to mechanical shaft power. The mechanical shaft power rotates the generator which is coupled with the AC generator's shaft.

Transmission System (System B). The electric transmissions require some electrical equipment. The transmissions system arrangement in the sequence was an alternating current generator, a diodes circuits, a wire, and a direct current electric motor. The windmill's shaft was coupled to the generator's shaft. The electric generator was 500 Watt alternating current brushless permanent magnet. The electricity production by the generator was alternating current (AC). The AC electric current was transformed to direct current (DC) by diodes circuits [7-8]. The diodes circuit is well-known as the Wheatstone bridge. The DC electricity is transferred by the wire 50 m long. The wire connected to the DC electric motor. The DC electric motor has 450 Watt with a permanent magnet. The DC electric motor's shaft is attached with the low-speed centrifugal pump tube afterwards rotating the pump.

Low-Speed Centrifugal Pump (System C). The centrifugal pump in this study was a low-speed centrifugal pump coupled with DC electric motor's shaft. The centrifugal pump uses a double U configuration as an impeller [6,9]. The centrifugal pump's shaft was connected to DC electric motor's shaft. The suction pipe, two long-arm on two sides, and double U pipes configurations are the three main parts of the centrifugal pump [9]. The centrifugal pump has 110.00 cm in diameter. The height between suction parts and double U pipe are 55.00 cm, 85.00 cm, and 115.00 cm. The suction part could be replaced for each requirement. The centrifugal pump is mounted below the rigid structure. The protective cover is installed around the centrifugal pump to prevent the water splashed everywhere.

The system efficiency in this wind-electric water pumping assessed from wind power (System A) to hydraulic power (System C).

The energy conversion of the wind electric water pumping begins with wind energy [11]:

$$P_{Wind} = 0.5\rho_{air}Av^3 \quad (1)$$

P_{Wind} as input power; ρ_{air} constant at 1.225 kg/m^3 ; A as sweep area of the windmill, remain constant at 3.14m^2 ; v as wind speed. The windmill system is shown in Fig. 2 of System A.

The energy conversion ends in the low-speed centrifugal pump while the pump starts pumping. The hydraulic power-driven by the wind speed. The wind speed changes into the volume flow rate due to this windpump system. The hydraulic power could be written as [12]:

$$P_{Hydraulic} = \rho_{Water}ghQ \quad (2)$$

$P_{Hydraulic}$ as output power; ρ_{air} persist constant at 1.03 kg/litre ; g as acceleration of gravity, steady at 9.81 m/s^2 ; h as the net head pump, there are 55.00 cm , 85.00 cm and 115.00 cm ; and Q as volume flow rate.

The system efficiency assess from input power (1) to output power (2). The equation to assess efficiency could be written as:

$$\eta = \frac{P_{Wind}}{P_{Hydraulic}} \times 100\% \quad (3)$$

As a result of this windpump system for developing salt farmers community in Demak-Indonesia, the volume in a day is certainly required, since the salt farmers used to gain advantages from the windmills. The wind speed and volume flow rate recorded every six minutes are assumed to remain constant.

3 Results and Discussions

Fig. 3 shows the relation between windspeed captured and volume flow rate produced by the wind pumping system. The wind speed available during the data collection process ranged between 2.20 m/s up to 3.90 m/s . The highest flow rate produced by the wind pumping system is windpump with 85.00 cm of the net head, followed by the 55.00 cm of windpump's net head. The highest wind energy captured by the wind pumping system could increase the volume produced by the pump. The average wind speed captured for

each variation for 55.00 cm and 85.00 cm is 3.10 m/s and 3.30 m/s, respectively. The wind pumping system with 85.00 cm of the net head has the greatest average wind speed and the 55.00 cm has the lowest, affecting the wind pumping system with 85.00 cm of net head producing more energy than 55.00 cm. The wind pumping system could drive the centrifugal pump if the windmill captured 2.5 m/s of a wind speed and up.

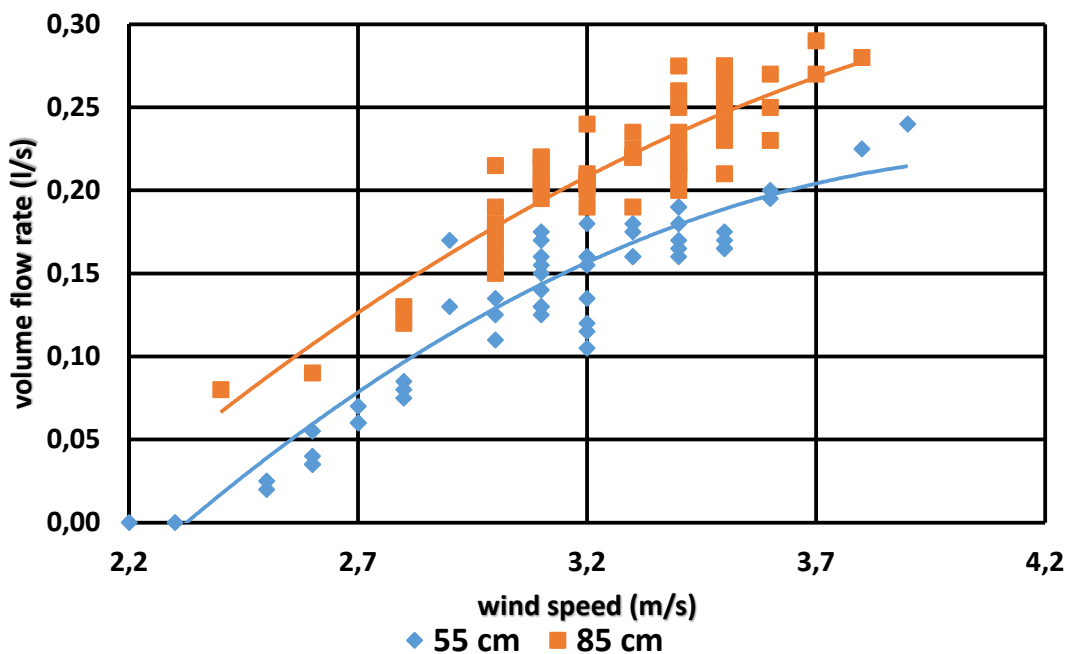


Figure 3. Relation of windspeed and volume flow rate of the wind pumping system

Fig. 4 shows the volume produced in a day as a result of the wind pumping system. The volume produced every 6 minutes is assumed to remain constant. The wind pumping system with 85.00 cm of the net head has the highest volume produced of 4640.58 liters, the net head of 55.00 cm produced volume of 2901.60 liters. The information has been recorded in Fig. 3 shows that the wind pumping system with 85.00 cm of the net head has the greatest average wind speed of 3.30 m/s produced 4640.58 liters of water. Although, the 55.00 cm has the lowest average wind speed of 3.10 m/s produced 2901.60 liters of water. The wind energy captured by the wind pumping system with 85.00 cm of net head

is more than 55.00 cm. The consequence are the centrifugal pump with 85.00 cm of net head produce more water than 55.00 cm of net head.

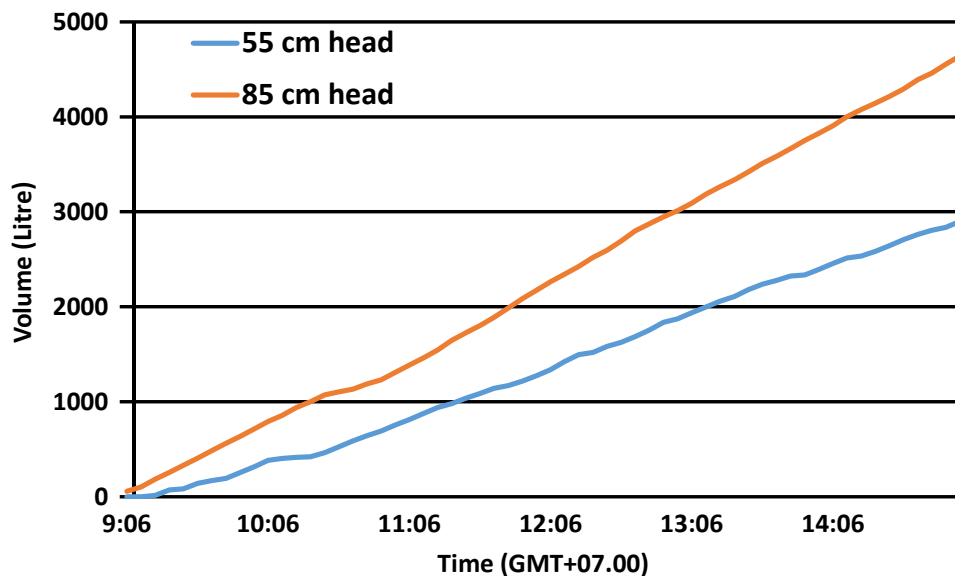


Figure 4. Volume produced in a day

There remains a substantial energy loss in the system which is shown in Fig. 2. The insufficiency of measuring types of equipment became essential during the data collection process. The calculation of system efficiency for each net head merely calculate the average efficiency. The average efficiency of the wind pumping system with 55.00 cm and 85.00 cm are 1.32% and 3.71%, respectively.

4 Conclusions

The experimental study of a wind pumping system with tree variations of the net head was complete. The wind pumping system with 55.00 cm and 85.00 cm of the net head has produced volume flow rate at maximum wind speed are 0.24 liter/s at 3.9 m/s and 0.28 liter/s at 3.8 m/s. The volume produced in a day are 2901.60 liters and 4640.58 liters,

respectively. The total average efficiency of the wind pumping system for 85.00 cm and 55.00 cm are 3.71% and 1.32%, respectively.

References

- [1] A. . Rositawati, C. . Taslim, and D. Soetrisnanto, “Rekristalisasi Garam Rakyat Dari Daerah Demak Untuk Mencapai SNI Garam Industri,” *J. Teknol. Kim. dan Ind.*, **2**(4), pp. 217–225, 2013.
- [2] S. D. C. Deo, S. D. Zevalukito, and Y. Lukiyanto, “Indonesian traditional windmill of Demak, Central Java for water pumping in traditional salt production,” *J. Phys. Conf. Ser.*, **1511**, 012117, 2020.
- [3] L. Mangialardi and G. Mantriota, “Continuously variable transmissions with torque-sensing regulators in waterpumping windmills,” *Renew. Energy*, **4**(7), 807–823, 1994.
- [4] P. E. Campana, H. Li, and J. Yan, “Techno-economic feasibility of the irrigation system for the grassland and farmland conservation in China: Photovoltaic vs. wind power water pumping,” *Energy Convers. Manag.*, **103**, 311–320, 2015.
- [5] S. D. Zevalukito, Y. B. Lukiyanto, and D. P. Utomo, “Two and Four Blades Windmill Characteristics of Traditional Salt Farmers from Demak Region,” in *ICIMECE 2019*, 2020, 1–5.
- [6] M. Velasco, O. Probst, and S. Acevedo, “Theory of wind-electric water pumping,” *Renew. Energy*, **29**(6), 873–893, 2004.
- [7] S. D. Zevalukito and Y. B. Lukiyanto, “The performance of salt farmer windmill from Demak for water pumping with a low-speed centrifugal pump,” *J. Phys. Conf. Ser.*, **1724**, 1–8, 2021.
- [8] Iswanjono, Y. B. Lukiyanto, B. Setyahandana, and Rines, “A Couple of Generator and Motor as Electric Transmission System of a Driving Shaft to Long Distance Driven Shaft,” *E3S Web Conf.*, **67**,1–4, 2018.
- [9] Y. B. Lukiyanto and E. Wahisbullah, “A Simple Double U Pipe Configuration to Improve Performance of a Large-Diameter Slow-Speed Centrifugal Impeller,” in

Proceedings of the 3rd Applied Science for Technology Application, ASTECHNOVA 2014, 2014.

- [10] B. Setyahandana, Y. B. Lukiyanto, and Rines, "Pipes Outlet Directions and Diameter of Double U Pipes Configuration on Centrifugal Reaction Pump," *Proceeding 15th Int. Conf. QiR (Quality Res.)*, 324–332, 2017.
- [11] T. M. Letcher, "Wind Energy Engineering: A handbook for onshore and offshore wind turbines", Chennai: Joe Hayton, 2017.
- [12] Y. A. Cengel and J. M. Cimbala, "Fluid Mechanics Fundamentals and Application, 1st ed", New York: McGraw-Hill, 2006.

Response Surface Modelling of the Mechanical Properties of Oil Palm Empty Fruit Bunch Fibre Reinforced Polyester Composites

Chinwe Evangeline Kamma^{1*}

¹*Department of Sustainable Environment and Energy Systems, Middle East Technical University, Northern Cyprus Campus 99738 Kalkanli Guzelyurt via Mersin 10 Turkey*

*Corresponding Author: kammachie@gmail.com

(Received 02-09-2022; Revised 16-09-2022; Accepted 21-09-2022)

Abstract

This work presents a systematic approach to evaluate and study the effect of fibre aspect ratio and fibre volume fraction on the tensile strength, ultimate elongation, modulus of elasticity, strength and impact energy of oil palm empty fruit bunch fibre reinforced polyester composites. Hand-lay-up technique was used in the fabrication of the composite materials. Response surface methodology was used to study the effect of the selected factors on the mechanical properties of oil palm empty fruit bunch fibre reinforced polymer-based composite. The optimum fibre aspect ratio and fibre volume fraction for each mechanical property was determined. From the result of optimization, the maximum value for tensile strength obtained was 12.15N/mm^2 at a fibre aspect ratio of 64 and fibre volume fraction of 26%. The maximum value for ultimate elongation was obtained as 1.939% at a fibre aspect ratio of 124 and fibre volume fraction of 50%, the maximum value for modulus of elasticity was obtained as 1509 N/mm^2 at a fibre aspect ratio of 124 and 34% volume fraction. The maximum value for toughness was obtained as 0.12 N/mm^2 at a fibre aspect ratio of 89 and a volume fraction of 30%. The maximum value of impact energy was obtained



d as 307.72J/m (5.77ft-lbs/in) at 28% fibre volume fraction and an aspect ratio of 69. The maximum value of impact strength was obtained as 4.57N/mm² at a 36% volume fraction and an aspect ratio of 64.

Keywords: Polyester Composites, Response Surface Model, Mechanical Properties, Oil Palm Empty Fruit Bunch

1 Introduction

Polymer matrix composites are composed of a variety of lengths of fibres bonded by a polymer matrix [1]. They are designed such that the mechanical loads to which the structure is subjected in service are supported by the reinforcement. According to [2], composites are materials that consist of two or more chemically and physically different phases separated by a distinct interface. The different systems are combined such that a system is achieved in which useful structural or functional properties are non-attainable by any of the constituents alone.

The wake of engineers' uses of composites started when it was discovered that they have great advantages above steel and its alloys such as low weight and higher resistance, high fatigue strength and faster assembly [3, 4].

Composites are used extensively as materials in making aircraft, electronic devices, packaging, vehicles, home building, etc. They comprise the matrix and reinforcing materials and their use until now has been more traditional than technical. They have served many useful purposes for a long but the application of the material for the utilization of natural fibres as reinforcement in polymer matrix took place quite recently [3]. These natural fibres have advantages such as low density, low cost, low weight, high toughness, acceptable specific length recovery, biodegradability and enhanced energy recyclability [5, 6].

The fruit bunches which are by-products of oil processing are presently industrial wastes. The oil palm empty fruit bunch can be found littered everywhere in oil palm producing areas of Nigeria since the wastes have presently no industrial application. Recently, because of the environmental impact of using oil palm empty fruit bunch as

fuel has been discouraged in Nigeria [18]. Its handling in the oil mills consumes energy. However, oil palm empty fruit bunch used locally to prepare local delicacies like ukwa (breadfruit), ugba (oil bean salad), abacha (slice cassava, popularly called African salad), and in rare cases now, in the production of local black soap because of the large potassium content of the bunch. This study hopes to help find a place for the usefulness of oil palm empty fruit bunch as fibre reinforcement for composites.

Several factors affect the performance of natural fibre reinforced polymer composites such as fibre-matrix adhesion properties, fibre length, fibre volume fraction, and fibre aspect ratio [7]. Composites are generally a combination of heterogenous materials [21], thus to improve the fibre-matrix interaction and adhesion, the fibre is mercerized to remove certain impurities and reduce the hydrophilic characteristics of the fibre leaving the fibre with a rough surface [4, 8-16]. The mixing procedures, type of compatibilizers, and processing and treatment conditions of fibres and the polymer resin have been shown to affect the quality of interfacial bonding between the fibre and the resin [17, 18]. Recent work conducted by Athijayamani et al. highlighted the effects of fibre length and content on composite tensile and flexural strength. The study showed that the tensile and flexural strength of a hybrid roselle/sisal polyester composite increased with increased fibre length and fibre content, while the impact strength reduced correspondingly [19].

Sapuan et al. studied the mechanical properties of woven banana fibre reinforced epoxy composites and found that the composites can be used for household utilities [20]. The industrial potentials of oil palm empty fruit bunch have not been well addressed in the literature to our knowledge. Therefore, the purpose of this work is to evaluate the tensile, and impact strength of short random oil palm empty fruit bunch fibre reinforced polyester composites for application in the automobile industry.

The high demand for low density, low cost, high impact resistance, and renewable and biodegradable materials have led to many works and research on fibre-reinforced polymer composites. However, there has not been rife work in modelling and optimization of the mechanical properties of oil palm empty fruit bunch fibre reinforced polyester composites concerning their fibre aspect ratio and volume traction using the response surface model.

This work hopes to address the above limitation by studying the effect of fibre aspect ratio and fibre volume fraction of oil palm empty fruit bunch fibre reinforced polyester composites on the mechanical properties and modelling the mechanical properties of oil palm empty fruit bunch fibre reinforced polyester composites using surface response technology to determine the optimum fibre aspect ratio and volume fraction for optimum mechanical performance.

2 Research Methodology

A brief description of the materials and methods to be used for the preparation of composites is given in this section. The chemicals to be used for various fibre treatments are discussed. A brief description of the different analytical techniques to be used for the characterization of fibres and composites is also given in this section.

2.1 Oil Palm Empty Fruit Bunch Fibre (RPF)

The Oil Palm Empty Fruit Bunch Fibre used in this work was obtained from the eastern part of Nigeria where the crop is grown for consumption as well as for commercial use.

2.2 Unsaturated polyester resin

General Purpose-grade Unsaturated polyester resin (HSR 8113M), was obtained from Nycil Industrial Chemicals, Ota, Ogun State Nigeria.

2.3 Chemicals for fibre modification

The Sodium hydroxide used for fibre surface modification is of reagent grade and was obtained from new concepts laboratories Obinze, Imo state, Nigeria.

2.4 Fibre preparation and surface modification

Extraction of the OPEFBF and preparation was carried out as follows: The fruits from the bunch were extracted mechanically leaving behind an empty fruit bunch, which was then retted utilizing tank water retting for about three days, and the fibres so obtained were sun-dried.

2.4.1. Mercerization

For preparing randomly oriented oil palm empty fruit bunch fibre composites, the fibres were treated with NaOH of 6wt% at 90mins at room temperature. Finally, the fibres were repeatedly washed and then dried in air and oven. Fibres of an average diameter of 0.41mm and fibre volume fractions of 10%, 20%, and 30% and fibre aspect ratios of 24.39, 73.171, and 121.9512 were obtained.

2.4.2 Preparation of OPEFBF-polyester reinforced composites and test specimens

Randomly oriented OPEFBPF-polyester composites containing fibres of specific length and fibre volume fraction were prepared by hand lay-up method using a stainless steel sheet female mould with a marble tile male mould. Before the composite preparation, the mould surface was polished well and a mould-releasing agent (mirror-glaze) was applied to the surface of the mould. General unsaturated polyester resin (GP) was mixed with 5% by vol. MEKP accelerator and 10% by vol. cobalt naphthenate catalyst. The fibre material was then placed in the mould and the resin mixture was poured evenly on it. After which the mould was closed and the excess resin allowed to flow out as a 'flash' by pressing, the pressure was held constant during the curing process at room temperature for 24 hours. The composite sheet will then be post-cured at 80°C for 4 hours. Test specimens according to ASTM standards were cut out from the sheet.

2.5 Mechanical property measurements: The standard mechanical properties were determined by the procedures found in ASTM (American Society for Testing and Materials) standards for plastics. The mechanical property tested for in this work is ultimate tensile strength and impact strength.

2.5.1 Tensile properties

The tensile properties were tested at the Civil Engineering Laboratory, University of Nigeria, Nsukka (UNN), using a Hounsfield Monsanto Universal Tensometer Machine. The Hounsfield Tensometer is a universal testing machine capable of testing metals,

plastics, textiles, timber, composites, fibres, papers etc. Provisions are made for such tests as tensile, compression, flexural or bending, shear, hardness etc. an important feature of the equipment/machine is the ease with which an auto-graphic record can be made. It contains a spring beam with ranges that are readily interchangeable and used in conjunction with special attachments. This enables tests to be performed on a wide variety of materials. Like most testing machines, the load is applied at one end and the magnitude of the load is measured at the other. The test piece, held in suitable chucks fixed to the spherically seated nosepieces by the chucks attachment pins, is loaded either by hand or employing a motor-driven unit through a worm gearbox. This causes the operating screw to move to the right and so transmits pull to the test piece. The other end of the test piece is connected via the tension head and bridge to the centre of a precisely ground spring beam. The deflection of this spring-beam, which is supported on rollers, is transmitted through a simple lever system to a mercury piston which displaces mercury in a uniform bore glass tube, thus magnifying the beam deflection and providing an easily read scale of load. The advance of the mercury column is followed manually by the cursor and its attached needle which is used to puncture the graph sheet at frequent intervals; thus recording force. The movement of the worm gear which causes the test piece to elongate is transmitted through a gear train to the recording drum, the rotation of which is proportional to the elongation of the test piece. The resultant graph produced by joining successive punctures shows the load against the cross-head movement which is virtually a true stress/strain diagram from which the modulus of elasticity and tensile strength of the material could be determined. The force will then be recorded and the area of the cross-section's test piece, the mechanical properties are determined such as tensile strength, ultimate elongation and modulus of elasticity.

2.5.2 Impact test

The impact properties such as impact strength and impact energy of the composite sheet were tested in the civil engineering laboratory, university of Nigeria Nsukka (UNN), using a notch impact-testing machine. Force was applied to the composite sheet until it

fractured, and the impact strength was recorded. The impact strength of composite material is the fracture energy of the material.

3 Results and Discussions

Cross-sectional area of composite = 60.8mm^2

Average diameter of fibre = 0.41mm

Table 3.1. Mechanical Properties of OPEFBF Composites at Varying Volume Fractions and Aspect Ratios Using *Shape-Preserving-Linear-Interpolant* Type of Fitting to Obtain the Youngs' Modulus and Toughness.

S/N	Fibre volume fraction (%)	Fibre aspect ratio	Ultimate tensile strength (N/mm^2)	Ultimate elongation (mm)	Youngs' modulus (N)	Toughness (N/mm^2)
1	10	24.39	7.40	0.0086	362.52	0.032
2	10	73.17	8.31	0.011	514.00	0.048
3	10	121.95	6.58	0.012	133.00	0.047
4	30	24.39	10.77	0.0013	1198.60	0.074
5	30	73.17	13.98	0.022	738.026	0.170
6	30	121.95	6.17	0.020	908.05	0.100
7	50	24.39	4.77	0.013	805.44	0.044
8	50	73.17	4.95	0.013	1028.00	0.040
9	50	121.95	4.11	0.017	370.68	0.048

3.1.1 Tensile Test Results

Table 3.2 Analysis of Variance Result for Ultimate Tensile Strength

Source	Sum sq.	d.f.	Mean square	F	Prob>F
X1	48.66	2	24.33	6.67	0.053
X2	18.13	2	9.06	2.48	0.19
Error	14.60	4	3.65		
Total	81.38	8			

From Table 3.2, the ANOVA results of tensile strength, it is seen that the prob>F value for fibre volume fraction (X1) of 0.0532 falls within the acceptable range (≤ 0.05), thus the fibre volume fraction is a significant factor at 95% confidence bound. In comparison with the aspect ratio, fibre volume fraction has a more significant effect on the ultimate tensile strength of the composites. Figure 3.1 reveals that there is an increase in the ultimate tensile strength up to an optimum after which there was a corresponding decrease. Circular contour lines from the plot imply that factors significantly affect the property tested and that the optimum so obtained is a global optimum so improvement may not be possible. The coefficient of determination (R^2) obtained was 0.8207, implying 82% variability of ultimate tensile strength as shown in Table 3.3.

The ultimate tensile strength of the polyester laminate is 48N/mm^2 so from the results it can be seen that the addition of fibres to the resin reduced the tensile properties. However, the young's modulus which is about $400\text{-}1000\text{N/mm}^2$ increased to 1500N/mm^2 after the addition of fibres, which implies that added fibres to the polyester resin increased the young's modulus and reduced the tensile strength.

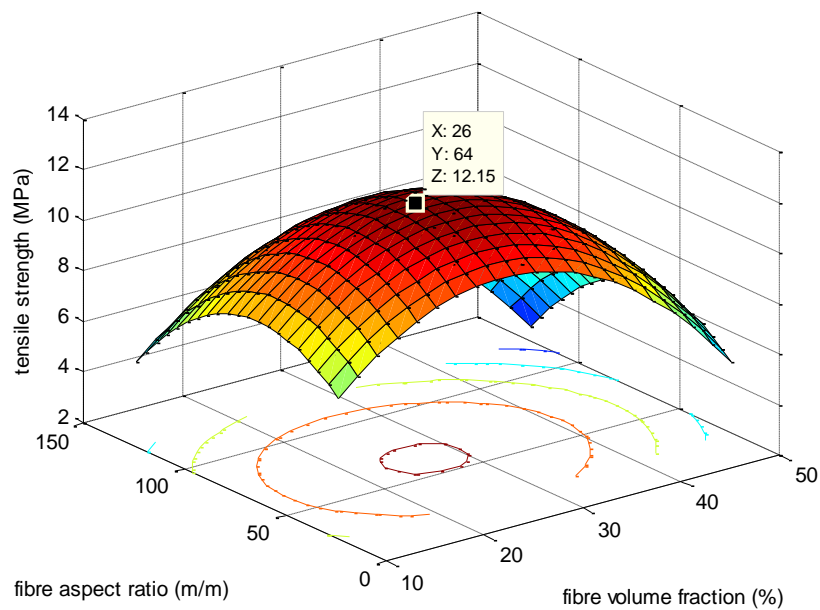


Figure 3.1. 3D plot of tensile strength versus fibre aspect ratio versus fibre volume fraction

Table 3.3. Numerical Results for Model Fit to Experimental Data for Tensile Strength

Variable	Coefficient	Standard Error	T Stat	P-Val	F Stat
Constant	0.42	3.50	0.12	0.91	Sse=14.594
X1	0.57	0.21	2.77	0.050	Dfe=4
X2	0.13	0.084	1.53	0.20	Dfr=4
X1²	-0.011	0.0034	-3.17	0.034	F=4.576
X2²	-0.0010	0.00057	-1.81	0.14	P-val=0.084953
	R ² =0.8207	AdjR ² =0.6413			

$$y=0.42381+0.5725*x1+0.12962*x2-0.010716*x1^2-0.0010277*x2^2$$

Where y is the ultimate tensile strength, x1 is the fibre volume fraction and x2 is the fibre aspect ratio.

The optimum tensile strength of 12.15 N/mm² occurred at a fibre volume fraction of 26% and fibre aspect ratio of 64m/m as can be seen from the surface plot.

3.1.2 Ultimate Elongation

Table 3.4 Analysis of Variance Result for Ultimate Elongation

Source	Sum sq.	d.f.	Mean square	F	Prob>F
X1	0.000030	2	1.50044e-005	0.41	0.6886
X2	0.00013	2	6.59244e-005	1.8	0.2767
Error	0.00015	4	3.65828e-005		
Total	0.00031	8			

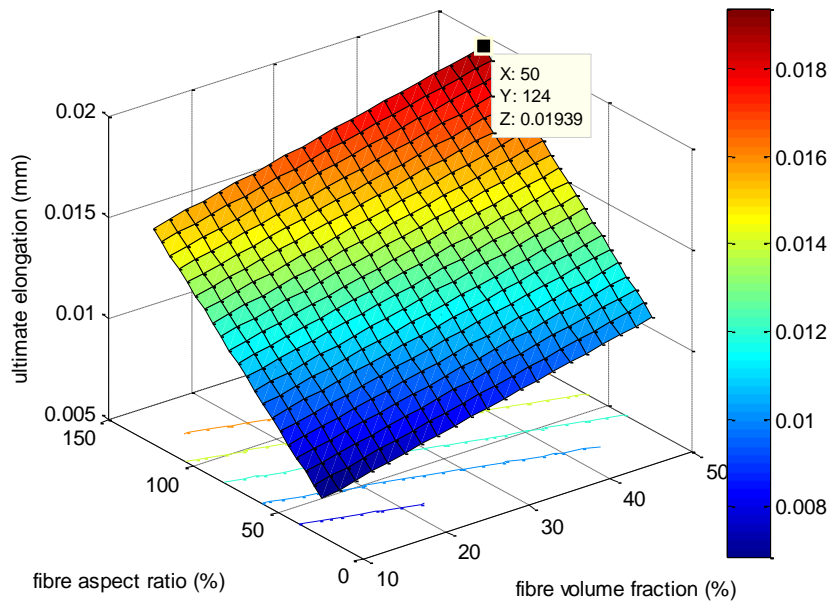


Figure 3.2 3D plot of ultimate elongation vs. fibre aspect ratio and volume fraction

From Table 3.4 ANOVA results for ultimate elongation, it can be seen that the prob>F values for both fibre volume fraction and fibre aspect ratio were greater than 0.1 (90% confidence) suggesting that both factors do not affect significantly the ultimate elongation. In fig 3.2, the contour lines which are parallel indicate that factors do not have a good interaction between them. The P values from t-stats and f-stats in table 3.5 indicate

the same as they didn't fall within the acceptable range of 0.1-0.01(90%-99%) confidence bounds.

Table 3.5. Numerical Results for Model Fit to Experimental Data for Ultimate Elongation

Variable	Coefficient	Standard Error	T Stat	P-Val	F Stat
Constant	0.0038	0.0050	0.75	0.48	Sse=0.000176
X1	0.000093	0.00011	0.84	0.43	Dfe=6
X2	0.000088	0.000045	1.94	0.10	Dfr=2
R²=0.4278	Adj R ² =0.2371			P-val=0.18733	

$$y=0.0038+0.0000933*x1+0.0000881*x2$$

x1 is fibre volume fraction; x2 is fibre aspect ratio, and y is ultimate elongation

The optimum ultimate elongation occurred at 0.01939 at a fibre volume fraction of 50, and fibre aspect ratio of 124 as can be seen from the surface plot.

3.1.3 Young's Modulus Results

Table 4.6 Analysis of Variance Result for Young's Modulus

Source	Sum sq.	d.f.	Mean sq.	F	Prob>F
X1	578352.9	2	289176.5	5.26	0.0758
X2	185903	2	92951.5	1.69	0.2934
Error	219717.9	4	54929.5		
Total	983973.8	8			

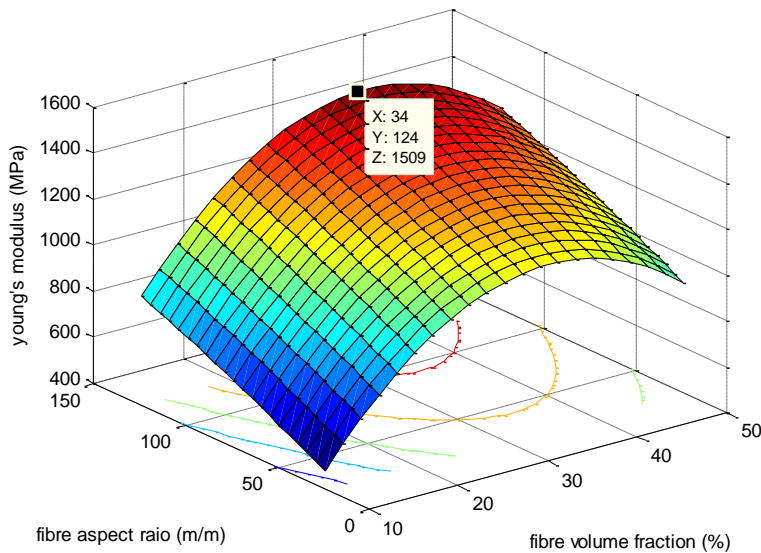


Figure 3.3. 3D-plot of Young modulus versus fibre aspect ratio versus fibre volume fraction.

Table 3.6 indicated that the fibre volume fraction played a more significant role in affecting Young’s modulus of elasticity than fibre aspect ratio based on their prob>F values. From table 3.7 the P-value for t-stats for volume fraction is less than 0.05 which indicates as well how significant a role fibre volume fraction played in the values of Young’s modulus of OPF composites. Fig 3.3, indicated that from the contour lines, there was a good interaction between the factors. R^2 of 0.7767 obtained implied a 78% variability of Young’s modulus.

Table 3.7. Numerical Results for Model Fit to Experimental Data for Young’s Modulus

Variables	Coefficients	Standard error	T stat	P-val	Fstat
Constants	-246.41	430.12	-0.57	0.60	Sse=2.19e-005
X1	71.85	25.31	2.84	0.047	Dfe=4
X2	4.75	10.38	0.46	0.67	Dfr=4
X1²	-1.031	0.41	-2.49	0.068	F=3.4784
X2²	-0.055	0.069	-0.79	0.48	P-val=0.12732

R2=0.7767 Adjusted R2=0.5534

$$y = -246.41 + 71.848 * x_1 + 4.7508 * x_2 - 1.0315 * x_1^2 - 0.0054756 * x_2^2;$$

x1 is fibre volume fraction; x2 is the fibre aspect ratio, and y is the young's modulus

Optimum occurred at a fibre volume fraction of 34 and a fibre aspect ratio of 124.

Optimum Young's modulus is obtained as $1509\text{N/mm}^2 = 1500\text{N/mm}^2$

3.1.4 Toughness

Table 3.8 Analysis of Variance Result for Toughness

Source	Sum sq.	d.f.	Mean square	F	Prob>F
X1	0.011	2	0.0057	4.39	0.098
X2	0.00081	2	0.0004	0.3	0.75
Error	0.0052	4	0.0013		
Total	0.017	8			

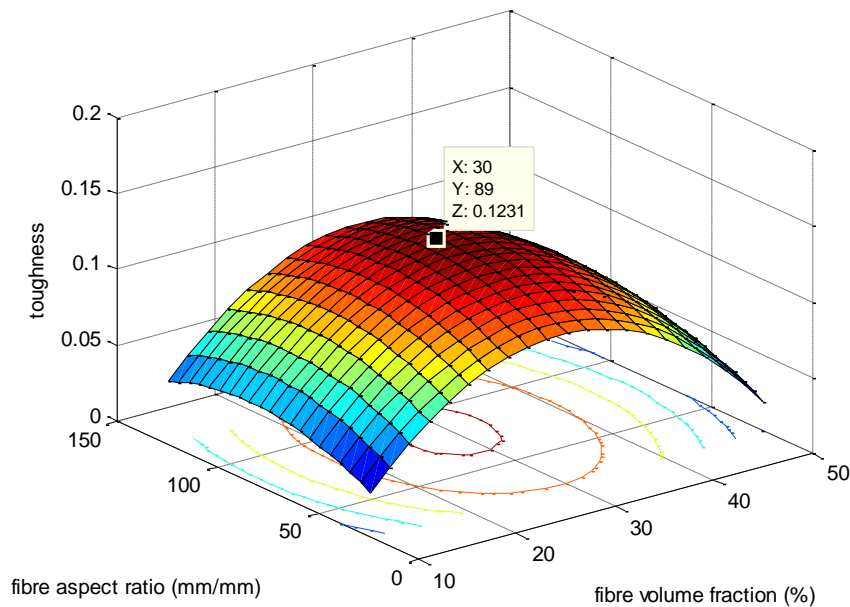


Figure 3.4 3D-plot of toughness versus fibre aspect ratio versus fibre volume fraction

Tables 3.8 and 3.9 showed that the aspect ratio played a more significant role in the toughness of the composites based on their P-value from t-stats and the ANOVA table. Fig 3.4 revealed a quadratic increase in the toughness until optimum was obtained after

which there was a corresponding decrease. The circular contour lines in the plot indicated a good interaction between factors. In addition, the circular contour line indicated a global optimum so an improvement on the optimum may not be possible. R² value of 0.7015 obtained indicated 70% variability in the toughness of the composites.

Table 3.9. Numerical Results for Model Fit to Experimental Data for Toughness

Variables	Coefficients	Standard error	T stat	P-value	Fstat
Constants	-0.085	0.066	-1.28	0.27	Sse=0.0052198
X1	0.011	0.0039	2.83	0.048	Dfe=4
X2	0.0011	0.0016	0.70	0.52	Dfr=4
X1²	-0.00018	-0.000064	-2.94	0.042	F=2.3501
X2²	-0.0000067	0.000011	-0.62	0.57	P-val=0.21412
R²=0.7015	AdjR²=0.4030				

$$y = -0.085091 + 0.011027 * x_1 + 0.0011183 * x_2 - 0.00018798 * x_1^2 - 0.0000066892 * x_2^2$$

x₁ is fibre volume fraction; x₂ is fibre aspect ratio.

Optimum occurred at a fibre volume fraction of 30 and a fibre aspect ratio of 89.

Optimum toughness is obtained as 123.1N/mm².

For the rational type of fitting, Tables 3.11 and 3.12 indicated in correspondence to the values obtained above that the fibre volume fraction played a more significant role than the aspect ratio. However, in comparison, the optimum obtained here is higher than that obtained previously, which indicates a better model fit with rational (linear-quadratic fitting).

Moreso, from tables 3.13 and 3.14, fibre volume fraction had a more significant effect on Young's modulus of elasticity based on their respective values from ANOVA and t-stats and f-stats. An R² value of 0.9247 was obtained showing a better fit when compared to that obtained from a linear fit.

Table 3.10 Mechanical Properties of OPEFBF Composites at Varying Volume Fractions and Aspect Ratios using *Rational* Type of Fitting to Obtain the Youngs’ Modulus and Toughness.

S/N	Fibre volume fraction (%)	Fibre aspect ratio	Ultimate tensile strength (N/mm ²)	Ultimate elongation (mm)	Youngs’ modulus (N)	Toughness (N/mm ²)
1	10	24.39	7.40	0.0086	523.012	0.032
2	10	73.17	8.31	0.011	616.43	0.048
3	10	121.95	6.58	0.012	884.19	0.048
4	30	24.39	10.77	0.0013	831.36	0.072
5	30	73.17	13.98	0.022	800.35	0.17
6	30	121.95	6.17	0.020	958.075	0.16
7	50	24.39	4.77	0.013	879.98	0.043
8	50	73.17	4.95	0.013	935.54	0.040
9	50	121.95	4.11	0.020	837.20	0.063

For the impact test, tables 3.15 and 3.16 showed that both fibre aspect ratio and fibre volume fraction played a very important role as their P-value are less than 0.05 (95% confidence bounds). Fig 3.7 showed a quadratic increase in impact energy up to optimum after which there was a corresponding decrease. The circular contour lines indicated a good interaction between the factors and a global optimum-improvement may not be possible. An R² value of 0.9373 was obtained which implied a good model fit and a 94% variability of the impact energy.

Also, from tables 3.17 and 3.18, the P-value indicated that both fibre volume fraction and fibre aspect ratios significantly affect the impact strength of the composites. The 3-D plot of fig 3.8 showed oval contour lines indicating a good interaction between the factors and a global optimum i.e there may not be a possible improvement on it. An R² value of 0.9117 obtained implies a good model fit and a 91% variability of impact strength.

3.1.5 Toughness

Table 3.11 Analysis of Variance Result for Toughness

Source	Sum sq.	d.f.	Mean square	F	Prob>F
X1	0.018	2	0.0091	7.13	0.048
X2	0.0028	2	0.0014	1.1	0.415
Error	0.0051	4	0.0013		
Total	0.026	8			

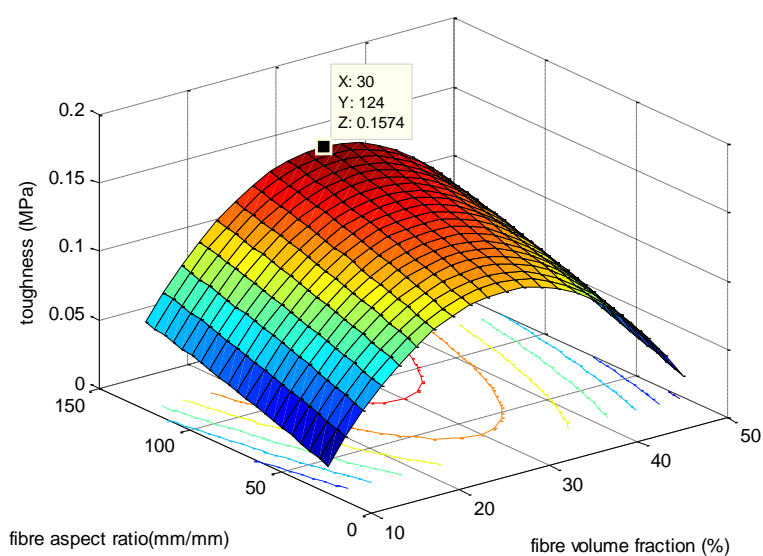


Figure 3.5 3D-plot of toughness versus fibre aspect ratio versus fibre volume fraction for rational model

Table 3.12. Numerical Results for Model Fit to Experimental Data for Toughness

Variables	Coefficients	Standard error	T stat	P-value	Fstat
Constants	-0.11	0.066	-1.69	0.17	Sse=0.0052146
X1	0.014	0.0039	3.67	0.021	Dfe=4
X2	0.00058	0.0016	0.36	0.73	Dfr=4
X1²	-0.00024	-0.000063	-3.77	0.020	F=4.1167
X2²	-0.00000091	0.000011	-0.086	0.94	P-val=0.099658
R²=0.8046	AdjR²=0.61				

$$y = -0.11124 + 0.014174 * x_1 + 0.00057795 * x_2 - 0.000238 * x_1^2 - 0.000000911 * x_2^2$$

x_1 is fibre volume fraction; x_2 is the fibre aspect ratio, and y is the toughness

Optimum occurred at a fibre volume fraction of 30 and a fibre aspect ratio of 124.

Optimum toughness is obtained as 157.4 N/mm^2

3.1.6 Young's Modulus Results

Table 3.13 Analysis of Variance Result for Young's Modulus

Source	Sum sq.	d.f.	Mean sq.	F	Prob>F
X1	80333.5	2	40166.8	3.02	0.1585
X2	35795.6	2	17897.8	1.35	0.357
Error	53137.4	4	13282.4		
Total	169266.6	8			

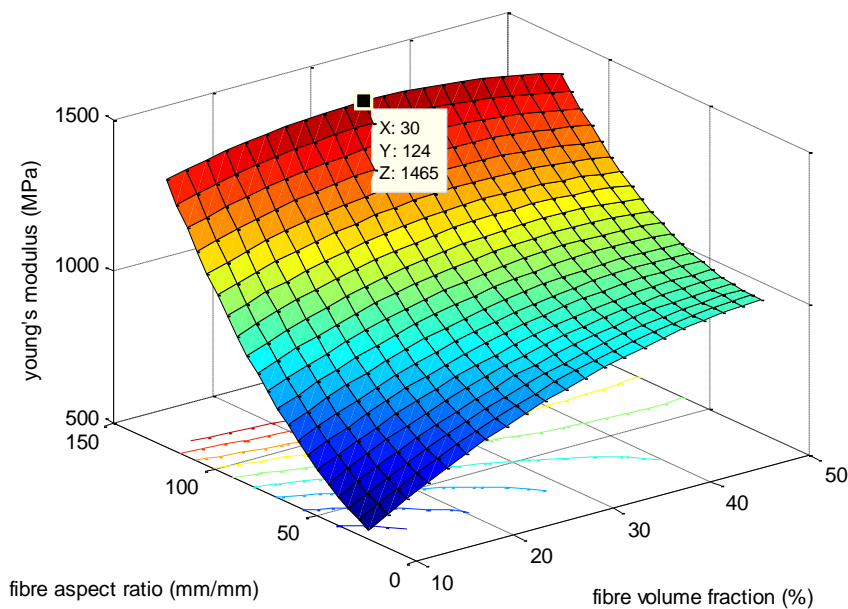


Figure 3.6 3D-plot of Young modulus versus fibre aspect ratio versus fibre volume fraction for rational model

Table 3.14. Numerical Results for Model Fit to Experimental Data for Young’s Modulus

Variables	Coefficients	Standard error	T stat	P-value	Fstat
Constants	235.38	140.30	1.68	0.19	Sse=12745
X1	25.33	7.45	3.40	0.042	Dfe=3
X2	2.45	3.10	0.80	0.480	Dfr=5
X1X2	-0.10	0.033	-3.08	0.054	F=7.3688
X1²	-0.21	0.12	-1.81	0.17	Pval=0.065459
X2²	0.015	0.019	0.76	0.50	
R²=0.9247	AdjR²=0.7992				

$$y=235.3800+25.3260*x_1+2.4531*x_2-0.1030*x_1*x_2-0.2088*x_1^2+0.04791*x_2^2$$

where y is young’s modulus, and x1 is fibre volume fraction; x2 is the fibre aspect ratio.

Optimum occurred at a fibre volume fraction of 30 and a fibre aspect ratio of 124.

Optimum Young’s modulus is obtained as 146.5N/mm²

3.1.7 Impact Energy Test

Table 3.15 Analysis of Variance Results for Impact Energy

Source	Sum sq.	d.f.	Mean sq.	F	Prob>F
X1	9.07	2	4.53	19.98	0.0083
X2	4.50	2	2.25	9.92	0.0282
Error	0.91	4	0.23		
Total	14.47	8			

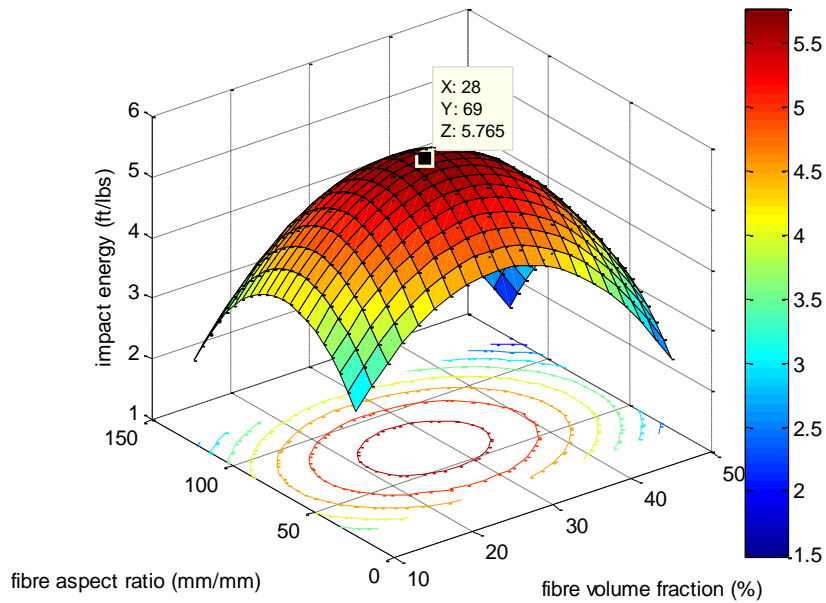


Figure 3.7 3D-plot of Impact energy versus fibre aspect ratio and fibre volume fraction

Table 3.16: Numerical Results for Model Fit to Experimental Data for Impact Energy

Variables	Coefficients	Standard error	T stat	P-value	Fstat
Constants	-0.78	0.87	-0.90	0.42	Sse= 0.90738
X1	0.27	0.051	5.28	0.0062	Dfe=4
X2	0.081	0.021	3.86	0.018	Dfr=4
X1²	-0.0049	0.00084	-5.84	0.0043	F= 14.9486
X2²	-0.00059	0.00014	-4.21	0.014	P-val= 0.0113
R²= 0.9373 AdjR²=0.8746					

$$y = -0.7827 + 0.2718 * x_1 + 0.0814 * x_2 - 0.0049 * x_1^2 - 0.0005960 * x_2^2$$

where y is the impact energy, and x1 is fibre volume fraction; x2 is the fibre aspect ratio.

The optimum 307.72J/m (5.77ft-lbs/in) occurred at a fibre volume fraction of 28, and an aspect ratio of 69 as can be seen from the surface plot.

3.1.8 Impact Strength Test Results

Table 3.17 Analysis of Variance Result for Impact Strength

Source	Sum sq.	d.f.	Mean sq.	F	Prob>F
X1	0.23	2	0.12	15.13	0.0136
X2	0.084	2	0.042	5.53	0.0705
Error	0.030	4	0.0076		
Total	0.35	8			

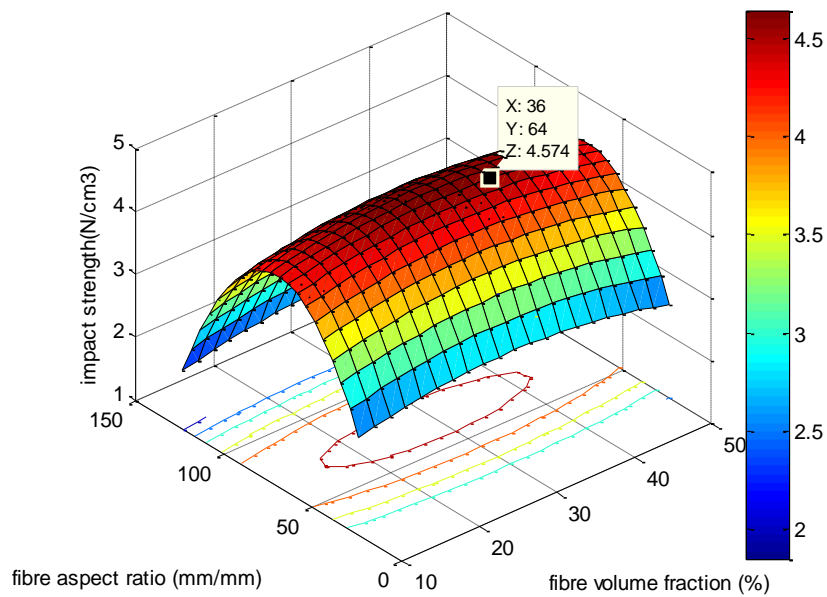


Figure 3.8 3D-plot of Impact strength versus fibre aspect ratio versus fibre volume fraction

Table 3.18. Numerical Results for Model Fit to Experimental Data for Impact Strength

Variables	Coefficients	Standard error	T stat	P-value	Fstat
Constants	-0.20	0.16	-1.27	0.27	Sse= 0.0305
X1	0.049	0.0094	5.16	0.0067	Dfe=4
X2	0.012	0.0038	3.04	0.038	Dfr=4
X1²	-0.00084	0.00015	-5.43	0.0056	F= 10.33
X2²	-0.00084	0.000025	- 3.24	0.032	P-val= 0.0220
R²= 0.9117 AdjR²=0.8235					

$$y = -0.2029 + 0.0487 * x_1 + 0.118 * x_2 - 0.0008375 * x_1^2 - 0.0008405 * x_2^2;$$

where y is the impact strength and x1 is fibre volume fraction; x2 is the fibre aspect ratio. The optimum 0.046N/mm² occurred at a fibre volume fraction of 36, and a fibre aspect ratio of 64 as can be seen from the surface plot.

Mean energy absorption capacity is given as s

$$U = \frac{A_{max}^2 \times A_0}{E_{mean}}$$

Where

A_{max} = maximum breaking stress of the sample

A₀ = original length of the sample = 160mm = 0.16m

E_{mean} = Mean Young modulus of elasticity calculated

$$E_{mean} = \frac{362.52 + 514 + 133 + 1198.6 + 738.0256 + 908.05 + 805.44 + 1028 + 370.6796}{9} = 673.15 \text{ N/mm}^2$$

$$= 673.15 * 10^6 \text{ N/m}^2$$

Mean energy absorption capacity is, therefore;

$$U_m = \frac{U_1 + U_2 + \dots + U_9}{9}$$

$$U_m = 0.2 \text{ J}$$

4 Conclusion

This project work is based on modelling the mechanical properties of OPR composites was done and the properties tested here include ultimate tensile strength, toughness, Young's modulus, impact strength and impact energy. Based on the results, optimization was carried out and the optimum value for each property tested was determined.

From this work, it was found that the fibre volume fraction significantly affects the properties more than the aspect ratio. For ultimate tensile strength optimization that the optimum obtained was a global one at fibre volume fraction and aspect ratio of 26% and 64 respectively. The optimum ultimate tensile strength was 12.15N/mm². For Young's modulus, optimization revealed that at a fibre volume fraction of 34% and aspect ratio of 124, the optimum value for Young's modulus was obtained to be 1509 N/mm².

For toughness, the optimization carried out showed an optimum value of 0.1231 N/mm² at a fibre volume fraction of 30% and an aspect ratio of 89. For the rational (linear-quadratic) type of fitting, the optimum obtained for toughness was 0.16 N/mm² at a fibre volume fraction of 30% and aspect ratio of 124. Also, the optimum obtained here for Young's modulus was found to be 1465 N/mm² at a 30% volume fraction and an aspect ratio of 124. For impact strength, optimization indicated a global optimum at values of aspect ratio and fibre volume fraction of 69 and 28% respectively. An optimum value of impact strength of 307.72J/m (5.77ft/lbs) was obtained.

Acknowledgements

I want to specially acknowledge Engr. Dr Emmanuel C. Osoka for his relentless effort in guiding and supervising this work and ensuring I conduct resourceful research.

References

- [1] R. M. Guedes and J. Xavier “Understanding and Predicting Stiffness in Advanced Fibre-Reinforced Polymer (FRP) Composites for Structural Applications”, In *Advanced Fibre-Reinforced Polymer (FRP) Composites for Structural Applications* (pp. 298-360). Woodhead Publishing. 2013.
- [2] J. P. Jose, S. Thomas, J. Kuruvilla, S. K. Malhotra, K. Goda, M. S. Sreekala, “Advances in Polymer Composites: Macro-and Microcomposites—State of The Art, New Challenges, and Opportunities”, *Polymer composites*, **1**, 3-16. 2012.
- [3] J. Kuruvilla, R. D. Toledo Filho, J. Beena, T. Sabu, and L. H. Carvalho, “A Review on Sisal Fiber Reinforced Polymer Composites”, *Revista Brasileira de Engenharia Agrícola e Ambiental*, **3**(3), 367-379. 1999.
- [4] X. Li, L. G. Tabiland, S. Panigrahi, “Chemical Treatments of Natural Fibre for Use in Natural Fibre-Reinforced Composites: A Review, *Journal of Polymers and the Environment*”, **15**(1), 25-33. 2007.
- [5] S.M. Lee, D. Cho, W.H. Park, S.G. Lee, S.O. Han, and L.T. Drzal, “Novel Silk/Poly (Butylene Succinate) Biocomposites: The Effects of Short Fibre Content on their Mechanical and Thermal Properties”, *Composites Science and Technology*, **65**, 647-657. 2005.
- [6] H. Y. Cheung, M. P. Ho, K. T. Lau, F. Cardona, and D. Hui, “Natural Fibre-Reinforced Composites for Bioengineering and Environmental Engineering Applications”, *Composites Part B: Engineering*, **40**(7), 655-663. 2009.
- [7] E. C. Osoka and O. D. Onukwuli, *The Optimum Condition for Mercerization of Oil Palm Empty Fruit Bunch Fibre*, *International Journal of Innovative Research in Computer Science and Technology*, **3**(4), 50-56. 2015.
- [8] D. Jones, G. O. Ormondroyd, S. F. Curling, C. M. Popescu, and M. C. Popescu, “Chemical Compositions of Natural Fibres. In *Advanced High Strength Natural Fibre Composites in Construction*”, (pp. 23-58), Woodhead Publishing, 2017.
- [9] M. Y. Hashim, A. M. Amin, O. M. F. Marwah, M. H. Othman, M. R. M. Yunus, and N. C. Huat, “The Effect of Alkali Treatment Under Various Conditions On

- Physical Properties of Kenaf Fibre”, In *Journal of Physics: Conference Series* **914**(1), 012030. IOP Publishing, 2017.
- [10] A. K. Mohanty, M. Misra, and L. T. Drzal, “Surface Modifications of Natural Fibres and Performance Of The Resulting Biocomposites: An Overview”, *Composite interfaces*, **8**(5), 313-343. 2001
- [11] A. Bismarck, A. K. Mohanty, I. Aranberri-Askargorta, S. Czaplá, M. Misra, G. Hinrichsen and J. Springer. “Surface Characterization of Natural Fibres; Surface Properties and The Water Up-Take Behavior of Modified Sisal and Coir Fibres”, *Green chemistry*, **3**(2), 100-107. 2001
- [12] L. A. Pothan, J. George, & S. Thomas, “Effect of Fibre Surface Treatments on the Fibre–Matrix Interaction in Banana Fibre Reinforced Polyester Composites”, *Composite Interfaces*, **9**(4), 335-353. 2002.
- [13] N. T. Phuong, C. Sollogoub and A. Guinault, “Relationship Between Fibre Chemical Treatment and Properties of Recycled Pp/Bamboo Fibre Composites”, *Journal of Reinforced Plastics and Composites*, **29**(21), 3244-3256. 2010
- [14] T., Padmavathi, S. V. Naidu & R. M. V. G. K. Rao. “Studies On Mechanical Behavior of Surface Modified Sisal Fibre–Epoxy Composites”, *Journal of Reinforced Plastics and Composites*, **31**(8), 519-532. 2012.
- [15] Petinakis, E., Yu, L., Simon, G., & Dean, K. (2013). “Natural Fibre Bio-Composites Incorporating Poly (Lactic Acid)”, *Fibre reinforced polymers-The technology applied for concrete repair*, 41-59. 2013.
- [16] O. Faruk, A. K. Bledzki, H. P. Fink & M. Sain, “Biocomposites Reinforced with Natural Fibres: 2000–2010”, *Progress in polymer science*, **37**(11), 1552-1596. 2012.
- [17] M. Y. Hashim, A. Zaidi, A. Mujahid, & S. Ariffin, “Plant Fiber Reinforced Polymer Matrix Composite: A Discussion On Composite Fabrication and Characterization Technique”. In *Seminar to Faculty of Civil and Environmental Engineering (FKAAS)*, Universiti Tun Hussein Onn Malaysia (UTHM). 2012.

- [18] C. M. Ewulonu and , I. O. Igwe. “Properties of Oil Palm Empty Fruit Bunch Fibre Filled High Density Polyethylene”. *International journal of engineering and technology*, **3**(6), 2012.
- [19] A., Athijayamani, M. Thiruchitrambalam, V. Manikandan and B. Pazhanivel, “Mechanical Properties of Natural Fibers Reinforced Polyester Hybrid Composite”, *International Journal of Plastics Technology*, **14**(1), 104-116. 2010.
- [20] S. M. Sapuan, A. Leenie, M. Harimi, and Y. K. Beng, “Mechanical Properties of Woven Banana Fibre Reinforced Epoxy Composites”. *Materials & design*, **27**(8), 689-693. 2006.
- [21] F. K. A. Nugraha, “Shrinkage of Biocomposite Material Specimens [HA/Bioplastic/Serisin] Printed using a 3D Printer using the Taguchi Method”, *International Journal of Applied Sciences and Smart Technologies*, **4**(1), 89-96. 2022.

This page intentionally left blank

Comparative Study of Master Oil (MO) and Lophira Lanceolata (Ochnaceae) Oil (LLO) Lubricants in Sewing Machines

J. B Yerima^{1,*}, G. O Mokoro¹, D. William² and S. D Najoji³

¹ Department of Physics, Modibbo Adama University, P M B 2076 Yola, Nigeria.

² Department of Industrial Mathematics, Modibbo Adama University, P M B 2076 Yola, Nigeria.

³ Department of Basic Science, Federal Polytechnic Damaturu, P M B 1006 Damaturu, Yobe State, Nigeria.

*Corresponding Author: bjyerima@gmail.com

(Received 15-09-2022; Revised 09-10-2022; Accepted 26-10-2022)

Abstract

In this paper the thermodynamic properties (Fire, Flash, Cloud, Pour points, and Volatility) of master oil (MO) and locally processed Lophira lanceolata oil (LLO) were determined using standard laboratory methods. The results show that LLO has lower volatility which means it can stay longer in moving parts of a machine than MO. Also, the results show that the flash and fire points of the lubricants lie within the maximum operating temperature range (<300 oC) of sewing machines. The high pour point (14 oC) and cloud point (23 oC) of LLO limit its use as a lubricant in low temperate regions of the world as opposed to -14 oC and -7 oC respectively for MO which has universal application. This implies LLO needs to be chemically blended with some additive agents that can lower its Pour point so that it can favourably compete with other lubricants used in sewing machines worldwide.

Keywords: lubricants, thermodynamic properties, volatility, temperature, and oil.



1. Introduction

Liquids are one of the three phases of matter. The molecules of a liquid are loosely packed together and a liquid seeks its level or it takes the shape of its container. Liquids have a definite volume and no form elasticity (no shear modulus), and they are characterized by their strong inter-atomic forces or low compressibility because a slight decrease in the already small inter - atomic separations gives high inter-atomic forces of repulsion [1]. Liquids exist in various forms such as water, oils, solutions, molten solids, and condensed gases to mention but a few. Oils are naturally occurring inorganic or organic substances that are not soluble in water. Most oils containing organic materials are made up of carbon, hydrogen, oxygen, and some elements like phosphorus. Oils are mostly extracted from living animals and plants as well as their dead remains in rocks underground. Liquids like other states of matter have both physical and chemical properties which make them have wide applications in everyday life. For instance, viscosity has made liquids useful as lubricants in moving parts of machines. Furthermore, viscosity is a good parameter for controlling oil quality because it is sensitive to minor variations in temperature, concentration, homogeneity, and the shape and size of molecules. Lubricant's viscosity and blending agents influence the rate at which sensitive components oxidize at the liquid's surface [2]. Other physical properties of liquids that make them useful lubricants include fire point, cloud point, pour point, flash point, and volatility. Thus, the knowledge of the physical properties of liquids is very important, and therefore there is a need to devise means of measuring or determining them.

There are many devices for measuring these physical properties of liquids available in the markets today. The simple and sophisticated forms of these instruments for measuring the physical properties of liquids are available and affordable in developed countries but they are expensive and inadequate in developing countries like Nigeria. This makes it difficult to explore and harness useful information on the potential of locally produced oils in Nigeria. For example, over the years, through personal investigations and interactions with some individuals in the Ganye local government area of Adamawa State, we observed that the majority of tailors make use of *Lophira lanceolata* oil (LLO) as a lubricant instead of the conventional Master oil (MO) in their sewing

machines. The tailors ascertained that LLO is a good lubricant, most available, and cheaper than MO. It is against this background that we were motivated to determine the pour, cloud, flash, fire and flash points, and volatility of LLO to ascertain its relative effectiveness as a lubricant in sewing machines.

2. Research Methodology

Lophira, an Ochnaceae family tree also called as Meni oil tree or False shea and known locally as Beung (in Chamba language) and Namijin Kadanya (in Hausa language), grows both in dry and moist evergreen mangroves of tropical Africa [3]. *Lophira lanceolata* is the predominant species in dry savannah areas, while *Lophira Procera* is found in West Africa's tropical rain forests. The *Lophira* tree blooms between the months of December and February. Most parts of the tree (bark, root bark, leaves, and leafy shoots) have been used for traditional medicine. The leaves are additionally employed in traditional rituals and given to livestock [4]. The fruit is bottle-shaped, lobed at the apex, and about 3 cm long, with continual sepals, two of which are expanded and wing-like. *Lophira lanceolata* seed contains 25 to 30% shell and 70 to 75% kernel, with the remainder yielding approximately 40% to more than 50% yellowish or cream-colored semi-solid fat [4]. In some Nigerian communities as well as other West African countries, the oil is used in preparing food as well as as a hair lotion and lice treatment. Despite their bitter and astringent taste, the seeds are consumed in some regions [4].

Lophira Lanceolata oil has the possibilities to be used as both animal feed and a source of food for humans. Currently, only the fat obtained from the seed is used, which represents about 40 - 50% weight by weight [4]. Whenever the lipid is collected, the cake is considered waste and thus discarded. Regardless of the fact that defatted cake could be an excellent source of protein, it is not utilized as such. There is insufficient knowledge and studies on the chemical makeup of *Lophira Lanceolata* seeds [5]. *Lophira Lanceolata* oil's viscosity and density decrease with temperature, suggesting that it is a non-Newtonian liquid, a great lubricant and refrigerant in non-vehicle engines, an attractive corrosion inhibitor, and has bio-fuel prospects [6]. And according to

some research findings [7], the chemical classification of *Lophira lanceolata* oil indicated that it contains polyunsaturated fatty acids (52.6%) and is significant in tocopherols (3.61 mg/100g). The bio - fuel potential was 38.78 (MJ/L), the iodine value was 72.4 (gI₂/100g), the saponification value was 223.6 (MgKOH/g), and the free acid was 1.074% [6]. *Lophira Lanceolata* seeds can be pressed into oil and used as a hair lotion or on the skin to avoid dry skin. This is because of the fact that it is a less volatile and efficient lubricant. [4].

Lubricating oil is the least volatile, most stable portion of petroleum products. Lubricating oils have hydrocarbon structures, with 20 to 70 carbon atoms per molecule, because petroleum products are primarily composed of hydrocarbons. Lubricating oil molecules are divided into three categories paraffinic, naphthenic, and aromatic. Paraffinic molecules mostly have straight chains, are waxy, have a high pour point, good viscosity, and are more temperature stable. Naphthenic molecules are straight chains with a high percentage of five-membered ring structures and a lower percentage of six-membered ring structures. They generally have a low pour point. As a consequence, they are used as cooling oils. They are extremely harmful to humans and are seldom used as lubricating oils. Aromatics are straight chains with six-membered ring benzene structures. In practice, no sharp distinction exists between these various groupings as many lubricating oil molecules are a combination, to varying degrees, of the different types of hydrocarbons [8]. Lubricating oils are fluids such as engine oils, gear, hydraulic oils, turbine oils, etc., used to reduce friction between moving surfaces. They also serve to remove heat from working parts in machinery created by moving surfaces and provide a protective layer on the metal surfaces to avoid corrosion. They as well serve as sealers, filling microscopic ridges and valleys in metal surfaces to enhance the effectiveness of machines and equipment. Furthermore, they act as a cleaning agent, removing dirt and other unwanted materials that might damage bearings or other parts that are operated in close tolerance. Waste is removed from the engine oil or transmission filters. Lubricating oils are typically blended with a range of chemical additives to produce products that last longer and make it possible for machineries to function better in tough operational conditions. Nevertheless, the effectiveness of the lubricants declines over time as the additives undergo chemical changes and

the oil becomes adulterated with a diverse array of undesirable pollutants as a result of numerous interactions between the components [9].

Oil is used to lubricate moving parts of sewing machines and for the parts to run low or dry of oil will cause the bearings and bushings to prematurely wear, tear, and possibly seize. The effects of running with low or no oil are the most common reason we see that machines are sent in for repair. They are two types of sewing machine oil; they include Synthetic oil (Master oil) and Petroleum oil. The sewing machine is comprised of base oil aromatic (LVI) plus naphthenic (MVI) and paraffinic (HVI) and additives. These additives give it lube protection, performance, and surface protection. The Flash point, fire point, cloud point, and pour point are all factors that affect the efficiency and dependability of sewing machine oil. The Flash point is the temperature at which the lubricant oil gives off enough vapors to kindle for a fraction of a second when a tiny flame is brought near it, while the Fire point is the lowest temperature at which the lubricant oil vapors burn continuously for a minimum of five seconds whenever a tiny flame is brought near it. The fire points are usually 5 to 40 °C higher than the flash points. The flash and fire points have no direct effect on the oil's lubricating property, but they are important when the oil is exposed to high-temperature service. An excellent lubricant must possess a flash point that is at least greater than the temperature at which it will be used. This protects against the risk of fire throughout operation. A cloud point is the temperature at which a cooling liquid would seem cloudy or hazy, even though the pour point is the temperature at which the lubricant oil ceases to flow or pour. The cloud and pour points of lubricant oil appear to suggest its appropriateness in cold conditions. Lubricant oil used in a machine operating at low temperatures must have a low pour point; otherwise, lubricant oil solidification will cause machine parts to jam.

It is worth noting that temperature is one of the factors that makes oils to have wide applications in science and engineering [11, 12].

3. Experiments

There were four separate experiments carried out in this work. All the experiments were carried out in the Petroleum Chemistry Department, America University of Nigeria, Yola, Adamawa state, Nigeria.

(a) Cloud Point of MO and LLO.

Samples of the MO and LLO were heated to a temperature slightly above room temperature and were poured into sample bottles with thermometers attached to them. The sample bottles were placed in a water bath of Seta Cloud and pour point Cryostat machine of accuracy ± 1.5 °C. The sample bottles were cooled down before being inspected at frequent intervals to check for cloudiness. Thus, every oil sample's cloud point was defined as the temperature when the portion of the thermometer submerged in the oil was no longer visible when seen as horizontally through the oil in the bottle.

(b) Pour Point of MO and LLO.

Samples of the MO and LLO at a temperature slightly above room temperature were poured into sample bottles in a water bath of Seta Cloud and pour point Cryostat machine of accuracy ± 1.5 °C. Each sample was assessed at regular intervals to see when it stopped flowing. The liquid's pour point was defined by the temperature when the oil surface did not sag for 5 seconds.

(c) Flash Point and Fire Point of MO and LLO

Specimens of MO and LLO were poured into separate sample bottles inside an automatic digital PM-93 flash and fire point tester machine of accuracy ± 0.1 °C. The flash and fire points were read directly from the tester machine.

(d) Volatility of MO and LLO.

A known mass of 7.4 g for each sample of oil was weighed utilizing a digital balance and placed in separate similar Petri dishes. The two oil samples in the Petri dishes were left to evaporate at the same temperature assuming other weather conditions remained constant. The masses of the oils remaining were recorded utilizing a sensitive digital balance at 20 minutes intervals.

4. Results and Discussion

Table 1. Cloud, Pour, Flash, and Fire points of MO and LLO.

Liquid property	Master oil (MO)	Lophira lanceolata oil (LLO)
Cloud point	-7.0	23.0
Pour point	-14.0	14.0
Fire point	200.5	294.3
Flash point	198.1	291.5

The experimental values of the cloud, pour, fire and flash points for MO are -7.0°C , -14.0°C , 200.5°C , 198.1°C and for LLO are 23.0°C , 14.0°C , 294.3°C , 295.1°C respectively (Table 1). These quantities for MO are less than those of LLO. The low pour point of MO shows the possibility of its use even in low-temperature regions of the world as opposed to LLO. For LLO to be applicable in low temperate regions its pour point should be lowered, if possible, below that of MO. This can be achieved by chemically blending LLO with some additives. The flash points and fire points of these oils lie within the maximum temperature range ($100\text{-}300^{\circ}\text{C}$) of sewing machines depending on the sewing conditions [10]. Thus, both oils can be safely used as lubricants in sewing machines in temperate regions except LLO needs some modifications such as lowering its pour point to make it applicable even in the Polar Regions of the world.

7.4 g each of MO and LLO kept in the same type of open containers so that they freely evaporated under the same weather conditions and the values of their masses M remaining after time t was recorded in Table 2. The interpretation of the mass-time data can be done in two ways namely linear and exponential relations. In the case of linear relation, mass is plotted against time while in the case of exponential relation, the natural logarithm of mass is plotted against time.

Table 2. Mass remaining at a given time for MO and LLO.

Time (minutes)	Mass (g)	
	LLO	MO
0	7.4	7.4
20	7.3	7.1
40	7.2	6.8
60	6.9	6.5
80	6.8	6.3
100	6.7	6.1

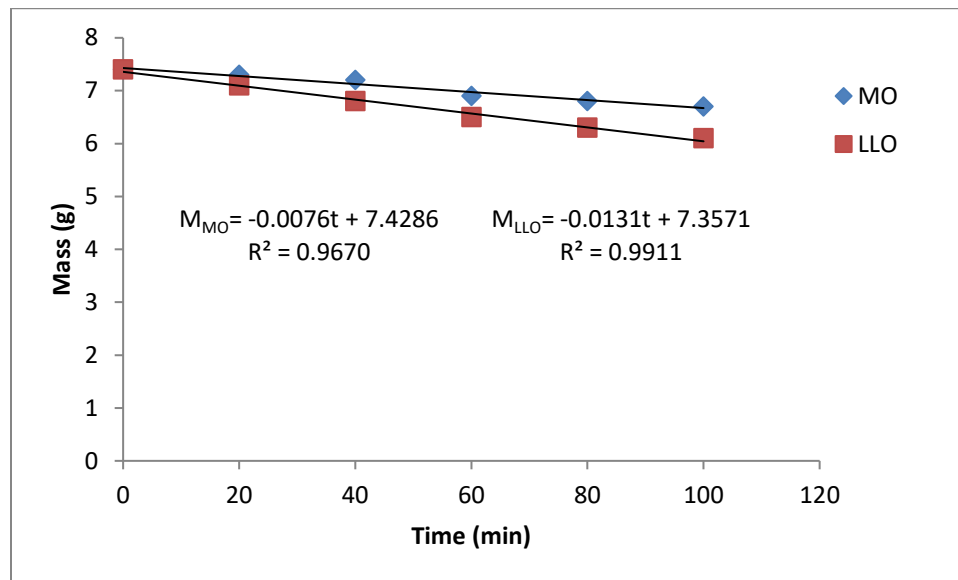


Figure 1. Mass-time lines for MO and LLO

Figure 1 represents the linear relationship and it shows that for both oils the mass remaining decreases with time. The graph of mass, M remaining against time, t yields the following regression lines

$$M_{LLO} = -0.0131t + 7.3571, \quad R^2 = 0.9911 \tag{4.6}$$

$$M_{MO} = -0.0076t + 7.4286, \quad R^2 = 0.9670 \tag{4.7}$$

where R^2 is the goodness of fit, the subscripts LLO and MO represent lophira lanceolata oil and master oil respectively. The regression lines show that the rate of evaporation of MO is higher than that of LLO. This means MO is more volatile than LLO. Therefore, LLO has the advantage of staying longer on the machine parts than the same amount of MO even though LLO is not treated as compared to the synthetic Master oil. The low volatility of LLO makes it a better lubricant than MO when they are used for a long period.

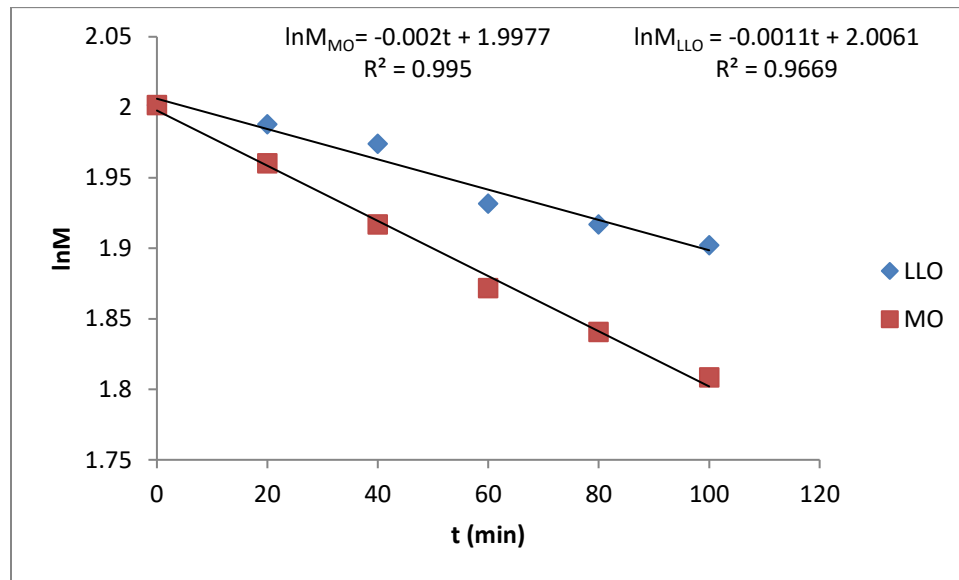


Figure 2. Natural log mass-time lines for MO and LLO

In the case of exponential law, since evaporation obeys the law of exponential decay, the mass M of oil remaining at a time t can be written as $M = M_0 e^{-\lambda t}$ where M_0 is the initial mass at $t=0$, λ is the decay constant and e is the number 2.718 to 3 places of decimal. The corresponding half-life or time required for half the amount of oil to evaporate is given by $t_{\frac{1}{2}} = \frac{0.693}{\lambda}$. Fig 3 represents the plot of the natural logarithm of mass of oil remaining at time t against time which yields the following regression equations

$$\ln M_{LLO} = -0.0011t + 2.0061, R^2=0.9669 \quad 4.8$$

$$\ln M_{MO} = -0.0020t + 1.9977, R^2=0.9950 \quad 4.9$$

The regression equations reveal that the values of the decay constant, λ , and half-life $t_{\frac{1}{2}}$ for MO and LLO are ($\lambda_{MO}=0.0020$, $\lambda_{LLO}=0.0011$) and ($t_{\frac{1}{2}}(MO) = 346.5 \text{ min}$, $t_{\frac{1}{2}}(LLO) = 630.0 \text{ min}$) respectively. This shows that MO has larger decay constant, almost twice that of LLO, meaning MO evaporates faster than LLO which is in agreement with the linear case. Finally, the exponential relations for LLO and MO are given by $M = M_o e^{-0.0011t}$ and $M = M_o e^{-0.0020t}$ respectively.

5. Conclusion

The study of the flash, fire, cloud, and pour points, and Volatility of master oil (MO) and locally processed lophira lanceolata oil (LLO) were carried out to compare and establish their suitability and effectiveness as lubricants in sewing machines. The results show that LLO has lower volatility than MO, that is, LLO lasts longer in moving parts of a machine than MO. Also, it is observed that the flash point and fire point of the lubricants, MO and LLO, lie within the maximum operating temperature range (<100-300 °C) of sewing machines. The pour point (14 °C) and cloud point (23 °C) of LLO are higher than those of MO at -14 °C and -7 °C respectively. The high pour point of LLO limits its use as a lubricant in low temperate regions of the world and therefore needs to be chemically blended with some additive agents that can lower its Pour point so that it can favourably compete with other lubricants used in sewing machines worldwide. Finally, the linear relations $M_{LLO} = -0.0131t + 7.3571$, $R^2=0.9911$ and $M_O = -0.0076t + 7.4286$, $R^2=0.9670$ and exponential relations $M = M_o e^{-0.0011t}$ and $M = M_o e^{-0.0020t}$ were obtained respectively where all the symbols have their usual meanings.

References

- [1] J.B. Yerima, J.S Madugu,P. Timtere, and Y.M David. “Dependence of viscosity and density of Nigerian lophira lanceolata oil (ochraceae) on temperature”. *Physical Review and Research International*.**2**(3):125-132. 2012.
- [2] B.F Adeosun, F.O Adu, K.O Ipinmoroti, “Thermodynamics of viscous flow of some Nigerian vegetable oils”. *NJET*, **14**(2), 165-170. 1997.
- [3] R. Ghogomu, and B.L Sondengam. “Two new cleaved bioflavonoids from Lophira lanceolata”. *J. Nat. Prod.* **52**(2),284-288. 1989.
- [4] H.M Burkill, “A Review of Daziel’s the useful Plants of West Africa”. *Royal Botanical Garden Kew* .**1**(3),12-34. 1985
- [5] I.C Eromosele, “Studies on the Chemical composition and Physicochemical properties of Seeds of some Wild plants”, *Plant Foods for Human Nutrition*. **46**, 361-365. 1994.
- [6] F. Samuel, and I.K Maimuna, “Biomass potentials of lophira lanceolata fruit as a renewable energy source”, *Africa journal of biotechnology*, **7**(3),308-310. 2008.
- [7] G. Nonviho, C. Paris, and L. Muniglia, “Chemical characterization of Lophira lanceolata and Carapa procera seed oils: Analysis of Fatty Acids, Sterols, Tocopherols and Tocotrienols”. *Research Journal of Chemical Sciences*. **4**(9), 57-62. 2014.
- [8] H. Yu-Lung and L. Chun-Chu. “Evaluation and Selection of Regeneration of Waste Lubricating Oil Technology”. *J. Environ Monit.* 2010.
- [9] W.B Dennis, "Used oil: resource or pollutant?". *Technology Review*, 46-52. 2010
- [10] A. Mazari, and A. Havelka. “Sewing machine needle temperature of an industrial lockstitch machine,” *J. Industria Textila*. **65**(6), 335-339. 2014.
- [11] K. C Wanta, I.C.N Simanungkalit, E. P. Bahri, R.F Susanti, G.P Gemilar, W. Astuti, and H. T. B. M Petrus. “Study of Nickel Extraction Process from Spent Catalysts with Hydrochloric Acid Solution: Effect of Temperature and Kinetics Study”, *International Journal of Applied Sciences and Smart Technologies*, **3**(2), 161–170. 2021

- [12] P.S. Prabowo, S. Mardikus, and E. Credo. “Heat Transfer Characteristic on Wing Pairs Vortex Generator using 3D Simulation of Computational Fluid Dynamic”, *International Journal of Applied Sciences and Smart Technologies*, **3**(2), 215–224. 2021.

Design of Someone's Character Identification Based on Handwriting Patterns Using Support Vector Machine

R. A. Kumalasanti^{1,*}

¹Department of Informatics, Faculty of Science and Technology, Sanata Dharma University, Yogyakarta, Indonesia

**Corresponding Author: rosalia.santi@usd.ac.id*

(Received 01-11-2022; Revised 21-11-2022; Accepted 28-11-2022)

Abstract

Image processing has a fairly broad scope and is rich in innovation. Today, image processing has developed with various reliable methods in almost all aspects of life. One of the uses of technology in the field of image processing is biometric identification. Biometric is a system that utilizes specific data in the form of individual physical characters in the process of identifying and validating data. There is also a biometric attribute that will be developed in this study is handwriting. The handwriting pattern of each individual has a different character and uniqueness so that it can be used as an identity. The uniqueness of this handwriting will be studied with the aim of recognizing a person's character or personality. If someone's personality data has been obtained, this can help the process of recruiting prospective employees in a company by simply reading from handwriting patterns. Handwriting can be studied by combining the science of Psychology so that it can provide output in the form of a person's characteristics or personality. This research will be developed using the multi class Support Vector Machine (SVM) classification. The preprocessing stage in the form of

binarization, thinning and data extraction will also greatly affect the reliability of the system. Simulations with variations of variables and parameters are expected to obtain optimal accuracy.

Keywords: handwriting, biometric, SVM

1 Introduction

Digital image processing is digital manipulation and interpretation of images using a computer. Image processing has a fairly broad scope and is still being developed in various aspects of life. This shows that image processing has a good impact on technological developments in this era. Digitalization is something that is already familiar to hear because almost all daily activities utilize digital data. Information in the form of digital data has a flexible nature so that it can be used for certain purposes. when COVID-19 hit, activities & social interactions were increasingly restricted in order to break the chain of the virus. This has an impact on social sustainability which is increasingly limited. An example is the recruitment of prospective employees which is quite complex, starting from a psychological test to interviews. The Phycotest aims to find out the character of the prospective employee and an interview test is conducted to see the gestures and how to answer each question given to the prospective employee to be assessed. Some of these tests are sometimes added to other tests which are quite time-consuming. This becomes less effective when it has to be done in the present because social needs are being restricted. Here image processing can be a solution, namely by using digital data to identify a person's character through handwriting. Handwriting is one of the biometric attributes that can be used to identify other than fingerprints, facial recognition, voice, and many more. A person's hand writing has its own uniqueness because it can be seen from the firmness of the strokes, the distance between one word and another, the distance between the lines / boundaries of the paper used [1]. These characteristics can be used to see explicitly the characteristics of a person as an individual. If a person's character has been obtained, the recruitment activities for prospective employees can run effectively and efficiently without having to meet face to face.

In this research, we will try to use SVM (support Vector Machine) with the same data set, namely handwriting. Handwriting will be retrieved from manual writing offline (on paper) and then scanned for pre-processing to the testing stage. Handwriting will be trained and tested to get the characteristics of each individual.

2 Research Methodology

Handwriting is one of the biometric attributes that can be used as authentic data because each individual's handwriting is unique. Emphasis when writing, the firmness of the strokes, the distance between one word and another, the distance between the lines and the margins of writing and much more. In this study, handwriting is used to read a person's character. Computer science and psychology will be collaborated to find optimal solutions.

2.1 Biometrics. Biometrics is a science and innovation to describe information from the human body naturally [2]. Biometrics refers to individual differences based on physiological or social attributes. Some of the biometrics on the human body are iris, hand geometry, signatures, fingerprints, face, handwriting and many more. Biometric values themselves can be in the form of individual physiological or social attributes that meet completeness needs.

2.1 Preprocessing. Preprocessing is a stage that aims to improve the quality of the images obtained so that they are easier to process at a later stage [3]. The data set in the form of handwriting will be scanned to obtain a digital image. The stages of this preprocessing are cropping, negative images, image binaryzation, and thinning. Cropping is used to maximize the information retrieved so that there is not too much information that is not needed. Binaryzation is used to process data from RGB to black and white. This aims to ease data computation and can provide optimal data sets in the next stage. Thinning is also done to thin out the writing so that the writing has the same thickness even though the thickness of the pen varies.

2.2 SVM (Support Vector Machine). This research will utilize the Support Vector Machine (SVM) method in conducting data training and testing. SVM is a technique for finding hyperplanes that can separate two data sets from two different classes [4]. There are also advantages of SVM, namely being able to determine distances using support vectors so that the computation process becomes faster and more effective. SVM is one of the methods in supervised learning which is usually used for classification and regression [5]. In classification modeling, SVM has a more mature and clearer concept mathematically compared to other classification techniques [6]. SVM can also solve linear and non-linear classification and regression problems.

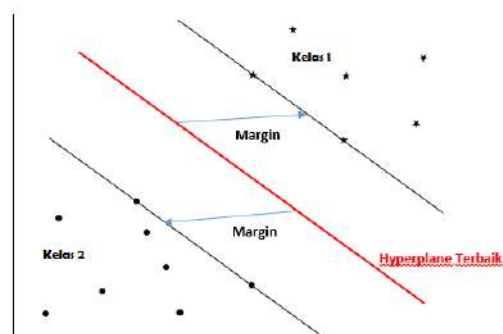


Figure 1. Illustration of Class Separation in SVM [4]

The best hyperplane as seen in figure 1 can be found with

$$\max L_D = \sum_{i=1}^n a_i - \frac{1}{2} \sum_{i=1, j=1}^n a_i a_j y_i y_j x_i x_j$$

In condition that

$$\sum_{i=1}^n a_i y_i = 0, a_i \geq 0$$

Not all data can be separated linearly, while SVM is basically only able to separate data linearly, so a development is needed to make SVM able to separate non-linear data, one of which is by adding a kernel function. By adding the kernel function to SVM, data x will be mapped to a higher vector space so that a hyperplane can be constructed. Hyperplane illustration can be seen in figure 2.

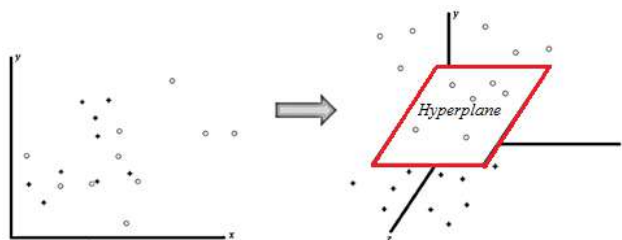


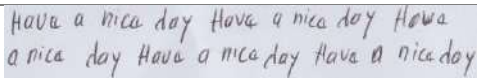
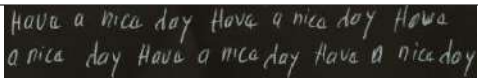
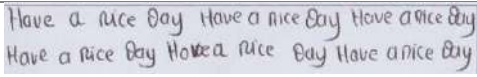
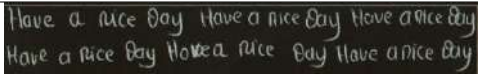
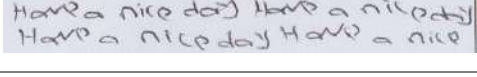
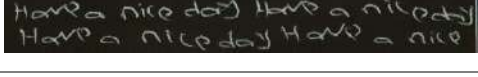
Figure 2. Hyperplane illustration in a higher dimension [4]

3 Results and Discussions

Identification of handwriting characteristics which is still being developed because the dataset is in the form of biometric data is an interesting thing to develop. In today's digital era, it is possible to model all forms of activity as concisely as possible and as effectively as possible. Moving on from instantaneous individual needs, the time-consuming process of recruiting prospective employees can be completed in a short and effective way using image processing.

The raw data in the form of handwriting after being scanned is then immediately given preprocessing to go to the next stage. Raw data and preprocessing results can be seen from table 1.

Table 1. Sample Image from Preprocessing results

ID	Raw Data	Preprocessing Result
1		
2		
3		

The appropriate input data will be calculated the distance, namely the distance between words in handwriting. Furthermore, if the distance results have been obtained, then the kernel calculation will be carried out with the SVM kernel function, namely the linear kernel. The results and predictions obtained after the SVM kernel calculation process will then be carried out by cross validation calculations to obtain accurate

results from the classification process in kernel calculations. The SVM flowchart can be seen in Figure 3 below.

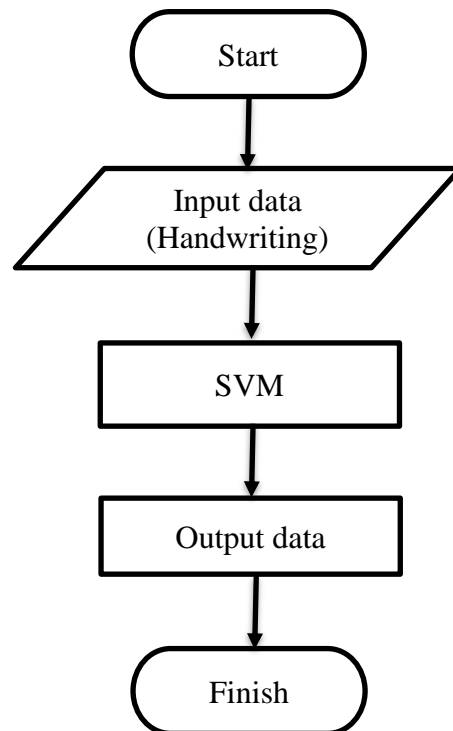


Figure 3. SVM Flow Chart

Calculation of handwriting patterns using word spacing patterns is given to training images and test images. This research uses computer science and psychology in application. Based on the results obtained from the SVM calculation, it will then be classified according to a person's character or personality. Here it takes a lot of attributes to compare one character with another so that the results obtained can be better.

4 Conclusions

The results and predictions of the handwritten character identification design using SVM and the accuracy obtained after calculations using cross validation are expected to provide optimal accuracy. The results of a person's character classification will be able to help make decisions regarding the recruitment of prospective employees. It is hoped that the results obtained will not only be utilized in the pandemic era but can also be developed in the future.

References

- [1] G. Thilagavathi, G. Lavanya and N. K. Karthikeyan, "Tamil Handwritten Character Recognition Using Artificial Neural Network," *International Journal of Scientific & Technology Research* , **8**(12), 1611-1616, 2019.
- [2] O. C. Ahuja, M. A. Mabayoje and R. Ajibade, "Offline Signature Recognition & Verification using Neural Network," *International Journal of Computer Applications*, **35**(2), 44-51, 2011.
- [3] S. Saidah, M. B. Adinegara, R. Magdalena and N. K. Pratiwi, "Identifikasi Kualitas Beras Menggunakan Metode K-Nearest Neighbor dan Support Vector Machine," *Jurnal Telekomunikasi, Elektronika, Komputasi, dan Kontrol*, **5**(2), 114-121, 2019.
- [4] M. Athoillah, "Pengenalan Wajah Menggunakan SVM Multi Kernel dengan Pembelajaran yang Bertambah," *JOIN (Jurnal Online Informatika)*, **2**(2), 84-91, 2017.
- [5] S. Khedikar and U. Yadav, "Identification of Disease by Using SVM Classifier," *International Journal of Advanced Research in Computer Science and Software Engineering*, **7**(4), 81-86, 2017.
- [6] P. A. Octaviani, Y. Wilandari and D. Ispriyanti, "Penerapan Metode Klasifikasi Support Vector Machine (SVM) pada Data Akreditasi Sekolah Dasar (SD) di Kabupaten Magelang," *Jurnal Gussian*, **3**(4), 811-820, 2014.

This page intentionally left blank

Optimization of Vacuum Forming Parameter Settings to Minimize Burning Defect on Strawberry Packaging Products Using the Taguchi Method

Th. Adi Nugroho^{1,*}, Adhi Setya Hutama¹ and Perwita Kurniawan¹

¹ *Manufacturing Design Study Program, Politeknik ATMI Surakarta
Jl. Adisucipto / Jl. Mojo No.1 Surakarta*

**Corresponding Author: adi.nugroho@atmi.ac.id*

(Received 23-10-2022; Revised 30-10-2022; Accepted 02-11-2022)

Abstract

Packaging products are being developed by PT. ATMI IGI – Center. The process of making these products uses the Vacuum forming method. The packaging product is made of PP (Polypropylene) and is used to pack strawberries. There are several problems during the production process, one of which is that there are still product defects burning or often called burn marks. These problems are caused by the machining parameters that have not been standardized, and based on trial error or experience of the operator. The vacuum forming machine used in this production is the Formech 508FS Vacuum Forming machine. The optimized parameters are heat zone, heat time, and stand by temperature. Optimizing these parameters using the Taguchi method, with an orthogonal array with 9 trials, and the selected signal to noise ratio (SNR) is smaller is better. The response of this research is the reduction of burn mark product defects. The results showed that to reduce burn mark product defects, is to set the parameter heat zone 1 by

90%, heating zone 2 is 80%, heating time 45s, and stand by temperature 60%. Based on this arrangement, the product defects obtained only reached 13%. PT. ATMI IGI-Center is expected to be able to use these parameter settings for the strawberry packaging production process.

Keywords: vacuum forming, defect product, Taguchi method, smaller is better

1 Introduction

PT ATMI-IGI Center is a company that engaged in the manufacture of Molding for plastics production and plastic product molding. Beside producing Mold and molding of plastic products with Injection method, the company is currently also starting to try to get into the field of Vacuum Forming production is in the form of Mold for Strawberry packaging products made with aluminum material. Production is carried out using the Thermoforming process, which is apply the Vacuum Forming system in the Formech 508FS machine. Thermoforming is an industrial process in which a thermoplastic sheet (or film) is processed into a new shape using heat and pressure [1].

The problem that occurs in the production of strawberry packaging is that the product often experiences burning defects or often called burn marks, as shown in Figure 1. Burn marks are product defects, where the product changes colour such as burning, dimensions, and weight [2]. Burn marks in the packaging process happen because there is no standardization for the operation of the parameters, so the operation is only based on the estimation and experience of the operator. This certainly affects the length of time and cost of the experiment because it is done by finding the right estimate of the number of parameter variables that can be used for production. On the Formech 508FS engine, the machining parameters used are heating zones, heating time and stand-by temperature. also stated that the parameters on the vacuum forming machine that need to be optimized include temperature, heating time, and heating zone [3].



Figure 1. Burning problem on the strawberry packaging product

This research was conducted focusing on optimization parameter setting, to find the parameter that optimal in overcoming the burning defect that often occurs in the production process of strawberry packaging. This research result later can be used for strawberry packaging production, and the method can be used to find optimal parameters of the next mold in the future produced by PT ATMI-IGI Center.

2 Methodology

2.1 Research Methodology

2.1.1 Taguchi Methods

The Taguchi method is used to optimize the parameters contained in the Formech 508FS. The Taguchi Method is one of the methods in experimental design that can be used to control product quality, such as to obtain optimal parameters and material compositions [4] [5]. The Taguchi method belongs to the DOE (Design of Experiment) realm, in which there are two main variables, namely the response variable and the independent variable [6].

In this study, the manufacture of Strawberry Packaging used 3^k factorial design, where at each level identify low, medium, and high. Characteristics in search of strawberry packaging product parameters using the smaller is better type, namely the characteristics of quality with a value limit of 0 and non-negative so that the value of which is getting smaller or closer to zero is the value that desired [7].

In this study the independent variables consist of three variables, namely heating zones, stand-by parameters, and heating time, each variable has 3 levels, low, medium,

high. Determination of the value of the independent variable level for stand-by temperature and heating time according to machine manuals, work journals and manuals, by conducting initial experiments.

The first step is to look at the temperature recommendation on TDS (Technical Data Sheet), parameter journal and the Formech 508FS engine operating manual, which will be medium level with forecast best setting, as shown in Figure 2. Next, to determine the high and low levels is to add a value according to the range obtained in the initial experiment. Results from initial experiments obtained parameter level for stand-by temperature 40% for low level (range -20% of the experiment) , 60% medium level, and 80% high level (range +20% of test). Heating time is 45s (low level according to trial), 50s (medium level according to the manual use of the Formech 508FS engine), and 55s (high level according to experiment). Medium level heating zones already available in the initial settings (which is usually used for PP material) and high and low levels are obtained through initial trial. The heating zone used is 40%, 60%, and 80%. In Zone 2 in heating zones the temperature increased by 10% due to the need to form more complicated clamping contour than the center of product.

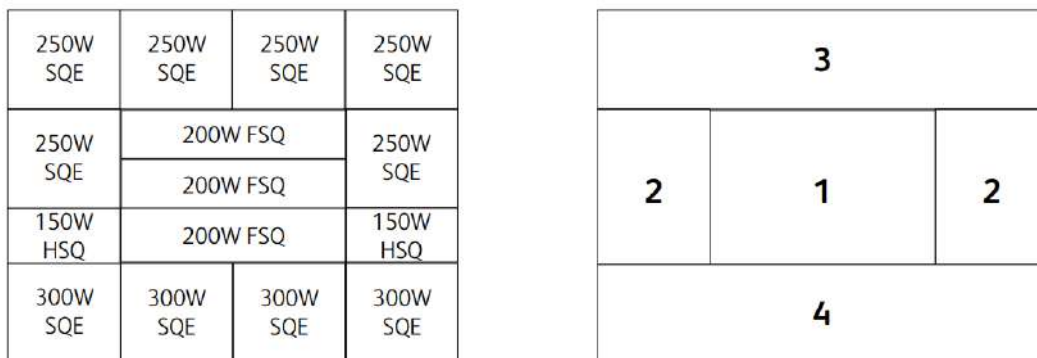


Figure 2. Heating Zone formation on Formech 508FS machine

2.1.2 Orthogonal Matrix

The use of the Taguchi method in design experiment based on Orthogonal Array (OA) in order to obtain the optimal amount of information with minimal trials. Orthogonal array is a matrix of a number of rows and columns [8]. Each column

represents a certain factor or condition that can change from one experiment to another, and the row represents the level of the factor in the experiment being performed.

Selection of the type of Orthogonal Array used in the experiment depends on the number of degrees of freedom. Determination of degrees of freedom means to see how many minimum numbers of experiments performed [9].

The formulation can be seen in the following equation:

$$\text{Degrees of freedom} = \sum_{k=1}^n (l_k - 1) \tag{1}$$

with, $k = 1, 2, \dots, n$

Research conducted using 3 independent variables with each parameter having 3 levels.

2.1.3 Experimental Result Analysis

The analysis used to determine the effect relative of the various controls in this study is to use the analysis of the average (Analysis of Mean/ ANOM).

ANOM or mean analysis, is used to looking for a combination of control parameters so that optimal results are obtained as desired [10].

2.1.4 Average Value (Mean)

The average or complete average of calculations, for quantitative average contained in a sample calculated by dividing the number of data values by lots of data [11]. Suppose there is a data distribution $y_1, y_2, y_3, \dots, y_n$. So, the average is:

$$\bar{y} = \frac{y_1 + y_2 + y_3 + \dots + y_n}{n} = \frac{\sum_{i=1}^n y_i}{n} \tag{2}$$

2.2 Data Collection Process

2.2.1 Matrix Orthogonal Selection

Orthogonal Matrix Selection is done by MINITAB 15 software assistance, according to the number of Independent Variables/Factors and Levels used in study. Research conducted using 3 independent variables with each parameter having 3 levels. The degrees of freedom (dof) obtained in this study are:

DoF = Independent variable * (level-1)

$$\text{DoF} = 3 \times (3-1) = 6$$

The value 6 of the degrees of freedom is the sum of minimum for the experiment to be carried out. Study it uses an orthogonal array L9 which has The number of experiments is 9. Based on these choices, on the Taguchi Design – Design table on MINITAB, column L9 is selected.

The research carried out took the L9(3³) orthogonal matrix with a total of 9 trials. The table of variations of the orthogonal array matrix is shown in table 1 has been entered according to the variation of parameters.

Table 1 Parameter Variations

No	<i>Heating Zones</i>	<i>Stand-by Temp</i>	<i>Heating Time</i>	<i>Cacat Produk (%)</i>
1	40	40	45	...
2	40	60	50	...
3	40	80	55	...
4	60	40	50	...
5	60	60	55	...
6	60	80	45	...
7	80	40	55	...
8	80	60	45	...
9	80	80	50	...

2.2.2 Vacuum Forming Trial Process

The materials used in this research are Polypropylhene (PP) plastic sheet with size 530x470mm for each sheet.

As for the machine used is a machine Vacuum Forming Formech 508FS. The machine has prepared in advance with the heating stage heater with high heating parameters. Then Parameters according to Orthogonal Matrix are inputted and stored in machine memory. Setting according to independent variable and level to the parameters of the Heating Zone, StandBy Temperature and Heating Time.

Determination of Assessment Aspects is determined based on finished product requirements, initial trial results, and requirements list from PT ATMI-IGI Center. Aspect The assessment uses the percentage of damage, for qualifies Taguchi Smaller is

Better Method. There are 5 Aspects that are the basis for the assessment the success of an experimental specimen, namely Burning/Not Burning, Thickness, Contour, Angle and Lock Holes/Pins.

2.3 Experimental Result Data Analysis

Assessment based on the assessment aspect is carried out after all parameter variations and all replications have been completed. The assessment data uses percent (%) units to mark the percentage of damage that occurs in vacuum forming printed products.

Analysis of Experimental Results was carried out using manual calculations in Microsoft Excel and confirmed by calculations on the MINITAB 15 software.

2.3.1 Analysis on Top Section

After the experiment was carried out, the average of the experimental results was obtained to determine the parameters that had the most influence on defects in the Top part of the product. The experimental data are shown in table 2.

Table 2 Top Section Experimental Data

No	Heating Zones	Stand-by Temp	Heating Time	Cacat Produk (%)
1	40	40	45	60%
2	40	60	50	47%
3	40	80	55	60%
4	60	40	50	60%
5	60	60	55	47%
6	60	80	45	47%
7	80	40	55	60%
8	80	60	45	7%
9	80	80	50	40%

The calculation of the average manually for the response to product defects as follows:

- Average for response in Heating Zones Level 1

$$\text{Holding Time Lvl.1} = (60\% + 47\% + 60\%) / 3 = 56\%$$

Then the average table for the product defect response is obtained (Table 2.4)

As for the calculations in the effect table, shows the variables with the greatest effect on product defects are as follows:

- Variable Effects of Heating Zones:

Highest Response for Means – Lowest Response for Means

$$56\% - 36\% = 20\%$$

Then the magnitude of the effect on each factor is obtained as shown in table 3 below.

Table. 3 Response for Means (Smaller is Better)

Level	Heating Zones	Stand-by Temp	Heating Time
1	56%	60%	38%
2	51%	33%	49%
3	36%	49%	56%
Efek	20%	27%	18%
Optimum Level	3	2	1

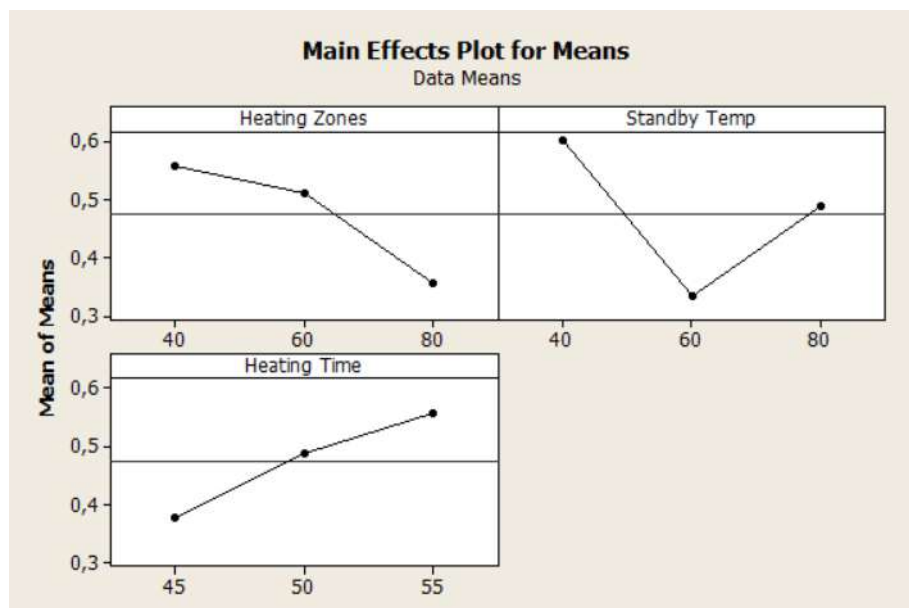


Figure 3. MINITAB calculation for Response for Means

Figure 3 above shows the results of the average graph (means) in the Top section which is processed using Minitab 15 software.

Parameter Heating Zone The means graph shows the lowest value is at level 3, which is 36%. While the StandBy Temperature parameter shows the lowest value is at level 2, which is 33%. Then the Heating Time parameter shows the lowest value is at level 1, which is 38%.

2.3.2 Analysis on Base Section

After the experiment was carried out, the average of the experimental results was obtained to determine the parameters that had the most influence on defects in the Base part of the product. The experimental data are shown in table 4.

The calculation of the average manually for the response to product defects as follows:

- Average for response in Heating Zones Level 1

$$\text{Holding Time Lvl.1} = (20\%+33\%+60\%)/3 = 38\%$$

Then the average table for the product defect response is obtained (Table 5)

Table 4 Base Section Experimental Data

No	Heating Zones	Stand-by Temp	Heating Time	Cacat Produk (%)
1	40	40	45	20%
2	40	60	50	33%
3	40	80	55	60%
4	60	40	50	60%
5	60	60	55	60%
6	60	80	45	33%
7	80	40	55	33%
8	80	60	45	13%
9	80	80	50	40%

As for the calculations in the effect table, shows the variables with the greatest effect on product defects are as follows:

- Variable Effects of Heating Zones:

Highest Response for Means – Lowest Response for Means

51%-29% = 22%

Then the magnitude of the effect on each factor is obtained as shown in table 5 below.

Table 5. Response for Means (Smaller is Better)

Level	Heating Zones	Stand-by Temp	Heating Time
1	38%	38%	22%
2	51%	36%	44%
3	29%	44%	51%
Efek	22%	9%	29%
Optimum Level	3	2	1

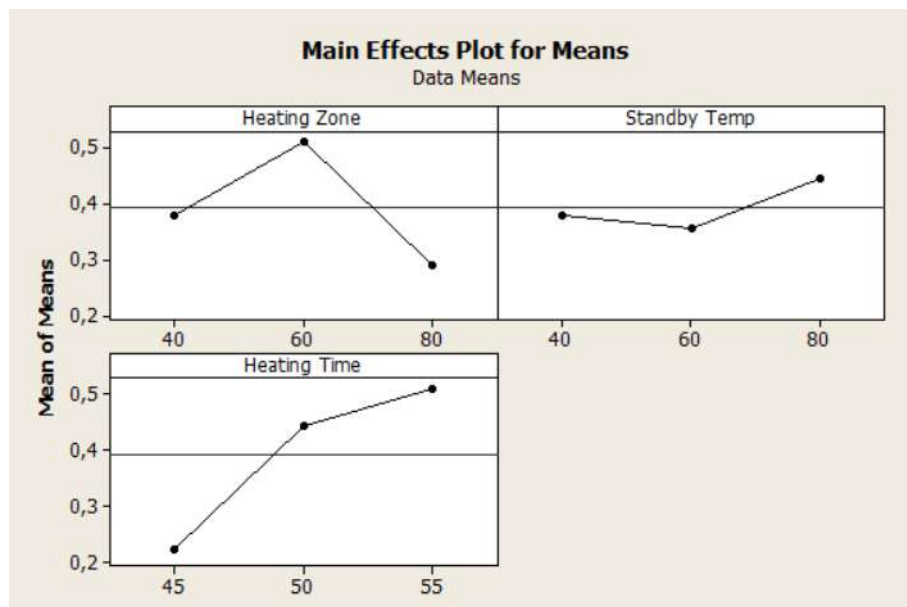


Figure 4. MINITAB calculation for Response for Means

Figure 4 above shows the results of the average graph (means) in the Top section which is processed using Minitab 15 software.

Parameter Heating Zone The means graph shows the lowest value is at level 3, which is 29%. While the StandBy Temperature parameter shows the lowest value is at level 2, which is 36%. Then the Heating Time parameter shows the lowest value is at level 1, which is 22%.

3 Results and Discussions

3.1 Research Result on Top Section

The results of processing experimental data and after the validation process is carried out, it shows that parameters that result in a formable product according to predetermined aspects and does not occur defect burning is parameter no.8. Process parameters vacuum forming for experiment no.8 has setting as follows:

- Heating Zone = Level 3 = 80%
- StandBy Temp. = Level 2 = 60%
- Heating Time = Level 1 = 45s

Table 2 shows the experimental data where parameter no.8 has a product defect percentage rate the smallest is 7%.

3.2 Research Result on Base Section

The results of data processing experimental results and after the validation process is carried out, it shows that parameters that result in a formable product according to predetermined aspects and does not occur defect burning is parameter no.8. Process parameters vacuum forming for experiment no.8 has setting as follows:

- Heating Zone = Level 3 = 80%
- StandBy Temp. = Level 2 = 60%
- Heating Time = Level 1 = 45s

Table 4 shows the experimental data where parameter no.8 has a product defect percentage rate the largest is 13%.

3.3 Validation of Research Result

Validation of research results from parameter recommended showing results that have the most perfect formation and still can maintain thickness and there are no parts which has defect burning. Finished products that have been cut according to the part used as strawberry package and already assembled like shown in Figure 5, Table 4 shows the experimental data where parameter no.8 has a product defect percentage rate the largest is 13%.



Figure 5. Assembling result on Validation Product

4 Conclusions

Based on the research that has been done, then can be concluded as follows:

- Optimal parameter setting to minimize product defects burning and able to shape the product during the vacuum forming process on the Formech 508FS machine for Strawberry Packaging products on the Top is a combination of parameters in the Heating Zone by 80%, StandBy Temperature by 60%, and Heating Time by 45s which resulted in an average percentage of product defects of 7%. As for the Base part is with a combination of parameters in the Heating Zone of 80%, StandBy Temperature of 60%, and Heating Time of 45s which results in an average percentage of product defects of 13%.
- Setting parameters that affect the process of making Strawberry Packaging products from the Top section on Burning product defects and being able to shape the product based on the results of calculations carried out, contained in Table 5.5 are StandBy Temperature which has an effect of 27%, then there is Heating Zone which has an effect of 20%, and followed by Heating Time which has an effect of 18%. Meanwhile, for setting parameters that affect the process of making Strawberry Packaging products from the Base section on Burning product defects and being able to form products based on the results of calculations carried out, contained in Table 5.7 is Heating Time which has an effect of 29%, then there is Heating Zone which has effect by 22%, followed by StandBy Temperature which has an effect of 9%.

References

- [1] P.W. Klein, “Fundamentals of Plastics Thermoforming”, Morgan & Claypool Publisher, Ohio, 2009
- [2] K.A. Widi and L.D. Ekasari, “Studi Analisa Pengembangan Produk Limbah Plastik Berbasis Tekanan Teknologi Injection Moulding”. *Jurnal Flywheel*, **8**(2), 14-18, 2017
- [3] C.R. Permana, C. Budiyanoro, and B. Prabandono, “Manufaktur dan Uji Kinerja Proses Vacuum Forming untuk Bahan Polymethyl Methacrylate (PMMA)”, *Jurnal Material dan Proses Manufaktur*, **3**(1), 1-9, 2019
- [4] A. Nugroho, A.S. Utama, and C. Budiyanoro, “Optimasi Keakuratan Dimensi dan Kekasaran Permukaan Potong Material Akrilik dengan Proses Laser Menggunakan Metode Taguchi dan PCR-TOPSIS”, *Jurnal Material dan Proses Manufaktur*, **2**(2), 75-82, 2018
- [5] A.S.Hutama, P. Kurniawan, A. Nugroho, and W.S. Hayu, “Studi Karakteristik Mekanis Material Limbah Polypropilene (PP) untuk Pembuatan Produk Cone Benang dengan Penambahan Material Kalsium Karbonat”, *Jurnal Rekayasa Sistem Industri*, **11**(1), 101-107, 2022
- [6] A. Nugroho, A.S. Utama, “Metode Taguchi - PCR Topsis Untuk Optimasi Energi Dan Kecepatan Grafir Mesin Laser”, *Politeknisains*, **18**(1), 6-11, 2019
- [7] F.K.A. Nugraha, “Shrinkage of Biocomposite Material Specimens [HA/Bioplastic/Serisin] Printed using a 3D Printer using the Taguchi Method”, *International Journal of Applied Sciences and Smart Technologies*, **4**(1), 89-96, 2022
- [8] H.A. Pamasaria, T.H. Saputra, A.S. Utama, and C. Budiyanoro, “Optimasi Keakuratan Dimensi Produk Cetak 3D Printing Berbahan Plastik PP Daur Ulang dengan Menggunakan Metode Taguchi”, *Jurnal Material dan Proses Manufaktur*, **4**(1), 12-19, 2020
- [9] N. Sunengsih. S. Winarni, T.G. Amazaina, “Kajian Terhadap Metode Taguchi TOPSIS pada Optimasi Multirespon”, *Seminar Statistika FMIPA Unpad*. Bandung, 2017

- [10] W.S. Hayu, “Optimasi Parameter Injection Molding untuk Mengurangi Cycle Time dan Berat Produk Cone Benang dengan Metode Taguchi”, *Tugas Akhir*, Politeknik ATMI. Surakarta.
- [11] R.E. Walpole, “Pengantar Statistika”, PT. Gramedia, Jakarta, 1995

The Effect of the Number of Cooling Pads on the Output Air Condition and Effectiveness of Air Cooler

Wibowo Kusbandono^{1,*}

¹*Department of Mechanical Engineering, Faculty of Science and Technology, Sanata Dharma University, Indonesia*

*Corresponding Author: bowo@usd.ac.id

(Received 01-11-2022; Revised 18-11-2022; Accepted 21-11-2022)

Abstract

To get comfortable air, it can be done by using an air conditioner or air cooler. The electrical power used for the air cooler is relatively lower. This research aims to see the effect of the number of cooling pads on the output air condition and on the effectiveness of the air cooler. The research was conducted experimentally. The research was conducted by varying the number of cooling pads used, thick. The distance between the cooling pads is 1.5 cm. The air temperature inlet of the air cooler has a dry bulb air temperature of $30^{\circ}C$ with an air humidity (RH) of 60%. The lowest dry bulb air temperature achieved was $24,04^{\circ}C$ when the number of cooling pads was 6 pieces. The highest air cooler effectiveness achieved was 0.99. Research has given satisfactory results. However, research can be developed by varying the cooling pad material or cooling pad pattern in order to obtain a small number of cooling pads.

Keywords: air cooler, effectiveness, cooling pad



1 Introduction

Air cooler is equipment used to produce cool air. Unlike the air conditioner (AC) which uses the working fluid of Freon, the air cooler uses the working fluid of water. Therefore the air cooler is more environmentally friendly. In its operation, the AC engine uses a steam compression cycle to produce cold air, while the air cooler uses an evaporative cooling process to get cold air. In the AC engine, the freon circulation system is in a closed flow system, while in the air cooler, the water flow system is open. In an open flow system, the fluid makes contact with the outside air. The use of the air cooler does not require it to be placed in a closed room, so that the air cooler can be placed in a room with free air circulation. Thus the need for oxygen from the air for users is not lacking. Of course, the air flow in the room is conditioned relatively calmly, it doesn't interfere with the air flow from the air cooler. From the psychrometric chart, it can be seen that for the condition of the air entering the air cooler at a dry bulb air temperature of 35°C with a relative humidity (RH) of about 46%, the lowest dry bulb air cooler outlet air temperature that can be achieved is around 25°C . Meanwhile, if the incoming air is with dry bulb air temperature of about 30°C with a RH of about 60%, the lowest dry-bulb output air temperature can be reached 24°C .

The air cooler is not used to condition all the air in the room. The air output of the air cooler is intended for users only. The output air flow is only directed to people who want to enjoy the air from the air cooler. With the air cooler, the output dry bulb air temperature can reach 24°C - 26°C . At that air temperature, the user can feel the coolness of the air it produces. In the design of the air cooler, in addition to the condition of the output air being in a comfortable area, it must also have high effectiveness. Unlike the AC machine, if the AC machine is designed to produce dry air [1], the air cooler is designed to produce relatively higher air humidity. The higher the RH, the cooler the air produced.

The manufacture of air coolers has actually been done for a long time. It has even been patented a lot [2-8]. But in Indonesia, the new air cooler is known after the air cooler was marketed in the last decade. Besides being cheap, the air cooler can also be carried anywhere (can be moved around). It's just that the condition of the output air produced by the air cooler depends on the condition of the air entering the air cooler [9]. The

minimum dry bulb output air temperature that the air cooler can produce is equal to the wet bulb air temperature entering the air cooler. When the dry bulb air temperature output reaches the temperature of the wet bulb air entering the air cooler, the relative humidity of the air reaches 100%. Because the RH of the air has reached 100%, it is impossible for water evaporation to occur on the cooling pad which causes a decrease in air temperature again. Unlike AC machines, the air cooler cannot produce the desired air condition. For areas in Indonesia, air coolers are suitable for use in air conditions, with dry bulb ambient air temperatures between 28⁰C to 35⁰C with low relative humidity (40%-50%). The lower the relative humidity of the air, the more profitable it is because the lowest air temperature produced will be lower.

Research on air cooler has been carried out by several researchers. The difference between the research that has been carried out by the author and that carried out by previous researchers lies in the shape of the cooling pad, cooling pad material, air cooler geometry and research variations. There are studies that vary the intake air temperature [10], there are studies that are carried out by varying the thickness of the cooling pad [11]. Some use a cooling pad made of sponge [11], some use coconut fiber [12,15]. Some vary the flow of air produced by a fan [12]. There are also those that vary the temperature of the water used [13, 14] and there are those that vary the water discharge [15]. In the research that has been done by the author, the cooling pad used is relatively thin, about 1 mm, and with different materials from previous researchers. The research was conducted by varying the number of cooling-pads. In the market, the cooling pad used for the air cooler is quite thick, with a thickness of more than 5 mm, some even more than 4 cm.

Some of the assumptions used in this research that have been carried out are: (1) when the air passes through the cooling pad, the air undergoes an evaporative cooling process (2) when the air undergoes an evaporative cooling process, the wet bulb air temperature remains (starting when the air enters the water). cooler until the air comes out of the air cooler) (3) the evaporative cooling process runs at a constant enthalpy, no energy enters and leaves. In the evaporative cooling process, there is a decrease in dry bulb air temperature, an increase in relative humidity, an increase in specific humidity, and an increase in dew point temperature.

2 Research Methodology

The research was conducted experimentally. The object under study is a homemade air cooler. Figure 1, presents a schematic of the air cooler used in the study. Figure 2, presents an image of the cooling pad. The maximum number of cooling pads used is 6 pieces. The thickness of the cooling pad moistened with water is 1 mm.

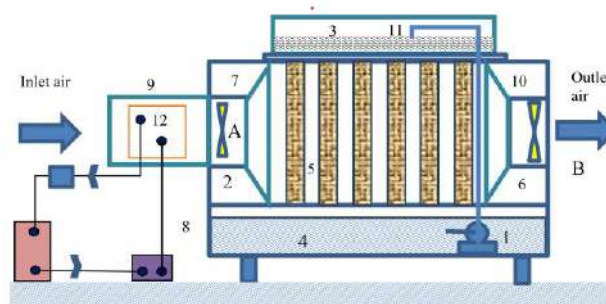


Figure 1. Schematic of an air cooler with 6 cooling pads

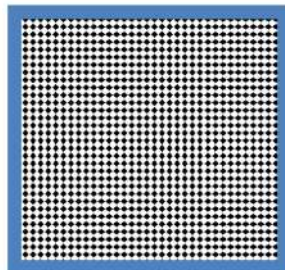


Figure 2. Cooling Pads

Air-cooler components in Figure 1

- | | |
|--|-----------------------|
| 1. Submersible pump (submersible pump) | 7. Water cooler frame |
| 2. Air intake fan | 8. Case |
| 3. Upper water reservoir | 9. Air inlet |
| 4. Bottom water reservoir | 10. Air outlet |
| 5. Cooling pad | 11. Water channel |
| 6. Bottom water reservoir | 12. Air heater |

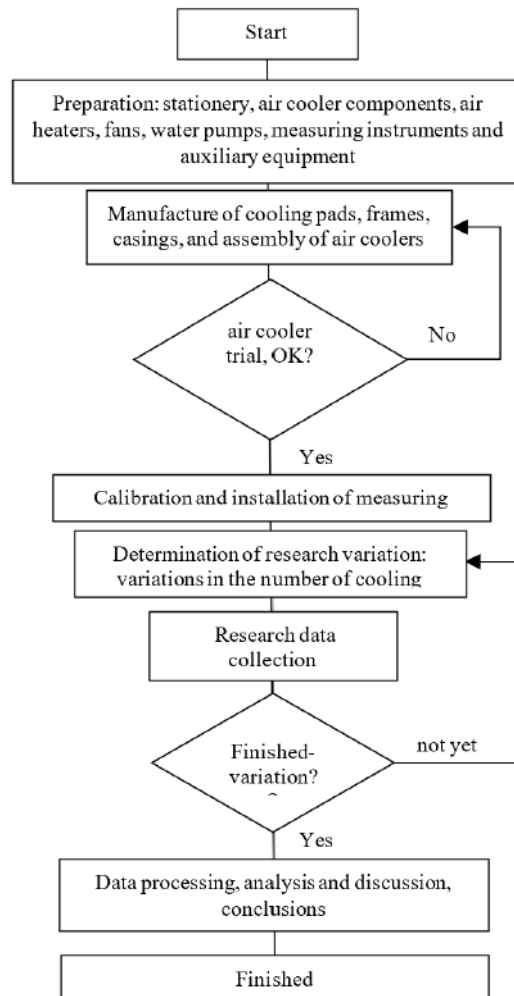


Figure 3. Research Flow

In this study, the air entering the air cooler was conditioned at a dry bulb air temperature of 30⁰C, with a relative humidity of 60%. If the dry bulb air temperature does not reach 30⁰C the air is preheated by the air heater before entering the air cooler, as desired. The air flow velocity is 1.5 m/s. The research implementation follows the research flow as presented in Figure 3. The research was conducted by varying the number of cooling pads, using 3 cooling pads, 4 cooling pads, 5 cooling pads and 6 cooling pads. To determine the air condition, a dry bulb thermometer and a wet bulb thermometer were used. Meanwhile, to measure the velocity of air flow used anemometer. Other air conditions can be searched by using psychrometric charts, such as relative humidity, absolute humidity, specific volume and air enthalpy.

The data from the research results are used to get the effectiveness of the air cooler. The effectiveness of the air cooler (ϵ) is the ratio between the actual (actual) decrease in dry bulb air temperature and the possible or ideal decrease in dry bulb air temperature [9]. The equation used to calculate the effectiveness of the air cooler is expressed by Equation (1).

$$\epsilon = \frac{(T_{db,A} - T_{db,B})}{(T_{db,A} - T_{db,C})} \dots (1)$$

In Equation (1)

ϵ : air-cooler effectiveness

$T_{db,A}$: dry bulb air temperature entering air-cooler, $^{\circ}\text{C}$

$T_{db,B}$: dry bulb air temperature out of air-cooler, $^{\circ}\text{C}$.

$T_{db,C}$: lowest achievable dry bulb air temperature air-cooler, $^{\circ}\text{C}$.

$T_{db,D}$: wet bulb air temperature in process evaporative-cooling, $^{\circ}\text{C}$

3 Results and Discussions

The results of the study are presented in Table 1. It appears that the condition of the output air from the air cooler is influenced by the number of cooling pads used. For air coolers with 6 cooling pads, the air cooler output air conditions produce the lowest dry bulb air temperature. As for the air cooler with 3 cooling pads, the air condition of the air cooler output produces the highest dry bulb air temperature. This is probably due to the large surface area of the water in contact with the air passing through the cooling pad. The more the number of cooling pads on the air cooler, the more surface area of the water in contact with the air when the water flows through the cooling pad. The larger the surface area of the water in contact with the air, the more water can evaporate into the air. Unlike the boiling process, the evaporation process can take place not at the boiling point temperature. The evaporation process can take place at any temperature. As long as the humidity has not reached 100% RH, the water flowing on the cooling pad can still evaporate into the air. The process of evaporation of water requires heat. In the process of evaporation of water in the cooling pad, heat is taken from the environment. In this case the environment is air. The heat is taken from the air flowing through the cooling

pad. The more water that evaporates, the greater the heat of vaporization required to change the water from the liquid phase to the vapor phase. The greater the heat taken by water from the air, the lower the air temperature. The amount of heat taken from the air is equal to the amount of heat used to change the liquid phase from the water to the water vapor phase. During the evaporative cooling process, the enthalpy value of the air remains constant. The heat taken from the air is sensible heat, while the heat used to change water from the liquid phase to the vapor is latent heat. In this case, it is assumed that no heat is taken from the water used to change the phase from water to steam.

Table 1. Conditions of air inlet and outlet of air cooler and effectiveness of air cooler

Number of cooling pad	Intake air condition <i>air cooler</i>				Air condition out of <i>air cooler</i>			Effectiveness of <i>air cooler</i> (ϵ)
	T _{db,A} (°C)	T _{wb,A} (°C)	RH _A (%)	W _A (gr/kg)	T _{db,B} (°C)	T _{wb,B} (°C)	W _B (gr/kg)	
3	30°C	24°C	60%	16,1	25,15 °C	24°C	18,1 9	0,81
4	30°C	24°C	60%	16,1	24,77 °C	24°C	18,3 5	0,87
5	30°C	24°C	60%	16,1	24,38 °C	24°C	18,5 2	0,94
6	30°C	24°C	60%	16,1	24,04 ^o C	24°C	18,6 6	0,99

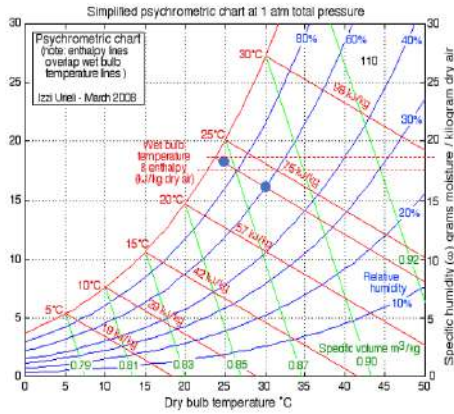


Figure a. Air cooler with 3 cooling pads

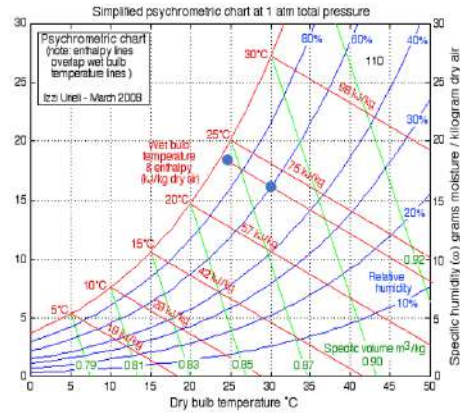


Figure b. Air cooler with 4 cooling pads

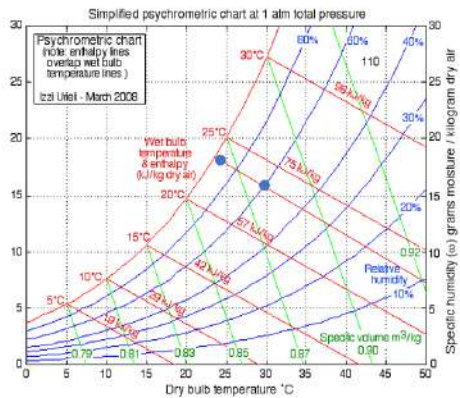


Figure c. Air cooler with 5 cooling pads

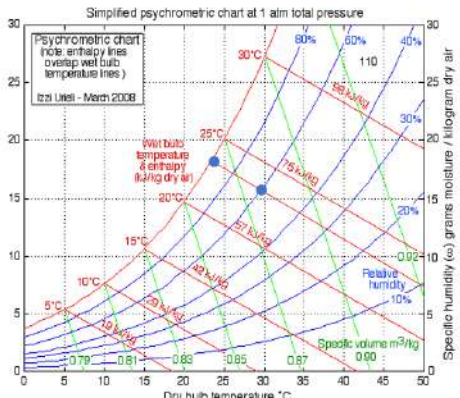


Figure d. Air cooler with 6 cooling pads

Figure 4. Conditions of air inlet and outlet of air cooler and effectiveness of air cooler with different number of pads. a. Air cooler with 3 cooling pads. b. Air cooler with 4 cooling pads. c. Air cooler with 5 cooling pads. d. Air cooler with 6 cooling pads

To get a cooler dry bulb air temperature from the air cooler, it can be done by increasing the use of cooling pads. The more the cooling pad is used, the lower the output dry bulb air temperature will be. But of course the number of cooling pads used has a limit. The limitation is, if the use of n number of cooling pads can produce output air with a relative humidity (RH) of 100%, then the addition of a cooling pad is no longer needed. The addition of a cooling pad will no longer reduce the dry bulb air temperature from the air cooler, because it is no longer possible to change the phase from water to steam anymore. In other words, the amount of water that evaporates is equal to the amount of water that

condenses. On the other hand, the more cooling pads used, the lower the output airflow rate. This is because the more the cooling pad is used, the greater the air resistance that occurs. Seeing the results of this study, the use of 6 cooling pads is sufficient. Because the relative humidity value of the resulting air is close to 100%. It is no longer necessary to add a cooling pad. Even if one additional cooling pad is added, the minimum output dry ball air that can be achieved is only 24 °C. Not so influential.

From Table 1 and Figure 4a-d, it appears that the lowest dry bulb air temperature that the air cooler can achieve is 24,04 °C. The air cooler is able to reduce the dry bulb air temperature by about 5,96°C, from the initial temperature of 30°C. Close to the decrease in the maximum dry bulb air temperature that the air cooler can achieve, by 6°C (with air intake conditions of 30 °C and 60% RH). For air humidity, the greater the number of cooling pads, the greater the specific humidity value (ω) produced. The specific humidity of the air increased from 16.1 grams of water/kg dry air to a maximum of 18.66 grams of water/kg dry air. This is because the water content in the air increases from the evaporation of water passing through the cooling pad. Likewise, the value of the relative humidity of the air (RH), increased from the original 60% to all above 90%. The highest produced by the air cooler, the air output of the air cooler has a RH of almost 100%.

The effectiveness of the air cooler depends on the number of cooling pads used. In this study, the effectiveness of the air cooler from the lowest value to the highest value, for the air cooler with a total of 3 cooling pads, 4 cooling pads, 5 cooling pads and 6 cooling pads, respectively, was 0.81; 0.87; 0.94; 0.99. This is understandable because the effectiveness value depends on the dry bulb air temperature from the air cooler outlet. The lower the dry bulb air temperature, the higher the effectiveness value (Equation (1)). Due to the difference in temperature between the dry bulb air temperature entering the air cooler and the dry bulb air temperature, the air cooler output is getting bigger. The effectiveness of the air cooler is directly proportional to the difference between the dry bulb air temperature inlet and the output. As is known, the difference between the lowest dry bulb air temperature that can be achieved by the air cooler (the temperature at which the air has a 100% RH) and the dry bulb air temperature entering the air cooler remains constant. From the results of this study, research can be developed with the target of producing outdoor air conditions that have a relative humidity of 100% of the air but with

a number of cooling pads that are smaller than 6 cooling pads. It can be done by using another cooling pad, it can be with a different cooling pad material or with a different cooling pad pattern.

4 Conclusions

The study resulted in conclusions (a) for air coolers with 3, 4, 5, 6 cooling pads, respectively producing dry bulb air temperatures of: 25,15⁰C; 24,77⁰C; 24,38⁰C and 24,04⁰C. (b) for air coolers with 3, 4, 5, 6 cooling pads, respectively, the effectiveness of the air cooler is 0.81; 0.87; 0.94 and 0.99. Research can be developed by minimizing the number of cooling pads, for example by using a cooling pad material or a different cooling pad pattern.

Acknowledgements

The author would like to thank the University of Sanata Dharma which has provided financial support, so that this research can be completed.

References

- [1] W. Arismunandar, S. Heizo, "Penyegaran Udara Edisi ke 4", Pradnya Paramita. Jakarta. 1991.
- [2] J. K. Jain, D.A. Hindoliya, "Experimental performance of new evaporative cooling pad material", Mechanical Engineering Department, Ujjain Polytechnic College, Ujjain (M.P.) 456010, India, 2011.
- [3] Charles W. Albrecht, Evanston, Wyo, "Evaporative Air Cooler", United State Patent, Patent Number 4,953,831, Date of Patent: Sep. 4, 1990.
- [4] James A. Brock, Alexander, Ark, "Portable Evaporative Air Cooler", United State Patent, Patent Number Des. 337,817, Date of Patent: Jul. 27, 1993
- [5] Peter Sydney Wright, Blackwood, Australia, "Off-Road Evaporative Air Cooler", United State Patent, Patent Number, Des. 433,111, Date of Patent: Oct. 31, 2000
- [6] William R. Calton, Scofield Dr., Cupertino, "Evaporative Cooling", United State Patent, Patent Number 5,715,698, Date of Patent: Feb. 10, 1998.
- [7] United State Patent, Patent Number 5,168,722, Date of Patent: Dec. 8, 1992

- [8] James A. Brock, Alexander, Ark, “Portable Evaporative Air Cooler”, United State Patent, Patent Number Des. 337,817, Date of Patent: Jul. 27, 1993.A
- [9] R.S. Khurmi, J.K. Gupta, “A Text Book of Refrigeration and Air Conditioning”, Eurasia Publishing House (P) Ltd, Ram Nagar, New Delhi-110055. 1995.
- [10] Doddy Purwadianto, Petrus Kanisius Purwadi, “Hubungan Kondisi Udara Masuk dengan Kondisi Udara Keluaran Air Cooler”, *Jurnal Ilmiah Widya Teknik*, **20**(2), 2021.
- [11] I Nyoman Suryana, I Nengah Suarnadwipa, Hendra Wijaksana, “Studi Eksperimental Performansi Pendingin Evaporative Portable dengan Pad Berbahan Spon Dengan Ketebalan Berbeda”, *Jurnal Ilmiah Teknik Desain Mekanika*, **1**(1), September 2014.
- [12] Ekadewi A. Handoyo, Fandi Dwiputra Suprianto, Selrianus, “Penggunaan Serabut Kelapa Sebagai Bantalan pada Evaporative Cooler”, *Seminar Nasional Teknik Mesin 3*, 30 April 2008, Surabaya, Indonesia, 2008.
- [13] Toni Dwi Putra, Nurida Finahari, “Pengaruh Perubahan Temperatur Media Pendingin pada Direct Evaporative Cooler”, *Proton: Jurnal Ilmu – Ilmu Teknik Mesin*, **3**(1), 2011.
- [14] Hendra Listiono, Azridjal Aziz, Rahmat Iman Mainil, “Analisis Evaporative Air Cooler dengan Temperatur Media Pendingin yang Berbeda”, *Jurnal Online Mahasiswa Fakultas Teknik*. **2**(2). 2015.
- [15] M.D. Amri, B. Yuniyanto, “Pengaruh Debit Aliran Air terhadap Efektifitas Direct Evaporative Cooling dilengkapi Cooling Pad Serabut Kelapa”, *Jurnal Teknik Mesin S-1*, **2**(2), 2014.

This page intentionally left blank

Pre-service Science Teachers' Competence and Confidence in Scientific Inquiry

Rohandi ^{1,*}

¹*Department of Physics Education, Sanata Dharma University,
Yogyakarta, Indonesia*

**Corresponding Author: rohandi@usd.ac.id*

(Received 05-11-2022; Revised 20-11-2022; Accepted 29-11-2022)

Abstract

The quality of science learning has a very important role in science education. The quality of science learning is largely determined by the quality of science teachers. Inquiry-based science learning is becoming a model that must be developed today. In order for inquiry-based learning to be carried out properly, science teachers must have adequate inquiry competencies. Teachers must also have adequate confidence in conducting inquiry-based learning with students in the classroom. The objective of this study was to examine students' competence and confidence in scientific inquiry. 42 pre-service science teachers were involved in this study. Data collected were analyzed using Rasch modeling. The results of data analysis show that mean of the Rasch score for students' competence (1.76 Logits; SD = 1.20) is higher than the mean of the Rasch score for students' confidence (1.41 Logits; SD = 1.01). These results show that although students feel competent to do inquiry, they do not yet fully have the confidence to carry out inquiry learning with students in classroom activities. Implications for a science teacher and pre-service science education based on these results are discussed.

Keywords: pre-service science teacher, scientific inquiry, learning science

1 Introduction

Science Education plays an important role in providing a good climate for students who have an interest in exploring science. The more students who are interested in science the more chances a scientist or researcher in science is born. The development of science cannot be separated from the development of scientific investigations by scientists. At the heart of the process of inquiry in the field of science is the process of hypothesis testing through a series of experiments.

The learning science outcomes besides students can have an understanding of science, they need to have experiences and skills in terms of testing their ideas in solving a problem through the process of inquiry. In the inquiry-based learning process, students are trained to think and reason properly and correctly. Engaging students in applying thinking and reasoning skills and promoting inquiry-based instruction has become the focus for many science educators. The process of inquiry promotes the exploration of questions raised by both students and the teacher. When the inquiry process skills are connected with science content, students discover meaningful concepts and understandings [1].

In this way, students will use these experiences to contribute to their identity in science in and outside the classroom and eventually a future career. In terms of students' science identity, they are able to demonstrate performance in relevant scientific practices with deep meaningful knowledge and understanding of science, and recognize themselves and get recognized as science persons by others. Students develop identities by engaging in science activities and in broader tasks in their community of practice in accordance with the science classroom.

Researchers have advocated for teachers to lead students to collaboratively solve problems in the context of real-world situations and students' culture [2] instead of conducting validation experiments based solely on textbooks. The fundamental of science learning activities is the interaction between students and objects or phenomena in the form of material objects and objects of events/phenomena. Students' interaction with nature objects is not just to describe the situation, but further than that, it is hoped that at least it will be continued with generalization activities, which can develop

students' cognitive and affective potential. Understanding science begins with a specific problem space, where scientists must formulate a problem-solving plan, form a hypothesis, perform an experiment, and gather evidence to explain the problem [3]. Similarly, students must learn to ask questions about specific issues and answer those questions based on evidence. They learn to explore, gather evidence from different sources, construct arguments, construct explanations based on available information, and communicate and defend their conclusions.

In inquiry-based learning, teachers act as facilitators and students take greater responsibility for their learning. Constructivism advocates that teachers help students think through and solve problems that require higher-order thinking and reconstruct their knowledge by interacting with the environment. Inquiry-based learning is an effective method to achieve this objective. It will lead students actively seek knowledge and generate new ideas are key features of inquiry-based science learning [4]. The essential characteristics of inquiry are connecting personal knowledge and scientific concepts, designing experiments, discovering, and building meaning from data and observations [5]. This characteristic describes that implementing inquiry teaching lead students to enhance their science learning by processing personal experience and connecting new and old knowledge. In summary, inquiry-based learning engages students to question, design, and implement discovery, analyze, and communicate their findings to expand their knowledge.

To ensure the achievement of the objectives of learning in science education, well prepared instructional design of learning science is needed so that it is guaranteed that students gain hands-on experience, and opportunities for conceptualization, and are trained to use science process skills in the inquiry process. Such a learning objective in science education will be possible to achieve if the (prospective) science teachers have adequate inquiry competence in teaching science to students which will have a good impact on student learning as well as training students in conducting science investigations (doing science). The skills and knowledge of scientific inquiry enable science teachers to be successful in their teaching of science.

In teaching science and accompanying students to learn science, science teachers need to do it with confidence. Besides competence in inquiry, science teachers'

confidence in conducting and guiding students to learn through the inquiry process is an important factor in the successful teaching of science. Confidence is a feeling of self-assurance arising from one's appreciation of one's own abilities or qualities. Science teacher confidence in the inquiry will promote students' learning even when facing difficulties. Teacher confidence in inquiry helps students feel ready for their inquiry activities and life experiences. When science teachers are confident in teaching through inquiry, they are more likely to move forward with students and opportunities to gain the students' potential in learning science.

In this study, pre-service teachers' competence and confidence were investigated and the Rasch model was used to analyze collected data. Pre-service teachers' competence and confidence will be mapped and discussed. Some implications are formulated from the results of the study.

2 Research Methodology

2.1 Sample

This study aimed to investigate pre-service science students' competence and confidence in inquiry at the School of Teacher Education. 42 students from the primary teacher education department who participated in the Teaching and Learning Science course were involved in this study.

2.2 Data Collection

An instrument used in this study was the questionnaire to measure students' competence and confidence in inquiry in learning science developed by Chang [6]. This questionnaire was designed to evaluate pre-service science teachers' competence and confidence in the inquiry. The questionnaire consisted of 14 items for both competence and confidence in the inquiry. As this instrument had not been used in Indonesia before, the questionnaire was first translated into Bahasa. The students' responses were categorized using a Likert scale. The extreme categories in the Likert scale are labeled "strongly disagree" (coded 1) and "strongly agree" (coded 4). These instruments were administered in the presence of a researcher who would provide assistance if the students encountered any difficulty. These instruments were distributed at the beginning

of the Teaching and Learning Science course. Overall, the administration of the questionnaires proceeded smoothly, all students had sufficient time to complete the questionnaire.

2.3 Data Analysis

The responses of pre-service teachers' competence and confidence in scientific inquiry were analyzed using *Winsteps* (Rasch-Model Computer program). In order for the items can be used in the Rasch model, the items *infit mean square* and *outfit mean square* should be distributed between 0.7 and 1.4, and the *item point measure correlation* should be greater than 0.3 [7].

The Rasch model has been implemented in analyzing data in this research. The Rasch model provides valuable data for the development, modification, and monitoring of valid measurement instruments. In this paper, the Rasch model was used to examine students' competence and confidence in inquiry in the primary teacher education department. The equal interval measures transformed by the Rasch model are used to map persons and items into a linear (interval) scale. Such mapping (called person-item maps) produces useful tools for evaluating students' competence and confidence of students in the inquiry. The person-item maps of students' competence and confidence of students in the inquiry provided ways for evaluating and interpreting the data. Items ordered in person-item maps illustrate the level of item difficulties. This means that items which more difficult to agree with or items which easier to agree with can be identified.

The Rasch model explains how the pre-service teachers' competence and confidence in scientific inquiry can predict a student's response to a particular test item involving competence and confidence in scientific inquiry. Students at the same logits value as an item have a 50% chance of correctly answering that item. Items above their ability level can still be answered correctly, but students have less than a 50% chance of correctly answering the item. Items listed below a student are those that the student has less than a 50% chance of correctly answering. Consequently, the higher position of the item on the single line means that the item is more difficult to agree with. Conversely, the lower position of the item on the single line means that the item is easier to agree with.

3 Results and Discussions

Before the output of *Winsteps* can be used for interpretation of the results of data analysis, all items used in the questionnaire are first evaluated (diagnosed) whether they meet the Rasch model criteria. The evaluation (diagnosis) results showed that for competence items, the *infit mean square* was distributed between 0.49 and 1.40; the *outfit mean square* was distributed between 0.46 and 1.4 and the *item point measure correlation* is greater than 0.3. In the evaluation results for confidence items, the *infit mean square* was distributed between 0.64 and 1.36; the *outfit mean square* was distributed between 0.64 and 1.36 and the *item point measure correlation* is greater than 0.3. The results of this diagnosis indicate that all items can be used in the Rasch model analysis. Furthermore, all data (42 students and 14 items) were transformed using Rasch analysis to order students along the continuum of the measure of competence and confidence in the inquiry.

The distributions of students ($n = 42$) according to competence and of items ($n = 14$) according to the difficulty are shown in Figure 1. On the left-hand side of Figure 1, the distribution of students is represented. Items located below a participant are items that the students were likely to agree to. Items located above are items that the students were unlikely to agree to.

The mean Rasch score for students' competence was 1.76 Logits ($SD = 1.20$). By looking at which items are located above and below this point, we can understand the student's average level of competence. Whereas, the mean Rasch score for items was 0.0 Logits ($SD=1.36$). Looking at the mean of Rasch score on persons and items and their respective standard errors, students' competence is compatible with the items difficulty score. It means that for this sample of students, their competence in inquiry could not be justified whether or not they tend to have more competence. However, the distribution of the items on the map has valuable information of students existing competence. Figure 1 displays an item–person map of inquiry competence in which students are placed relative to the hierarchy of items. On the right side, items are listed in order of difficulty, with the hardest item to agree to at the top (item12) and the easiest item to agree to at the bottom (item13).

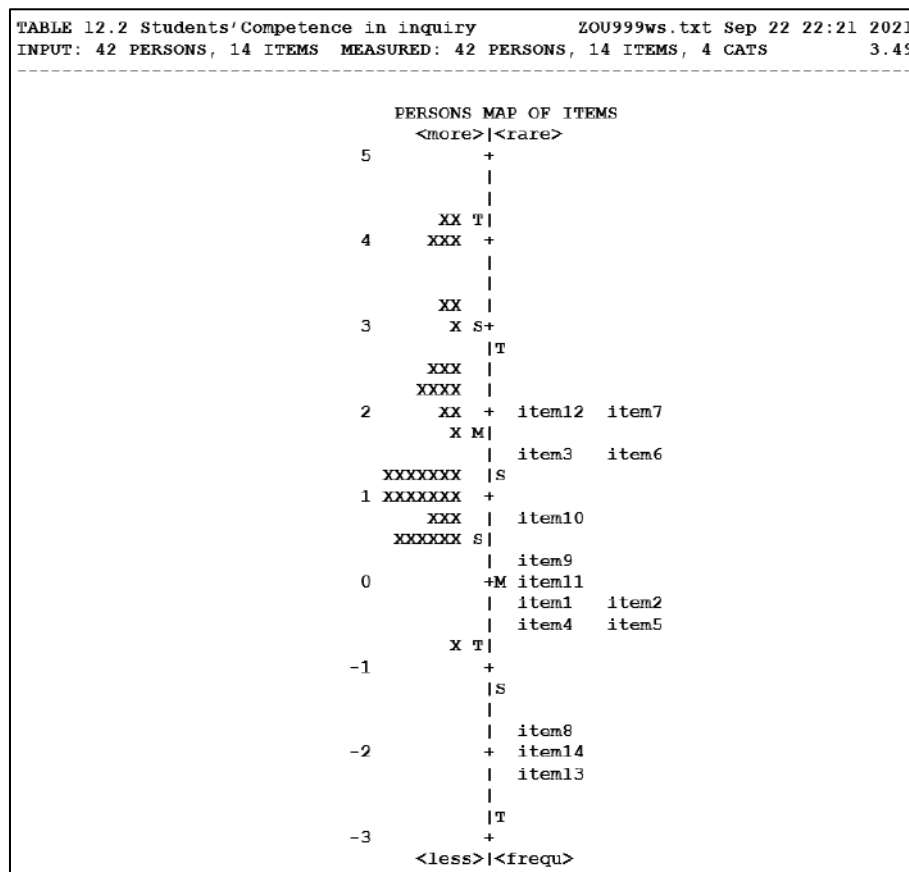


Figure 1. Item Map of Pre-service Teachers' Competence

The mean Rasch score for students' confidence was 1.41 Logits (SD = 1.01). The mean Rasch score for items was 0.0 Logits (SD=0.95). Looking at the mean of Rasch score on persons and items and their respective standard errors, students' confidence is compatible with the items difficulty score. It means that for this sample of students, their confidence in inquiry could not be justified whether or not they tend to have more confidence. However, the distribution of the items on the map has valuable information on students existing confidence. Figure 2 displays an item-person map of inquiry confidence in which students are placed relative to the hierarchy of items. On the right side, items are listed in order of difficulty, with the hardest item to agree to at the top (item12) and the easiest item to agree to at the bottom (item10).

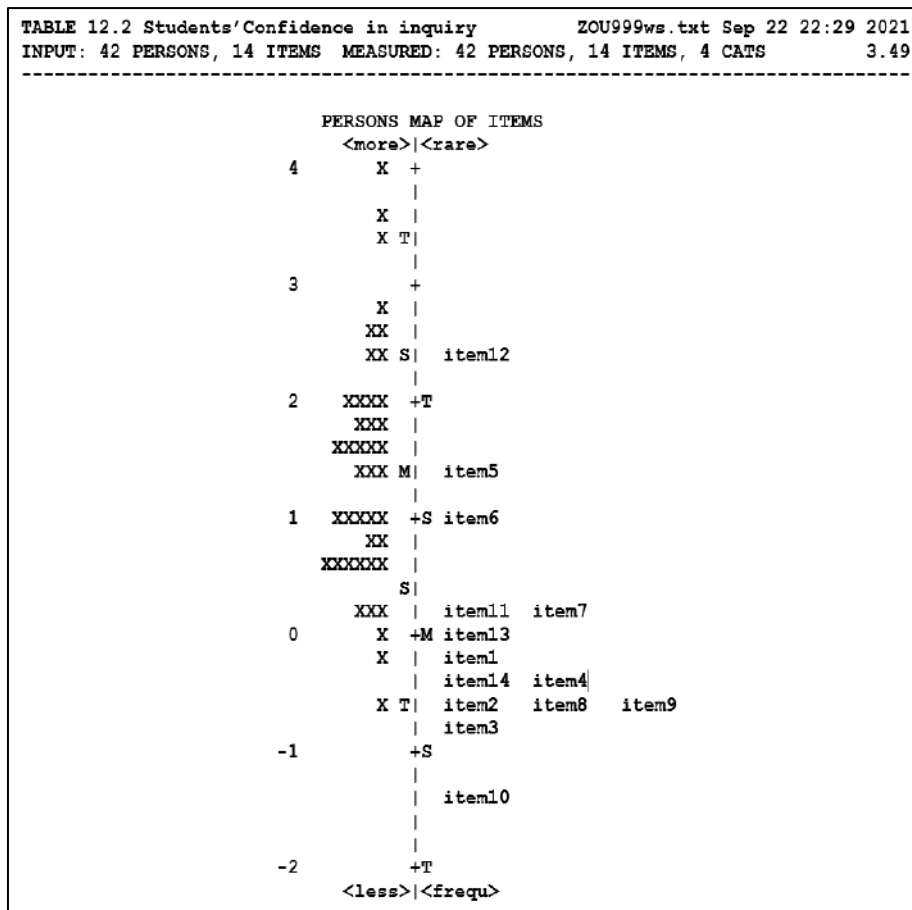


Figure 2. Item Map of Pre-service Teachers' Confidence

The results of data analysis show that mean of the Rasch score for students' competence (1.76 Logits; SD = 1.20) is higher than the mean of the Rasch score for students' confidence (1.41 Logits; SD = 1.01). These results show that although students feel competent to do inquiry, they do not yet fully have the confidence to carry out inquiry learning with students in classroom activities.

In terms of inquiry competence shown in Figure 1, students have difficulty in describing and interpreting data through scientific terminology (item12), controlling extraneous variables that may interfere with results (item7), and posing verifiable hypotheses according to data (item4). The three competencies require a high level of thinking skills. The results of this data analysis, show that students' thinking skills still need to be improved so that these three competencies can be done better. This difficulty is consistent with students' confidence in conducting inquiry learning. As shown in

Figure 2, students are least confident in using scientific terms learned to explain the meaning of experimental data (item12) in science class. In carrying out inquiry learning, it is also indicated that students are still not confident in choosing suitable study methods based on the question (item5), and considering possible factors that may influence the experiment (item6) in science class.

The results of data analysis (see Figure 1) also show that students are able to build conclusions according to collected data (item 13), infer according to collected data (item14), and conduct experiments according to a predefined plan (item8). These results are consistent with the analysis of students' confidence in conducting inquiry learning. Students are very confident (see Figure 1) in carrying out the experiment in accordance with the experiment's procedures (item 10). These results show and likely caused because students are very familiar with doing a practicum with a recipe model where all the things that must be done have been described in the practicum instructions. Students just need to follow the procedures that have been compiled with the order of their activities.

From the results of data analysis as outlined above, some implications in science learning in schools or in pre-service science education can be formulated as follows:

- Science learning activities in schools need to be directed to inquiry rather than prescription models. This is because, in this prescription model, students are given little or no opportunities to propose problems for investigation, ask questions, formulate hypotheses, design procedures, process answers, and explanations, predict and communicate results as well as identify assumptions, use logical and critical thinking and engage in argumentation.

It is also to respond to the demands of learning for the 21st century that most of the learning goals of 21st century skills can be taught within the context of scientific inquiry or project-based learning which requires teachers to be able to engage students in self-directed strategies, to organize activities that delegate learning decisions to students and monitor their progress, to facilitate learning activities such as collective problem solving, and to guide students in thinking about complex problems by giving them feedback following assessment [8]. Furthermore, Chu et al. [8] suggest that delivering inquiry-based tasks is

important in learning science. Inquiry-based tasks will facilitate students to become active agents in building knowledge through constructing their own understanding and through meaning-making, which requires them to have an inquiry mindset. Similarly, Kuhlthau et al. [9] argue that inquiry is a way of learning new skills and broadening our knowledge for understanding and creating in the midst of rapid technological change. Inquiry is the foundation of the information age school [9]. In the teacher preparation context, inquiry-based instruction can also improve the critical thinking and inquiry skills of students in pre-service teacher education [10, 11]

- The importance of conducting experiments in the laboratory or in the outside classroom by focusing not only on the results but also the process of inquiry. The model that needs to be developed is reflective inquiry. There is an element of reflection in each step of the experiment to; 1) recognize the extent to which students have confidence in carrying out the experiment correctly, 2) recognize the extent to which students need to learn/practice in performing steps in the inquiry, and 3) formulate an improvement action plan. This is in line with the research result that the use of the reflective worksheets showed that inquiry-based learning activities promoted students' scientific process skills such as defining the problem, formulating a hypothesis, and observing and interpreting results during the inquiry-based learning process. Students also improved in terms of ability such as using scientific terms, drawing scientific and comprehensible figures, and making scientific explanations. In addition to these, it was found that students had more positive opinions about the learning process [12].

To ensure the achievement of the objectives of science education, a planned instructional organization is needed, so that it is guaranteed that students gain hands-on experience, and opportunities for conceptualization, and are trained to use science process skills. Facilitating students' learning is a crucial factor. Inquiry-based approaches encourage science teachers to become a facilitative role. Proper teacher guidance will allow students to internalize inquiry skills in every step of the investigation. This is in line with the findings of the study Kuhlthau et.al. [9] that

students need considerable guidance and intervention throughout the process to enable a depth of learning and personal understanding. Without guidance, students often approach the process as a simple collecting and presenting assignment that leads to copying and pasting with little real learning. With the teacher's guidance, students are able to concentrate on constructing new knowledge and learning useful strategies in each stage of the inquiry process.

One of the strategies that focus on the process of acquiring inquiry skills is guided inquiry. With this model of inquiry, the teacher provides essential intervention at critical points in the inquiry process that fosters deep personal learning and transferable skills [9]. In inquiry learning, teachers need to restructure their learning environment so that students' beliefs about science, scientists, and themselves will lead to positive attitudes.

4 Conclusion

As the objective of this study was to examine students' competence and confidence in scientific inquiry, the results of data analysis show that mean of the Rasch score for students' competence (1.76 Logits; SD = 1.20) is higher than the mean of the Rasch score for students' confidence (1.41 Logits; SD = 1.01). This indicates that although students in pre-service science education feel competent to do inquiry, they do not yet fully have enough confidence to carry out inquiry learning with students in classroom activities. For the development of competence and confidence of pre-service science teachers in scientific inquiry, science activities in the classroom need to be directed towards the inquiry model with an emphasis not only on the results of the investigation but also on proper guidance during the inquiry process.

References

- [1] R. K. Alwardt, "Investigating the transition process when moving from a spiral curriculum alignment into a field-focus science curriculum alignment in middle school". Lindenwood University, 2011.
- [2] R. Rohandi and A. N. Zain, "Incorporating Indonesian Students' Funds Of Knowledge" Into Teaching Science To Sustain Their Interest In Science," *Bulgarian Journal of Science & Education Policy*, **5**(2), 2011.
- [3] C. C. Selby, "What makes it science," *Journal of College Science Teaching*, **35**(7), 8-11, 2006.
- [4] S. Abell, G. Anderson, and J. Chezem, "Science as argument and explanation: Exploring concepts of sound in third grade," *Inquiry into inquiry learning and teaching in science*, 100-119, 2000.
- [5] J. Hinrichsen, D. Jarrett, and K. Peixotto, "Science inquiry for the classroom: A literature review," *Programme Report. Oregon: The Northway Regional Educational Laboratory*, 1999.
- [6] H.-P. Chang, C.-C. Chen, G.-J. Guo, Y.-J. Cheng, C.-Y. Lin, and T.-H. Jen, "The development of a competence scale for learning science: Inquiry and communication," *International Journal of Science and Mathematics Education*, **9**(5), 1213-1233, 2011.
- [7] J. Linacre, "A User's guide to Winsteps-ministep: Rasch-model computer programs. Program Manual 3.68. 0," *Chicago, IL*, 2009.
- [8] S. K. W. Chu, R. B. Reynolds, N. J. Tavares, M. Notari, and C. W. Y. Lee, *21st century skills development through inquiry-based learning from theory to practice*. Springer, 2021.
- [9] C. C. Kuhlthau, L. K. Maniotes, and A. K. Caspari, *Guided inquiry: Learning in the 21st century: Learning in the 21st century*. Abc-Clio, 2015.
- [10] Irwanto, A. D. Saputro, E. Rohaeti, and A. K. Prodjosantoso, "Using inquiry-based laboratory instruction to improve critical thinking and scientific process skills among preservice elementary teachers," *Eurasian Journal of Educational Research*, **19**(80), 151-170, 2019.

- [11] A. Stavrianoudaki and A. Smyrniotis, "Effects of inquiry-based learning cooperative strategies on pupils' historical thinking and co-creation," in *Education beyond crisis*: Brill, 300-315, 2020.
- [12] A. Mutlu, "Evaluation of students' scientific process skills through reflective worksheets in the inquiry-based learning environments," *Reflective Practice*, **21**(2), 271-286, 2020.

Appendix:

A. Students' competencies in scientific inquiry:

1. Be able to pose questions according to data observed
2. Be able to pose an explorable question
3. Be able to describe a concept with an operational definition
4. Be able to pose a verifiable hypothesis according to data
5. Be able to pose a feasible explorative plan according to the question
6. Be able to manipulate variables related to plan
7. Be able to control extraneous variables that may interfere with results
8. Be able to experiment according to a predefined plan
9. Be able to collect data through different methods
10. Be able to record data through different instruments
11. Be able to compare and classify data collected from an experiment
12. Be able to describe and interpret data through scientific terminology
13. Be able to build a conclusion according to collected data
14. Be able to infer according to collected data

B. Students' confidence in inquiry teaching:

1. In science class, I could ask questions about what I don't understand through observation.
2. When learning science, I could collect information related to questions to obtain a deeper understanding.
3. When learning science, I could deduce possible answers to the questions.
4. In science class, I could describe what data should be collected in the experiment.
5. In science class, I could choose suitable study methods based on the question.
6. In science class, I could consider possible factors that may influence the experiment.
7. In science class, I could design the experimental steps based on the question.
8. In science class, I could observe and record the results of the experiment carefully.
9. In science class, I could operate the experimental apparatus to measure data.
10. In science class, I could carry out the experiment in accordance with the experiment's procedures.
11. In science class, I could compare or classify data collected in the experiment.
12. In science class, I could use scientific terms learned to explain the meaning of experimental data.
13. In science class, I could draw conclusions based on the mathematical relationship among experimental data.
14. In science class, I could explain experimental results or phenomena based on the experiment's conclusion.

AUTHOR GUIDELINES

Author guidelines are available at the journal website:

<http://e-journal.usd.ac.id/index.php/IJASST/about/submissions#authorGuidelines>

This page intentionally left blank